Project Report No. 412

May 2007

Price: £6.50

Development of rapid analytical methods for detecting mycotoxins in cereal grains

by

Richard Luxton

University of the West of England
Frenchay Campus, Coldharbour Lane, Bristol, Avon, BS16 1QY

This is the final report of a project lasting for 24 months which started in July 2004. The work was carried out by the University of the West of England and was funded by contracts of £53,000 from HGCA (Project No. 3008), £365,000 from Defra (Project No. FQS 61) and £312,459 of in-kind contributions from industry (£40,000 from RHM, £10,00 from Weetabix, £96,000 from CCFRA, £81,000 from Gwent Electronic Materials and £85,459 from Uniscan Instruments) making a total of £730,459.

Contents

Abstract

Mycotoxins are naturally occurring toxic compounds produced by fungal growth. In excess of 200 mycotoxins have been identified, although most analytical laboratories can only assay for up to 20 of these.

The potential health risk of exposure to mycotoxins in foods depends upon the type of mycotoxin due their differing degrees of toxicity. Some of the more common mycotoxins are genotoxic and carcinogenic. Acute effects require that large amounts of mycotoxin are ingested. Traditionally the analysis of mycotoxins uses affinity columns to purify the extract prior to high pressure liquid chromatographic (HPLC) detection. These assays are time-consuming and relatively expensive (~£100).

The increasing consumer demand for safe food is accompanied by the need for rapid and cost-effective analytical techniques capable of screening for the presence of mycotoxins to allow for the positive release of food ingredients before they enter the food chain. This requirement was addressed in the project by developing an analytical system using disposable biosensors capable of identifying and quantifying a pre-selected suite of mycotoxin residues. Six mycotoxins were selected by the project consortium members based on food industry analytical requirements and availability of antibodies. The six mycotoxins were: ochratoxin A, deoxynivalanol (DON) and aflatoxins B1, B2, G1, G2. Zearalenone and fumonisins FB1 and FB2 were identified for inclusion if any of the selected mycotoxins were problematic.

The overall aim of the FQS 61 project was to investigate the feasibility of developing an automated detection system for mycotoxins in foodstuffs and feeds. This involved combining a novel rapid extraction method with biosensor technology integrated in a twelve channel measurement system allowing simultaneous measurement of up to six different mycotoxins, in duplicate.

Rapid extraction techniques developed at CCFRA allowed mycotoxins to be extracted from grain in less than 10 minutes using a non-toxic, Pytosol solvent. The extraction method compared well with conventional methods. The measurement of mycotoxins was performed on an instrument developed by Uniscan Instrument which incorporates a competitive immunoassay, combined with an electrochemical detection step. Development of the mycotoxin immunoassays was undertaken at the University of the West of England. The immunoassays were performed using a biosensor which immobilised the mycotoxin antibodies on the biosensor surface. An array of 12 biosensors was produced by a screen printing method using conductive inks. Each biosensor could have a different antibody immobilised on the surface giving the potential of 12 separate measurements. Gwent Electronic Materials were responsible for designing and fabricating the arrays of biosensors and Applied Enzyme Technologies developed stabilisers for the antibodies immobilised on the biosensor surface. The electrochemical measurement was made by the instrument giving the concentration of mycotoxins present in the sample using neural network. The software can also evaluate any cross-reactivity between the specific antibodies and other mycotoxins.

During the course of the project a large number of antibodies were characterised for the different mycotoxin assays. Problems obtaining suitable antibodies for all six mycotoxins proposed resulted in only assays for total aflatoxin, aflatoxin B1, ochratoxin A and DON

being fully characterised. The instrument developed was able to automate the immunoassays, allowing 12 simultaneous measurements to be made. The neural network showed that there was no cross-reactivity between the assays used on the instrument, indicating that the antibodies were giving a high degree of specificity to each of the mycotoxins. The assays were optimised to cover the concentration ranges that are required to discriminate levels of mycotoxin above and below the MRL.

The evaluation stage of the project showed that the antibodies on the biosensor surface were stable at room temperature for at least six months and a preliminary end-user study of ochratoxin A extracted from grain samples showed that the system could in principle be used to measure mycotoxins. However, further optimisation is required to reduce the assay time from the current 77 minutes.

The project successfully demonstrated that arrays of biosensors can be integrated into an instrument allowing the automated measurement of multiple mycotoxins to be performed.

Summary

There is increasing consumer demand for food and drink of consistent high quality in terms of safety. This concern, backed with increasing government legislation that requires food processors, wholesalers and retailers to ensure due diligence and traceability of their raw food products, requires considerable effort and investment by the industry in ensuring that these criteria are fully met. There are a wide range of compounds that need to be addressed, i.e. agrochemical residues, natural and microbiological toxins and environmental contaminants to name the most important. Mycotoxins, produced either in the field or during storage, occur on a wide range of raw food matrices e.g. cereals, nuts, dried fruits, spices and herbs. Many of these materials are used across the food chain from animal feeds to raw ingredients for food manufacture. In this way mycotoxins can be introduced into the food chain to give rise to secondary contamination, e.g. aflatoxin M1 in milk derived from animal feed contaminated with B1. In addition, their stability means that some treatments, e.g. fractionation, can actually increase mycotoxin concentration while thermal processing fails to reduce the risk significantly, e.g. for aflatoxin and ochratoxin A in milling and baking. Furthermore, sources are often eaten without further processing e.g. nuts, some cereals and dried fruits, representing a direct risk to consumers.

Current EC legislation (EC 466/2001) prescribes maximum levels of aflatoxins between 2-15 µg/kg (2-15 ppb) dependent on the food matrix. For ochratoxin A no current EC legislation is in place but the Commission has stated that the establishment of a maximum limits on the basis of 'as low as reasonably achievable (ALARA) principal' (EC 472/2002). Currently limits in the range 5-10 µg/kg (5-10 ppb) are adopted within the food industry. The maximum limits for these mycotoxins are being reviewed by the Commission with a report due at the end of 2003 (EC 472/2002). While no EC regulations exist at present for trichothecene deoxynivalenol (DON) it is anticipated that a maximum limit of 500 µg/kg (500 ppb) will be adopted in the foreseeable future.

This 2 year project sought to integrate different areas of technology to investigate the feasibility of developing rapid sensor instrumentation, for mycotoxins, in raw food products, as a model system for further development and extension to other analytes that may be amenable to immuno-biosensors technology. The areas of technology that were integrated to produce the working system were: rapid extraction technology, immunobiosensor technology, instrumentation and pattern recognition software. The objectives of the project were:

I. To research an innovative multi-array disposable electrochemical immuno-biosensor device capable of rapidly identifying and quantifying mycotoxins in a range of raw food products.
II. To evaluate novel methods of rapid extraction of mycotoxins from a variety of raw foods.
III. To elucidate and overcome possible over-estimation of currently reported mycotoxins levels due to co-elution of interferents in classical techniques.
IV. To integrate immuno-biosensor technology into generic enzyme biosensor array instrumentation for use by semi-skilled personnel.

Initially six mycotoxins were chosen as the target compounds for the biosensor array: trichothecene deoxynivalenol (DON), ochratoxin A (OA), total aflatoxin, aflatoxin B1, zearalenone and fumonisin. The proposed approach to obtaining antibodies proved problematic and hence commercially available antibodies and conjugates were sourced. There were problems obtaining suitable antibodies for all the mycotoxin assays which resulted in only four assays being fully developed – DON, OA, total aflatoxin and aflatoxin B1.

The work packages associated with the project divided the research into three main areas, development of the extraction technology, development of the biosensor array and development of the instrumentation including the software. Also within the project was an evaluation period where the end-user would use the other instrument to assess its utility. Full details of the scientific studies and evaluations of the technology are included in the later sections of this report.

Extraction of mycotoxins

The rapid extraction system developed by Advanced Phytonics for the fragrance industry has been successfully modified and employed for the organophosphate residues in food products in FQS 12. The process utilises a new breed of refrigerant gases as solvents. These solvents are non-toxic, non-flammable and non-polluting. The nature of the solvents allows the extraction process to be applied to wet materials and to be carried out at pressures of less than 10 bar and at temperatures at and below room temperature. It is also possible to use added organic solvents to enhance the properties of the Phytosol solvents in the extraction process. After extraction the solvent can be reclaimed, “concentrating” the extract retained in the organic solvent and minimising waste. It is also possible to modify the extraction specificity of the system by altering the temperature and pressure at which the extraction is carried out. The outcome of the process can be an aqueous or solvent extract of minimal volume. The aqueous extract providing compatibility with the biosensor functionality. The lack of organic solvent is an important consideration for use with immuno-biosensors that naturally require an aqueous environment for optimum activity.

Development of the rapid extraction of mycotoxins undertaken in the project showed that good recovery, greater than 80%, was achieved (4 of the 5 mycotoxins gave recovery is greater than 90%) for all mycotoxins except ochratoxin A which had a recovery of approximately 50%. This compared well to classical methods of extraction and had the added advantage of being complete in less than 10 minutes. The residue remaining was dissolved in buffer containing 20% methanol to dissolve the mycotoxin in the extract and to allow compatibility with the enzymes on the biosensor.

Immuno-biosensors

The use of disposable screen-printed biosensors to detect organophosphates on raw food products has been described in defra-Link project FQS12 where this innovative technique combined the advantage of relatively inexpensive disposable carbon based sensors with the high sensitivity and selectivity of enzyme inhibition.

This project replaced the enzymes on the screen-printed biosensor with antibodies to give the measurements specificity to particular mycotoxins. The measurements of the mycotoxins were based on the principles of immunoassay but applied to disposable sensor technology, in the format of an array of immuno- biosensors utilising amperometry and chronoamperometry. The selected antibodies were stabilised using poly-electrolytes and complex sugars.

A competitive enzyme linked immuno-biosensor was developed which had advantages over sandwich assay approaches, particularly for small molecules such as mycotoxins. The assays were based on an indirect competition assay using an immobilised capture antibody where there was competition between free antigen (from the extract) and biotin-labelled antigen. This was followed by the addition of streptavidin-labelled enzyme (alkaline phosphatase), and then the addition of substrate solution (1-naphthyl phosphate) for the electrochemical assay. The formation of the product 1-naphthol, was detected electrochemically. A schematic representation of the assay format is shown in Fig 1 below; in this case the mycotoxin shown is aflatoxin B1 (AFB1).

A sensor comb of 12 sensors was fabricated using screen printing technology. The comb was used in conjunction with instrumentation designed and fabricated during the project. The sensor comb was inserted into the instrument which “dipped” the sensors on the comb into a series of wells containing sample, reagents and wash solutions placed in a commercially available 96 well microtitre plate. Finally, the instrument made the electrochemical measurement and displayed the result. Initially the sensors were screen printed on to a plastic substrate. Problems with cutting the sensor comb from the plastic substrate resulted in poor precision of the electrodes. Investigations into the use of a laser to cut the comb did not solve the problem. Screen printing sensors on to a ceramic substrate gave greatly improved reproducibility; the base sensors had a coefficient of variation between 2.4% and 4%.

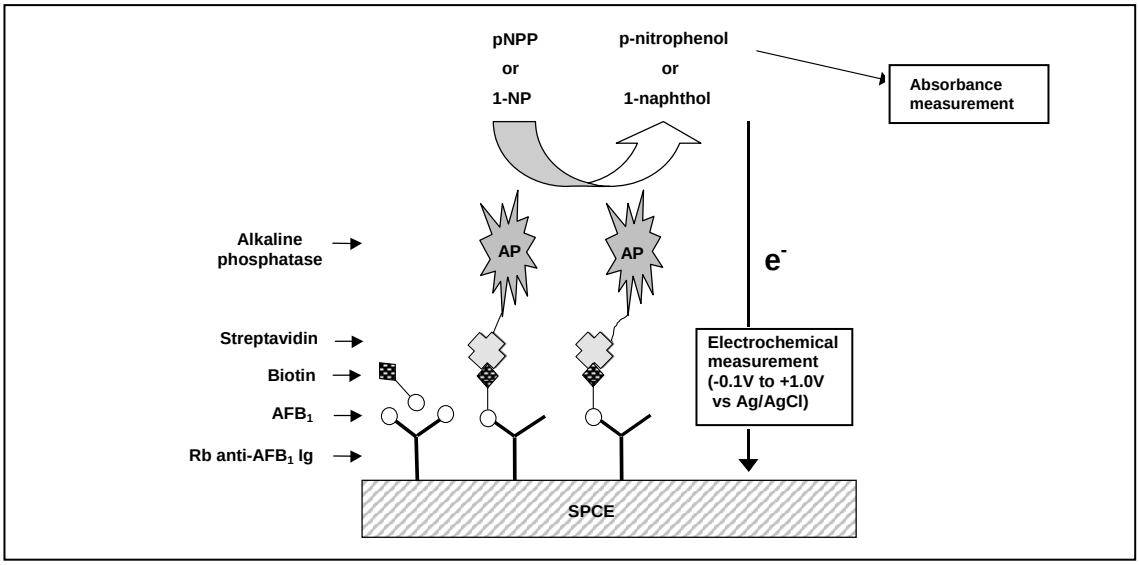

Figure 1. Schematic diagram of mycotoxin immunoassay

Four competitive immunoassays for DON, OA, total aflatoxin and aflatoxin B1 were developed for the biosensor array using commercially available reagents. The assays were optimised to give a response at the MRL for the particular mycotoxin. Parameters optimised included: antibody concentration, mycotoxin-biotin concentration, streptavidin-enzyme concentration and the concentration and type of blocking agent used. A precision of 4% was achieved for OA but the precision for the other assays was greater (9-18%). Studies demonstrated that the antibodies chosen for the aflatoxin assays showed some cross reactivity between different classes of aflatoxin. Figure 2 shows an example of the electrochemical response and dose-response curve for aflatoxin B1.

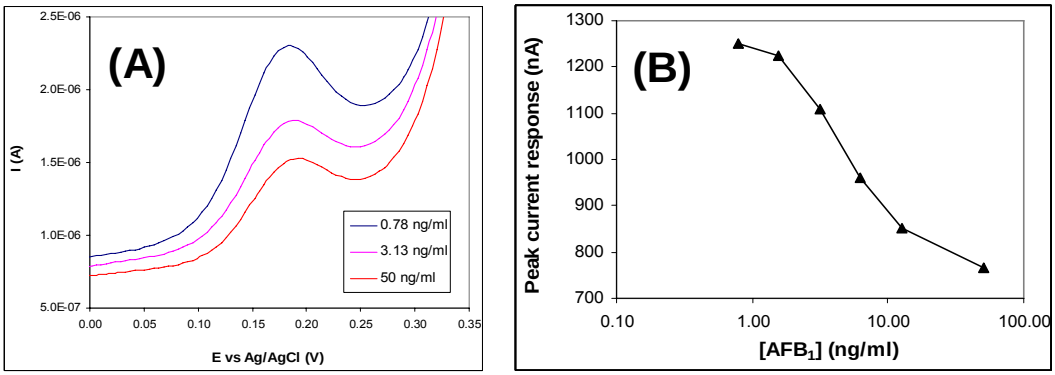

Figure 2. Electrochemical immunoassay for AFB1 (A) voltammograms, and (B) calibration plot for AFB1 in phosphate buffer solution.

The original project proposal was to have different assays on the biosensor comb and to use a neural network programme to interpret the patterns of activity from the different sensors. Problems with acquiring antibodies resulted in only single assays being evaluated on the sensor comb. A neural network programme was evaluated using data generated at UWE and analysed by Uniscan for ochratoxin A and aflatoxin B1. The results showed no cross-reactivity between these two mycotoxins, which is explained by the specificity of the antibody used in the sensors. There was insufficient data for the other mycotoxins to be fully analysed. As only single assays were being performed on the instrument the neural network was not implemented by the end of the project.

Antibody and enzyme label conjugate stabilisation

The immobilisation and stabilisation of the antibodies on the sensor surface was crucial to ensure maximum activity on the screen-printed carbon transducer. Proven protein stabilisation and immobilisation techniques developed in a previous project (FQS 12) was used a basis for the stability studies on the mycotoxin antibodies and enzyme labelled conjugate.

Polyelectrolyte stabilisers mixed with the antibodies produced protein-polyelectrolyte complexes, which are synergistically stabilised by water modifiers such as sugars and polyalcohols. The 3D matrix which was formed 'entraps' the antibody in a low water environment with polyelectrolyte present. Thermal stress was used as a means of accelerated degradation of the antibody and was cautiously used to give an estimated prediction of shelf-life.

The studies showed that antibodies were stabilised on the sensor surface using P2, a stabilising agent developed by AET. Accelerated testing at 37°C suggested the antibodies would be stable for at least six months.

Instrumentation

An instrument was developed and fabricated according to the project proposal. A working prototype instrument was available for the system evaluation. A sensor comb was mounted in the instrument which moved the comb into wells containing sample, reagents and wash solution. Each sensor comb contained 12 biosensor areas on which the assays were performed. Twelve parallel electrochemical measurements were optimised to give a precision better than 1% for instrumental response, but when the laboratory evaluation was undertaken it identified some issues with the material used to fabricate the sensor combs (see work package 3). Combs fabricated from Velox gave poor reproducibility but combs fabricated using a ceramic material a precision of 4% was achieved. The instrument represented a significant advance over the instrumentation developed for the defra-Link project FQS12

The system's components included:

Electronics Rack – An enclosure containing all the electronic modules. This included the array of potentiostats and modules to control pumps and solenoids. The rack hosted the electronic connections between all the system components.

Multi-Well plate – A standard 96 well (12 x 8) plate was used to hold the solutions, into which the sensors were immersed in specific, timed sequence to allow washing and addition of reagents to the sensor surface.

Well plate heater – An aluminium tray holding the Multi-Well plate. The tray incorporated resistive heaters and a temperature sensor capable of maintaining the Multi-Well plate at a constant temperature of 37 deg centigrade.

Linear translation stage – A motor driven linear translation stage on which the Well plate heater was mounted. The translation stage positioned the Multi-Well plate rows such that the array of 12 sensors was aligned with any of the 8 rows in the plate. The stage also provided extended movement to allow a sensor wash to be performed via wash

nozzles. In this case the waste liquid from the wash was collected in the wash tray.

Sensor Actuator – A structure which supported the sensor holder above the well plate and by action of a motor, lead-screw and linear bearing, lifted the sensors in and out of the well plate wells. This action was controlled by computer software.

Sensor Wash nozzles – a series of 12 nozzles provided a wash jet on to the sensor, activated by electrical switching of the wash pump under software control.

Base Plate – The plate on to which the system was constructed.

Wash tray – A tray which collected the waste from the sensor washing process.

Computer / Software – A Windows compatible PC ran a bespoke software application which provided all the control and data processing for the instrument.

Evaluation

The initial evaluation programme defined in the project proposal was not undertaken due to the delays in developing assays. A new evaluation programme was devised where the end users would evaluate one analyte using the instrument in their home laboratories. End users visited UWE to run OA contaminated samples on the instrument. Samples analysed included naturally contaminated wheat at a range of levels (<0.1µg/kg to 2.6µg/kg), and blank wheat spiked multiple times at 1µg/kg. The detailed evaluation was not performed as planned due to the problems in delays associated with the assay development and some problems with the instrument. The end users identified that the assay time would need to be reduced for the final system.

The following sections details the work undertaken during the project. Details of the extraction methods, development of the biosensor, optimisation of assays, development of the instrumentation and a review of the end-user evaluation are given.

Consortium Members

Project Management

Dr Simon Hook	Home-Grown Cereals Authority	(Project Manager)
Dr Richard Luxton	University of the West of England	(Project Coordinator)

Assay development

Prof John Hart	University of the West of England	(Lead Scientist)
Dr Roy Pemberton	University of the West of England	

Biosensor fabrication

Mr Robin Pittson	Gwent Electronic Materials Ltd
Dr Guido Drago	Applied Enzyme Technology Ltd

Instrument fabrication

Dr Graham Johnson	Uniscan Instruments
Dr Daniel Lonsdale	Uniscan Instruments
Mr John Griffiths	Uniscan instruments

Extraction method development

Mr Nick Byrd	Campden & Chorleywood Food Research Association
Dr Martin Hall	Campden & Chorleywood Food Research Association

End users

Dr Clare Hazel	RHM Technology Ltd
Mrs Sue Patel	RHM Technology Ltd
Ms Lynn Foster	Weetabix

1. Rapid Extraction of Mycotoxins from Cereals

Introduction

In order to be able to develop a rapid biosensor based analytical instrument it was essential that the initial extraction was efficient, robust, quick and safe. To ensure full compatibility with the biosensor and adhere to strict regulations regarding the use of solvents in food production sites, it was essential that only small amounts of permitted organic solvents were used in the extraction step.

Samples were fortified with known amounts of mycotoxin at the anticipated permitted maximum residue level.

Materials and Methods

A rapid mycotoxin extraction method is described for determining six selected mycotoxin residues in cereals. Analytes are extracted into a refrigerant gas (Phytosol) and the residues reconstituted into methanol prior to determination by the biosensor or lc/ms/ms.

Extraction Materials.

1. Methanol..-Fisher
2. Phytosol D (Composition: 1,1,1,2-Tetrafluoroethane >88%,
   Dimethyl ether >9%). Advanced Phytonics Ltd.

3. Mycotoxin standards.-
   Ochratoxin A - Sigma
   Deoxynivalenol - Sigma
   Aflatoxins B1, B2, G1, G2. – Sigma

Stock solutions of individual mycotoxins (10mg/L ochratoxin A and aflatoxins, 100mg/L deoxynivalenol) were prepared in methanol. Mixed working standard solutions were prepared to fortify samples at the required concentrations. Mixed calibration standards were prepared for lc/ms/ms quantitation. All standards were stored refrigerated for up to six months.

Apparatus

Liquid chromatograph / Triple quadrupole mass spectrometer (LC/MS/MS)

Perkin Elmer 200 series pump
Agilent 1100 autosampler
Applied Biosystems API 4000 LC/MS/MS

Column: Hyperclone BDS C18 (100mm x 4.6mm)
Mobile Phases:
A: 95% Water /5% Methanol 10Mm Ammonium Acetate
B: 5% Water /95% Methanol 10Mm Ammonium Acetate

Flow rate: 1ml/min

Extraction Vessel

A gas tight vessel designed by CCFRA and engineered by Jenway was used to extract mycotoxin residues.

Extractions were performed in a 130ml glass extraction vessel vertically enclosed within a perspex safety cylinder. The end of the glass extraction tube was sealed with an aerosol cap fitting to allow the input of gaseous phytosol extraction solvent, and to allow the release of extracted analytes. The collection vial was placed in a beaker containing water at 40°C (+/-2 °C).

Extraction Procedure

5g (+/-0.5g) of homogenised cereal sample was weighed directly into the extraction vessel, into which 2ml of methanol was pipetted. The vessel was sealed, Phytosol D added via the aerosol closure to approximately 1 cm above the level of sample, and the vessel shaken for at least 1 minute. The solvent was aspirated through silicon tubing into a collection tube placed in a beaker containing water at 40°C (+/-2°C). The phytosol extraction was repeated and the solvent transferred to the collection tube.

The combined extracts were allowed to evaporate to dryness and the residue redissolved and made up to the relevant volume in methanol.

Quantification was carried out by liquid chromatography with triple quadrupole mass spectrometric detection.

Results

Milled wheat samples were individually fortified with mycotoxin standards. Aflatoxin B1, B2, G1, G2 and ochratoxin A was fortified at a level of 0.01mg/kg, deoxynivalenol was fortified at 1 mg/kg. All samples were extracted using the phytosol extraction procedure. The recoveries of the fortified samples are shown in Tables 1.1, 1.2 and 1.3.

Analyte	% Recovery
Aflatoxin B1	89
Aflatoxin B2	92
Aflatoxin G1	81
Aflatoxin G2	92

Table 1.1. Recovery of aflatoxins from milled wheat fortified at 0.01 mg/kg

Analyte	% Recovery
Deoxynivalenol	93

Table 1.2. Recovery of deoxynivalenol from milled wheat fortified at 1 mg/kg

Analyte	% Recovery
Ochratoxin A	52

Table 1.3. Recovery of ochratoxin A from milled wheat fortified at 0.01 mg/kg

Discussion

The relatively simple and crude extraction procedure for the removal of the mycotoxins does not eliminate all of the co-eluting interferences that would make identification and quantification using classical HPLC techniques problematic. In order to be able to determine the extraction efficiencies of the phytosol extraction, a lc/ms/ms quantitation method was developed using an Applied Biosystems API 4000 triple quadrupole mass spectrometer.

LC/MS/MS conditions were optimised for the six selected mycotoxins as well as nine additional mycotoxins (nivalenol, fusarenon-X, 3-acetyldeoxynivalenol, 15-acetyldeoxynivalenol, neosolaniol, diacetoxyscipenol, HT-2 toxin, T2-toxin, zearalenone).

The ability to be able to identify and quantify a greater number of mycotoxins other than the initial six that were selected was to ensure that should additional mycotoxins be chosen at a later date, an instrumental method was in place capable of determining the efficiency of the extraction.

LC/MS/MS conditions are listed in Appendix 1.

The composition of the extraction solvent has a significant influence on the ability to recover mycotoxins from the wheat samples. Ideally a greater volume of methanol would have been added to the milled wheat to aid the extraction of ochratoxin A, however the maximum final percentage of methanol in the final extract was restricted to 20% to ensure optimal compatibility with the biosensor. Other solvents such as acetonitrile may have been able to improve the recovery of ochratoxin A, however as this is not a permitted solvent in food production sites, no development work was attempted.

The extraction solvent selected (2ml methanol, phytosol D & 5g sample) has proven to be extremely efficient at extracting the aflatoxins B1, B2, G1, G2 and deoxynivalenol. This extraction solvent should also prove to be similarly successful in extracting those additional twelve mycotoxins which were on the reserve list or where lc/ms/ms conditions were optimised.

All of the selected mycotoxins were successfully extracted from the fortified wheat with recoveries ranging from 52% to 93%. The extraction step is simple to perform, cheaper than classical mycotoxin extraction techniques and kinder to the environment, as only a minimal amount of non-chlorinated solvent is used. Potentially up to 10 pre-weighed samples can be extracted in one hour.

In conclusion, it has been demonstrated that the gaseous phytosol extraction procedure successfully extracts the six pre determined mycotoxins. Further work at CCFRA would be able to determine the feasibility of extending the scope of the extraction to include additional mycotoxins.

The use of a simple extraction procedure using a gaseous solvent allows samples to be extracted by non technical personnel and avoids the need for any costly laboratory apparatus for sample extraction and concentration.

2. Development of Biosensors

Introduction

Previous work by the group at UWE on other projects has created a precedent for successful electrochemical immunoassay protocols for other single analytes based on the use of screen-printed carbon electrodes (SPCEs). These protocols have utilised SPCEs coated with an appropriate capture antibody, which have then been utilised in a competitive immunoassay procedure, terminating in electrochemical detection of an appropriate electroactive enzyme-generated product. Since SPCEs can be mass-produced at low cost, there is clear potential for their adoption in a high-throughput analytical setting such as a cereal production unit, where the end-user stands to benefit in terms of rapid screening of raw materials for the presence of toxins. The link between UWE and Gwent Electronic Materials Ltd has been established over the past fifteen years as a reliable source of cooperative development in producing electrode materials and particularly SPCEs for research. Faced with the goal of screening foodstuffs for a variety of mycotoxins, this project therefore set out to investigate the use of SPCEs in an array format with the aim of being able to produce an assay or series of assays which could be performed automatically with minimal input or skill requirement from the end-user(s). The following sections summarise the results of investigations carried out to develop the electrode materials for the project, to test the resulting SPCE arrays for electrochemical behaviour and precision, and to develop/test an automated instrument for carrying out immunoassay using these arrays. The results of investigations into developing immunoassays for three mycotoxin families are presented, these being aflatoxins, ochratoxin A (OTA) and deoxynivalenol (DON).

Electrode materials and quality control tests

The aim of the present work was to design a screen-printed electrode array capable of aligning with a standard 96-well plate format with the capability of being moved from row to row during the timescale of an immunoassay. Hence it was important that the quality of the printing should be sufficiently good to define a relatively small working electrode area and associated counter/pseudoreference electrode with sufficient precision to produce good electrochemical behaviour across an entire array. The electrode design needed to be addressable via contacts from above, so that the array would integrate with the necessary instrumentation (see section 3), and so that electrodes could be lowered into, and function in, microwells containing up to 300 microlitres of solution. In considering the electrode design, it was also necessary that, in order to prepare immunosensors, the working electrodes could be coated with appropriate antibody reagents, either before or after being cut or snapped from their backing card as “comb” structures capable of meshing with the 96-well microplate format.

The choice of electrode materials for this project was based on previous studies in which carbon ink, code D14 from Gwent Electronic Materials Ltd. was used as the working electrode material in screen-printed electrodes comprising single or dual electrode configurations. In previous studies involving immunosensor development, carbon ink,

code D14 was printed successfully onto PVC or polyester card and was successfully coated in this format with the appropriate capture antibodies.

Paste Formulations:

All of the paste formulations are manufactured by GEM in their production facility. Each of the pastes is made to a specification, which includes the Fineness of Grind (F.O.G.), Solids Content, and Viscosity. Each of these attributes must be met and checked through Quality Control before the paste is considered acceptable for use. The working electrode, carbon/graphite paste formulations go through a further electrochemical test as part of their Quality Control to ensure that they are fit for purpose.

Printing Pastes Used:

Electrode Type	**Formulation**	**Product Code**
Working Electrode	Carbon/Graphite	C2000802D2
Reference Electrode	Silver/Silver Chloride	C61003P7
WE and RE Area Defining Mask	Polymer Dielectric	D2040917D2

Printing Screens:

Screens are checked for tension prior to printing and after printing and a lower limit is set for the tension of all screens. Once the tension of the screen reaches this point it is replaced.

Printing:

Electrodes were printed using DEK 248 Screen Printer which had been programmed with the optimised settings for each of the individual layers to be printed.

Polyester substrate

First print-run(13/10/04)

Polyester backing card was selected in order to obtain the best chance of good quality precision printing (for details, see details from GEM); the choice of carbon ink for best printing was a modification of the original D14 ink, known as GEM code C2000802D2. A counter/pseudoreference electrode of Ag/AgCl (60:40) (GEM code C61003P7) was printed alongside each working electrode. These were separated by a non-conducting dielectric material (GEM code D2040917D2). The electrode design for an array of 12 such dual electrodes is shown in Fig 2.1A. These arrays were printed onto polyester sheets in sets of five (60 electrodes per sheet) as shown in Fig 2.1B.

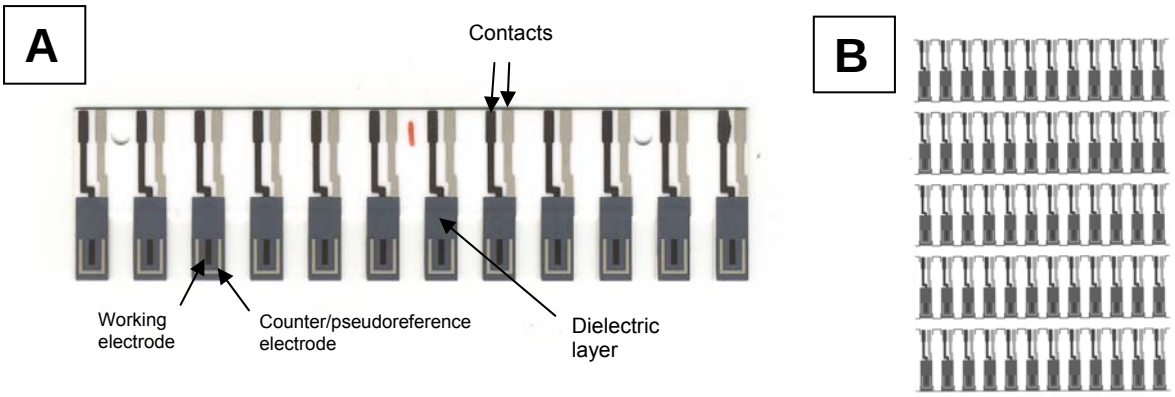

Fig 2.1. Screen-printed electrode design. (A) Array of 12 electrodes showing working, counter/reference and dielectric pattern (B) Sheet of 60 electrodes printed onto polyester backing card.

Combs of 12 electrodes, or individual electrodes were cut out from the backing sheet using scissors. In order to obtain a 12-electrode array capable of sitting in a 96-well microtitre plate it was necessary to remove the interdigitating rectangle of polyester between adjacent electrodes. This was achieved most effectively using a scalpel, resulting in less bending/distortion of the polyester "comb" than if attempted using scissors. This process was however time-consuming and required great attention in order to avoid touching the electrode surfaces or bending the polyester.

Quality control tests of the printed electrodes were performed by cyclic voltammetry of a 0.5mM solution of potassium ferrocyanide in 0.05M Na+/K+ phosphate buffer, pH 7.0. Initial experiments were conducted using a Autolab Type II potentiostat (Eco Chemie B.V, Netherlands; UK agents Windsor Scientific UK Ltd.). Individual sensors were cut out and mounted in an electrode holder comprising gold edge connectors and leads terminating at the potentiostat. The sensors were immersed into a 20 ml volume of ferrocyanide solution in a glass electrochemical cell. After an equilibration (wetting-up) time of 20s, the applied working potential was scanned from -0.3V to +1.0V and back at v = 100 mV s-1. A representative voltammogram for a single sensor is shown in Fig 2.2.

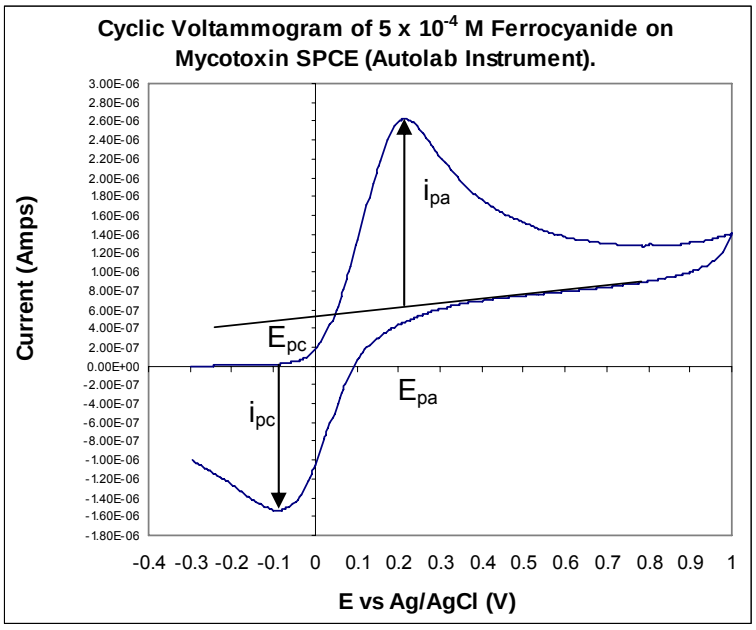

Fig 2.2**.** Example quality control cyclic voltammogram performed on bare SPCE

The size of the anodic and cathodic peak currents (ipa and ipc respectively) was recorded for each sensor. The values of applied potential at which these peaks occurred (ie. the anodic and cathodic peak potentials, Epa and Epc respectively) were also recorded. Voltammograms were obtained for sensors from various locations within a single card of 60 printed sensors, and from several cards from a single print run. The results of ip measurements are summarised in Figs 2.3- 2.6. Figure 2.3 shows the mean and coefficient of variation values for ipa measurements obtained for replicate sensors across, down or diagonally within a single card print. Peak current values over the entire card of 60 sensors ranged from 2.39 to 2.67 μA. Across the rows, CV values of between 1.7 and 3.8% were obtained, whilst a CV of 1.7% was obtained down column 1. Diagonally, the CV value was 3.7%. Taking all ipa values for the whole sheet, the CV was 3.0% (n = 30 electrodes tested). At less than 4% CV, these results indicate excellent precision for ipa values obtained within a single sheet of electrodes.

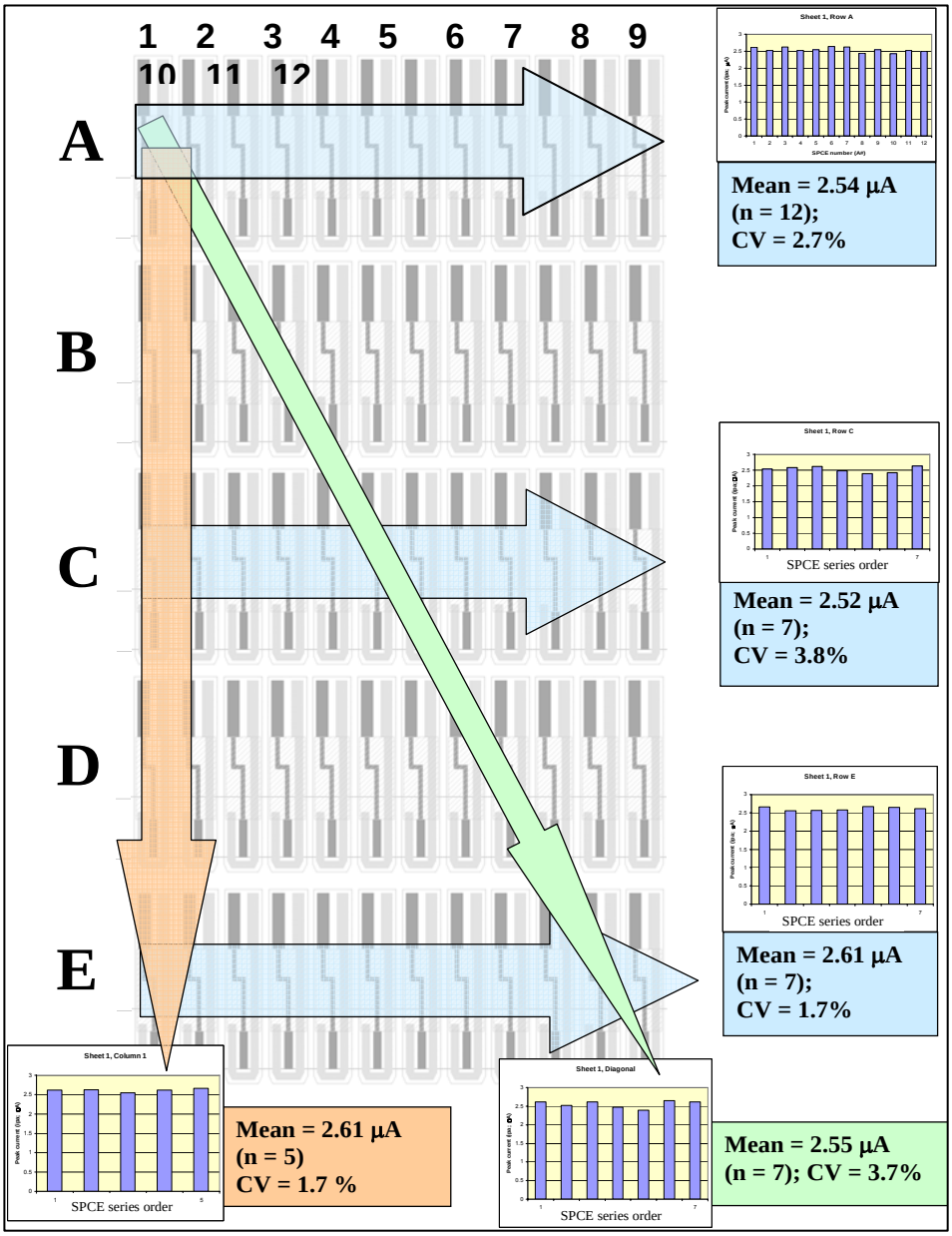

Fig. 2.3. Results of QC tests using cyclic voltammetry of ferrocyanide: i_{pa} measurements intra-sheet

Cathodic peak current (ipc) readings (not shown) gave precision values slightly higher than ipa values, at between 1.9 and 7.8% for a single sheet. As an indication of the reversibility of the electron transfer process at these electrodes, the ipc/ipa ratio was calculated for the various rows and columns on a single sheet of electrodes. Ratios of 1.0, indicating a completely reversible process, are never achieved in practice. The results obtained were consistent, at between 0.70 and 0.77, whether calculated across, down, or diagonally within a sheet. The best precision was obtained across Row A (1.9%), ranging up to 6.6% across Row E. Some variation was therefore evident as one moved down the sheet, and precision worsened from top left, to bottom right on a sheet. However, at less than 7%, these values were acceptable as levels of variation in ipc/ipa ratio.

The results obtained for ipa measurements between different printed sheets are summarised in Fig 2.4 for 3 separate sheets. Mean values for n=7 sensors taken from the same equivalent row (Row D) from different sheets ranged from 2.74 to 2.90μA. Precision ranged from 1.7% to 6.9% CV. This result indicated that some sheets showed better quality printing than others. The acceptable level of precision is 5%. Therefore, the majority of electrode sheets would fulfil this requirement at present, with a minority of sheets requiring some improvement.
Values for Epa were also obtained for electrodes from different locations within a single printed sheet of 60. Mean and precision values for replicate electrodes across, down and diagonally across a single sheet are shown in Fig 2.5.

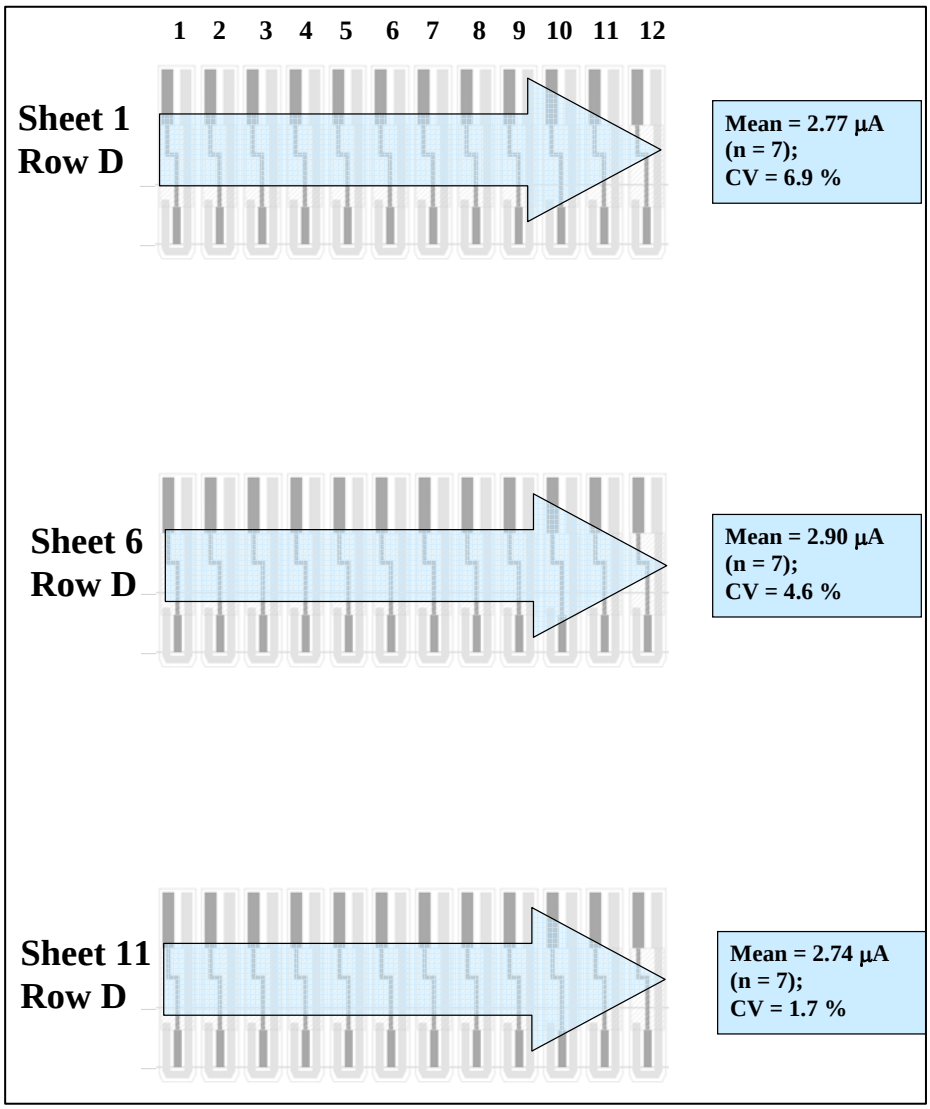

Fig. 2.4. Results of QC tests by cyclic voltammetry of ferrocyanide: ip_a measurements inter-sheet

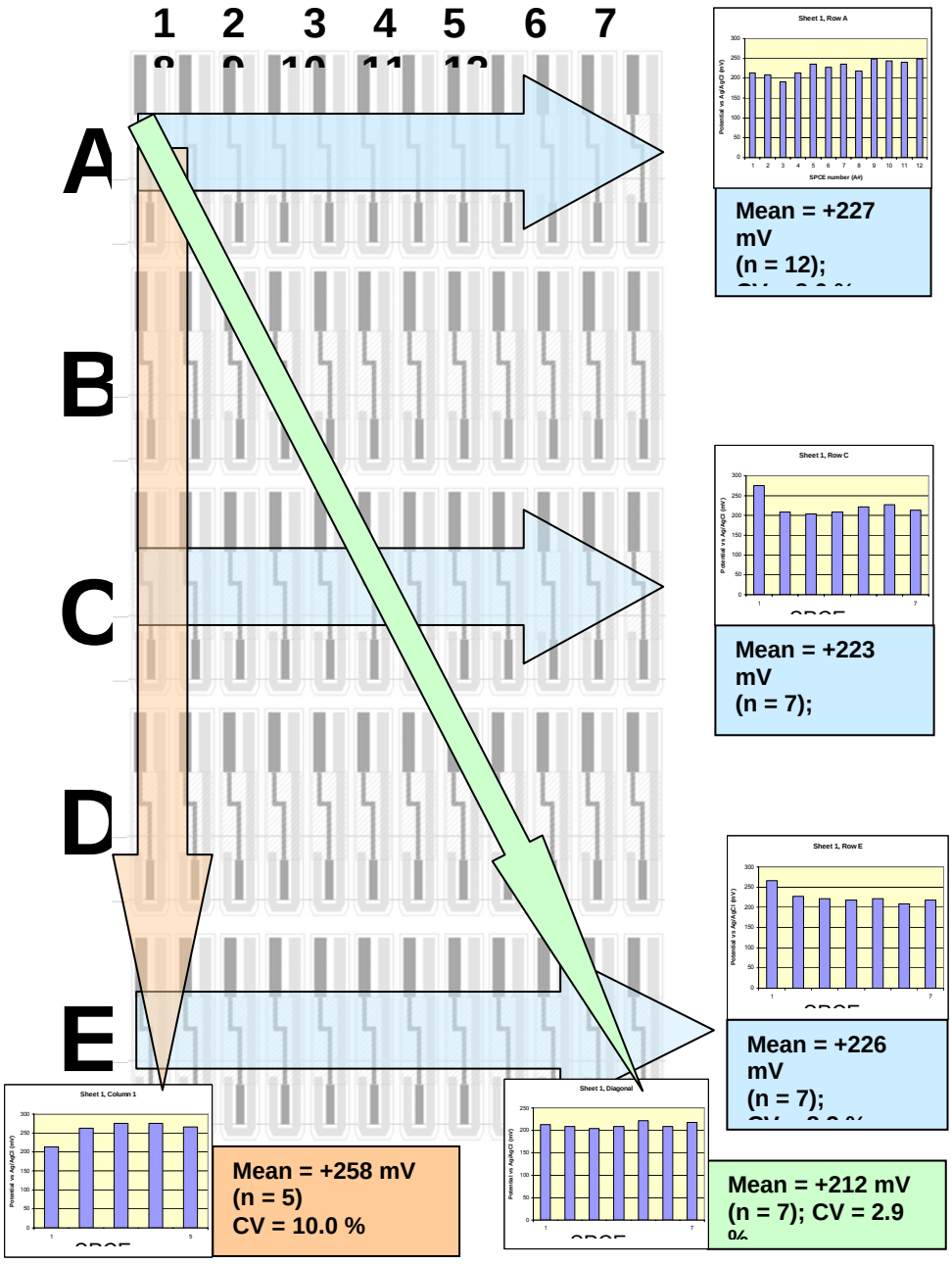

Fig. 2.5. Results of QC tests by cyclic voltammetry of ferrocyanide: E_{pa} measurements intra-sheet.

The overall mean Epa value for a single sheet was +230.8 mV, with a CV of 10.2% for the entire sheet. As shown in Fig 2.5, CV values for electrodes across or down the sheet ranged from 8.0 to 10.0%.
In order to obtain a measure of the variability in Epa between different sheets, mean and CV values were calculated for cyclic voltammetry of replicate electrodes from the same row on three different sheets of electrodes. Fig 2.6 summarises these results.

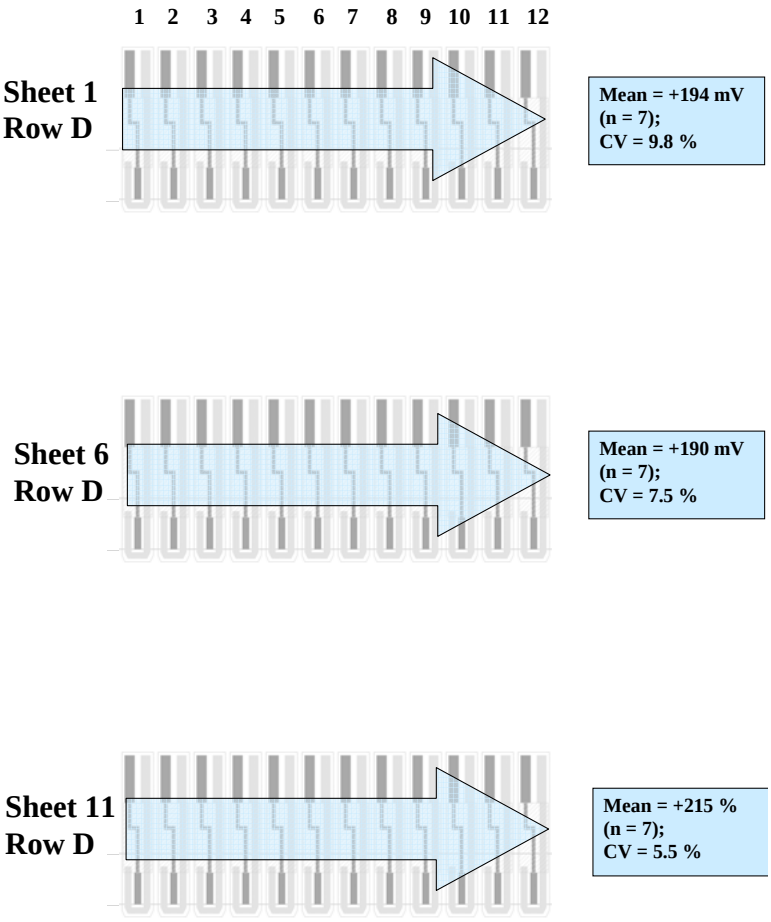

Fig. 2.6. Results of QC tests by cyclic voltammetry of ferrocyanide: E_{pa} values inter-sheet.

The inter-sheet values for Epa ranged from 5.5 to 9.8%. These compared favourably to the intra-sheet values. Overall, the Epa values showed more variability than ipa values, indicating that care should be taken in selecting the operating potential to allow for any drift in the reference electrode potential between different electrodes.

Second print-run (23/03/05)

Quality control tests were conducted as for the first print-run, using CV of potassium ferrocyanide. Measuring ipa values across each row from a card of 60 electrodes, CV values (n=6 electrodes) varied from 0.8% to 4.9%. This compared with values of 1.7 to 3.8% for the first print-run. This value was important since electrodes were to be tailored with antibody and tested in immunoassays as combs of 12 electrodes from a single row. Thus, precision values of up to 4.9% CV were evident before any additional variability due to the addition of reagents or to assay procedures.

A trend of decreasing current responses was observed for electrodes as one moved down the sheet(s). Mean ipa values for n = 6 sensors were: Row A 2855nA, Row B 2883 nA, Row C 2719 nA, Row D 2682 nA and Row E 2673 nA. Taking ipa values for a single column of electrodes, a value of 12.6% CV was obtained. If ipa values were calculated diagonally across the sheet, a value of precision of CV = 11.5% was obtained. These results indicated that there was a relatively large variability between different rows of electrodes for this print-run and that this would be translated into a variation between different 12-electrode combs of >10%, even before the addition of antibody reagents/assay procedures.
The overall mean ipa value for the entire sheet was 2754 nA and the overall CV for the sheet was 5.5%. This indicated more variability in printing than in the first print-run.

Ceramic substrate

For the following reasons, electrodes were screen-printed onto ceramic substrate rather than PVC as the project progressed:
To improve the precision of screen-printing dual electrodes in rows of 12
To enable combs of 12 electrodes to be easily "snapped out" from their substrate sheet
To avoid stretching/bending of the comb during handling/installation/use within the automated instrument. The polyester combs were prone to distortion which would add to variability and would not allow guaranteed meshing of electrodes with microwells during automated operation.

First print-run (23/03/06)

Dual electrodes were printed to the same design as that shown in Fig 2.1A, but onto 0.5 mm thick ceramic substrate, by colleagues at Gwent Electronic Materials. Thirty-six individual electrodes were printed onto each single sheet, in three rows of 12 electrodes each. It was possible to snap out each "comb" of 12 electrodes from the sheet by supporting the sheet along a straight-edge and gently applying pressure to the appropriate row of electrodes. In some cases difficulty was experienced due to printing ink having partially covered the laser-etched serrations; this was a problem of screen registration which was reported back to GEM and fed into improved printing of the second batch of ceramic electrodes. The formulation for the dielectric layer was the same as that used successfully for printing onto polyester. It was evident that this formulation was less than optimal for printing onto ceramic, since there was clear evidence of holes in the dielectric layer. This information was relayed back to colleagues at GEM for action to improve the dielectric printing in future print-runs.

Quality control tests using cyclic voltammetry of potassium ferrocyanide were performed on several combs of 12 electrodes as described for the polyester-based electrodes. A mean CV of 6.4% was obtained for 12 replicate electrodes. Cyclic voltammetry was also performed using a 10^{-3}M solution of 1-naphthol in 0.1M Tris-HCl buffer, pH 10, this being the final product which the electrodes would be detecting as biosensors in the mycotoxin assay procedure. CVs of 20.5% and 2.5% were obtained for separate combs (see Fig 2.7), indicating that excellent reproducibility could be achieved, but that a large degree of variability could also be seen.

Comb 1

Sensor	ip (μA)	Ep (mV)
1	18.61	190
2	24.00	190
3	18.66	190
4	15.88	190
5	15.18	180
6	15.14	180
7	14.88	180
8	15.24	180
9	16.02	190
10	9.52	170
11	15.92	180
12	16.32	190
Mean	16.28	184.17
SD	3.334384	6.685579
CV (%)	20.48043	3.630179

Comb 2

Sensor	ip (μA)	Ep (mV)
1	16.22	180
2	15.97	190
3	15.81	180
4	15.39	180
5	15.62	180
6	15.42	180
7	15.38	180
8	14.92	180
9	15.04	180
10	15.47	180
11	15.18	180
Mean	15.49	180.91
SD	0.391589	3.015113
CV (%)	2.527566	1.666646

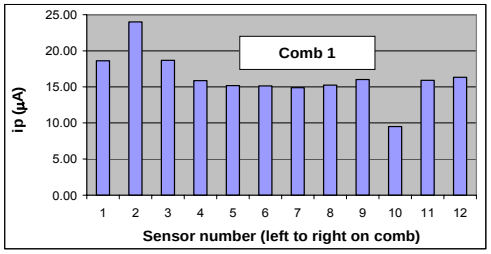

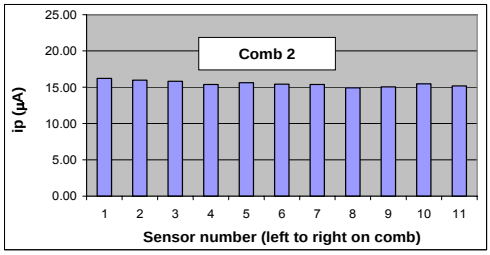

Fig. 2.7. Peak current responses for electrodes (combs of 12) printed on ceramic substrate and tested by cyclic voltammetry in 10^{-3}M 1-naphthol solution.

Representative combs of electrodes were also tested using the same solutions, but by chronoamperometry rather than cyclic voltammetry, at an applied potential of +0.5V vs Ag/AgCl. Data were captured over 120s after the application of the potential. Results for ferrocyanide solution are shown in Fig 2.8 for t = 20, 60 and 120s. Precision did worsen with increasing time, but was excellent throughout, ranging from 2.4 to 5.6%.

		I (nA)	
SPCE	20s	60s	120s
1	696.4	488.2	407.7
2	686.4	464.5	382.8
3	688.9	448.9	365.3
4	688.9	448.9	365.3
5	665.8	433.9	337.9
6	684.5	447	360.4
7	655.9	429.6	354.7
8	672.1	440.2	362.2
9	662.1	442	357.9
10	682.1	443.3	357.2
11	645.3	422.7	332.3
mean	675.3	446.3	362.2
SD	16.2	17.8	20.3
CV (%)	2.4	4.0	5.6

Fig. 2.8. Current responses and precision values for a comb of 12 (ceramic) electrodes after chronoamperometry in 5 x 10^{-4}M K^+ ferrocyanide solution in phosphate buffer, pH 7.0.

When combs of electrodes from the same run were tested by chronoamperometry in 1-naphthol solution (Fig 2.9), CV values were larger than those obtained for ferrocyanide solution at equivalent sampling times and increased greatly with increasing sampling time. However, at shorter sampling times, t=5s and t= 10s, lower precision values of less than 4% were obtained (Fig 2.9). This result indicated that the reproducibility of the electrodes was acceptable for the measurement of 1-naphthol over short sampling times. The increase in variability of the electrode response was likely to be due to changes in electrode surface area due to polymerisation of 1-naphthol which is known to occur as a result of electrooxidation.

			i (nA)		
SPCE	5s	10s	20s	60s	120s
1	5282	2973	744.9	260.7	198.6
2	5171	2911	726.2	254.5	192.4
3	4910	2731	533.8	124.1	0
4	5127	2868	707.6	254.5	198.6
5	4916	2706	527.6	124.1	0
6	5090	2781	701.4	248.3	192.4
7	4773	2626	521.4	117.9	0
8	5053	2824	713.8	254.5	192.4
9	4823	2632	552.4	130.4	0
10	5090	2750	664.2	248.3	180
11	4935	2799	564.9	124.1	0
12	5078	2886	720	248.3	192.4
mean	5021	2791	639.9	199.1	112.2
SD	149.9	108.2	90.7	66.4	99.2
CV (%)	3.0	3.9	14.2	33.3	88.4

Fig. 2.9. Current responses and precision values for a comb of 12 ceramic electrodes after chronoamperometry in 10^{-3}M 1-naphthol solution in Tris buffer, pH 10.

Second print-run (20/06/06)

Compared to the first print-run of ceramic electrodes, this batch displayed improved registration of the three printed layers (working, reference, dielectric), with respect to the laser-etched snapping-out lines on the ceramic substrate. Consequently, the combs of 12 electrodes were more easily separated, with less risk of damaging any of the electrodes. A modification to the dielectric layer also appeared to have improved the printing of this layer, resulting in fewer holes, although some were still evident. Three combs from this batch were tested by cyclic voltammetry in ferrocyanide as before. The resulting precision values were 1.8, 3.1 and 4.0%, indicating an improvement in printing compared to the first print-run. Chronoamperometry of a 10^{-3}M solution of 1-naphthol produced a CV value of 6.8% at 5s, rising to a maximum of 14% at 14s, decreasing to 6.4% and 6.9% at 30 and 100s respectively. This result indicated a more consistent effect of 1-naphthol oxidation on surface area from electrode to electrode than that seen for the first print run on the ceramic substrate.

Instrumentation

Comparison of Autolab and Uniscan instrument performance
Initial QC tests (cyclic voltammetry and chronoamperometry) on electrodes printed onto polyester substrate were conducted using an μAutolab Pstat II potentiostat. Since the final instrument for conducting the mycotoxin immunoassays for this project was to be based on the PG580 potentiostat from Uniscan, it was important to compare the two instruments for their performance in cyclic voltammetric tests. Both instruments were used to test a comb of 12 electrodes (on polyester) by cyclic voltammetry in potassium ferrocyanide solution. Results are summarised in Fig 2.10.

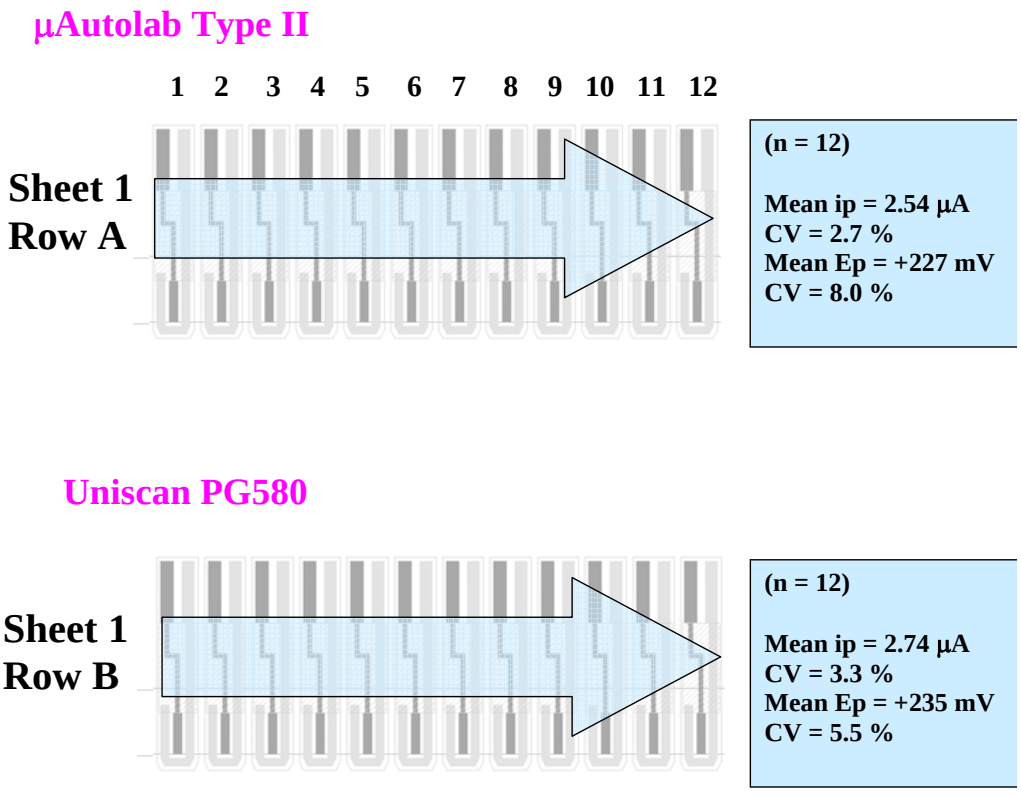

Fig. 2.10. Results of QC test by cyclic voltammetry of 5 x 10^{-4}M K^+ ferrocyanide conducted using either Autolab or Uniscan potentiostat.

The Uniscan PG580 performed well for cyclic voltammetry using the new SPCEs and gave comparable results to the Autolab instrument in terms of ipa value and precision (both instruments less than 3.5%). Epa values were also similar for the two instruments. The combination of Uniscan PG580 and SPCEs gave satisfactory performance characteristics for analysis using cyclic voltammetry, leading to the conclusion that the Uniscan instrument should be used for future experiments. Consequently, QC tests on the second print run of polyester substrate electrodes and those on the ceramic electrodes were conducted using the PG580 instrument.

Automated 96-well assay stage and 12-channel potentiostat

(See documents from Uniscan for instrument specification)
Photographs of the instrument are shown in Fig 2.12.

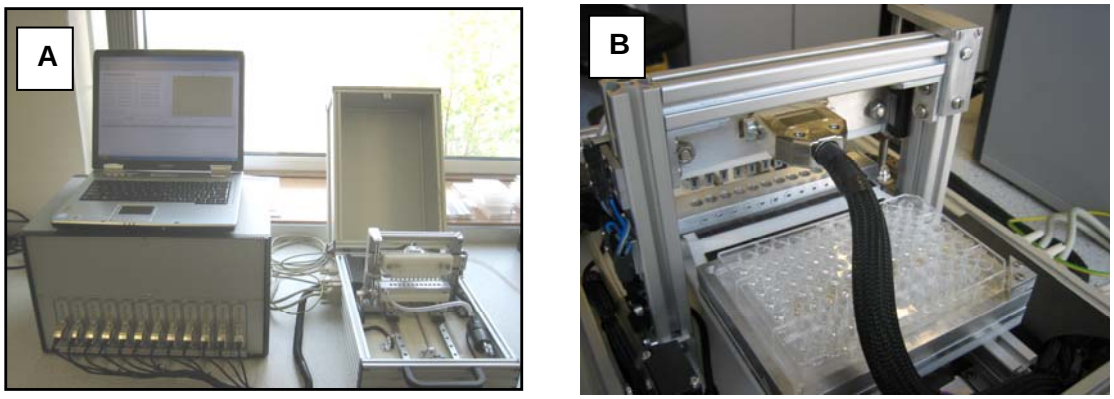

Fig. 2.12. Photographs showing (A) Uniscan automated 96-well assay stage and 12-channel potentiostat (B) Close-up of sensor gantry, wash station and 96-well plate.

The automated instrument was computer-controlled (see Uniscan spec) and its operation was programmable via a configuration menu. It was set up so that each row of 12 wells on a 96 well plate could be programmed individually, according to the following eight parameters:
1) Well (ie.Row) number
2) PreDelay (ie. time sensors are in wells)
3) Agitate (0 or 1 if sensors required to agitate during time in wells)
4) Well time (secs, ie. time operating potential is applied to sensors for)
5) Wash time (secs, if wash cycle required before moving sensors onto next row)
6) Sample rate (ie. rate of data capture during chronoamperometry, in Hz)
7) Current range (exponent, eg. -4 for 10-4Amps = 100 μA)
8) Temperature setpoint (temperature of plate platform below 96-well plate, in degrees C)

An operating procedure for setup and operation of the automated instrument is given in Appendix 1

A typical layout for the ochratoxin assay is given as an example Fig 2.13. Refer to sections on appropriate immunoassays for full description of reagents for each assay.

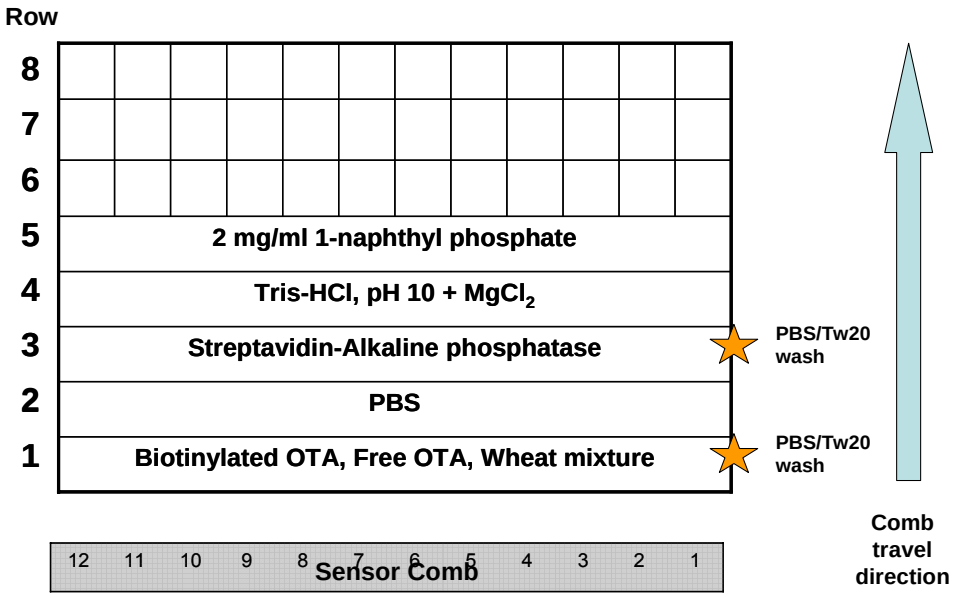

Fig. 2.13. Typical 96-well plate setup, indicating wash steps and direction of travel of sensor comb, for computer-controlled automated immunoassay using Uniscan 12-channel potentiostat/automated stage.

The configuration settings for operation of the assay based on this plate configuration, using five rows for the full assay, are given in Table 2.1.

	Row				
	1	2	3	4	5
PreDelay (s)	1200	80	1200	80	300
Agitation (0 or 1)	1	1	1	1	0
Well time (s)	0	0	0	0	120
Wash time (s)	30	0	60	0	0
App Potential (V)	oc	oc	oc	oc	+0.5
Sample Rate (Hz)	5	5	5	5	5
Current range (e) (100μA)	-4	-4	-4	-4	-4
Temperature (°C)	25	25	25	25	25

Table 2.1: Configuration settings for Rows 1-5 in typical automated mycotoxin immunoassay

Biological reagents

Reagents for the various mycotoxin immunoassays were sourced from various supplies and tested for activity/binding with their respective antigens. Tables 2.2 – 2.4 below summarise the data for aflatoxin B, ochratoxin A and DON reagents respectively. Refer to section 5 for details of reagent use. Highlighted Rows indicate those reagents selected for the final assays.

Table 2.2. Aflatoxin B assay reagents

ANTIBODY	TYPE	SOURCE	TESTED	OUTCOME
Mouse Monoclonal Clone AT-B1	Mouse ascites (IgG1)	Sigma	Via rabbit IgG in ELISA (96 well)	V. poor specific binding
Rabbit Polyclonal	Serum Ig fraction	Sigma	ELISA (96 well) & Electrochemical biosensor	Good specific binding
Rat Polyclonal	Cell supernatant	Tepnel	Not tested	Not tested

ENZYME CONJUGATE	TYPE	SOURCE	TESTED	OUTCOME
Streptavidin-alkaline phosphatase	lyophilised	Sigma	With Tepnel B1-biotin antigen conjugate	Good

LABELED ANTIGEN	TYPE	SOURCE	TESTED	OUTCOME
Aflatoxin B1-biotin (Batch 1) Aflatoxin B1-biotin (Batch 2)	Synthesised " "	Tepnel "	With mouse mAb AT-B1 and rabbit polyclonal serum	Good binding to rabbit polyclonal; poor to mouse mAb

Table 2.3: Ochratoxin A assay reagents

ANTIBODY	TYPE	SOURCE	TESTED	OUTCOME
Rabbit Polyclonal	Serum fraction	Tepnel	ELISA (96 well)	Not binding Ochratoxin A - biotin
Rabbit serum	Protein A cut	Tepnel	Electrochemical immunoassay	Tested: Good binding

ENZYME CONJUGATE	TYPE	SOURCE	TESTED	OUTCOME
Streptavidin-alkaline phosphatase	lyophilised	Sigma	With Tepnel OTA-biotin antigen conjugate	Good

LABELED ANTIGEN	TYPE	SOURCE	TESTED	OUTCOME
Ochratoxin A-biotin	Synthesised	Tepnel	With rabbit polyclonal serum fraction	Tested: Good binding (with rabbit serum)

Table2. 4: DON assay reagents

ANTIBODY	TYPE	SOURCE	TESTED	OUTCOME
Rabbit serum R177	Polyclonal	Institute of Food Research (IFR), Norwich	By ELISA	Specific binding of DON-biotin – requires mouse or goat capture antibody
Rabbit serum R178	Polyclonal	Institute of Food Research (IFR), Norwich	By ELISA	No specific binding in absence of capture antibody

ENZYME CONJUGATE	TYPE	SOURCE	TESTED	OUTCOME
Streptavidin-alkaline phosphatase	lyophilised	Sigma	With Tepnel DON-biotin antigen conjugate	Good

LABELED ANTIGEN	TYPE	SOURCE	TESTED	OUTCOME
DON-biotin	Synthesised	Tepnel	With rabbit sera R177 and R178	Specific binding

Electroactivity of Grain Extracts

Before embarking on testing wheat or other extracts for the presence mycotoxins, it was important to determine whether the extracts themselves contained any electrochemical interferences which might affect the performance of the electrochemical immunoassays. Wheat and chilli extracts were supplied by N.B (CCFRA). Suspensions were prepared from these as follows:

- Pellets were supplied following extraction from 5 g of grain or chilli.
- Pellets were resuspended in 1ml methanol, then diluted 1/10 in appropriate buffer (PBS or Tris).
- Extracts from 5 g were therefore reconstituted into a final volume of 10ml.
- Tested by linear sweep voltammetry on bare SPCES for electrochemical interferences.

Direct voltammetry in wheat or chilli suspension at pH10.

The electrochemical activity of extracts was determined by direct voltammetry of extract-containing solutions at bare electrodes, as follows:
(Wheat or chilli was at 5 g in 10 ml 10% methanol/Tris-HCl, pH 10/ 10 mM $MgCl_2$).
300 μl of this preparation was added to a microtitre well.
A bare SPCE was incubated in the solution for 5 min at open circuit voltage (o.c.v.)
Measurement was by linear sweep voltammetry from -0.1 V to +1.0 V (100 mV/s).
Resulting voltammograms are shown in Fig 2.14.

The wheat extracts showed a small peak of electrochemical activity at +0.4 V and a shoulder at +0.65 V. The chilli extract showed a large peak at +0.23 V and a shoulder at +0.65 V.

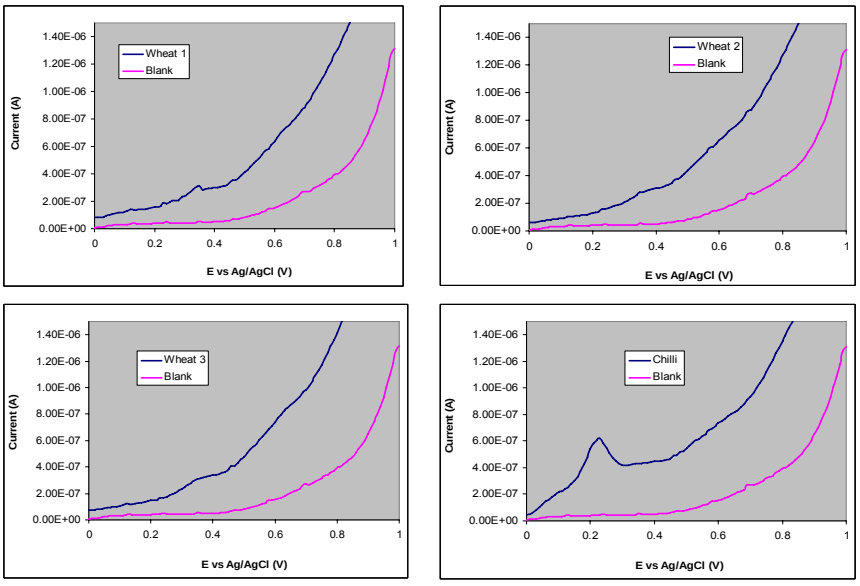

Fig. 2.14. Voltammograms of three different wheat and one chilli extracts.

Ability to remove interferent species by washing.

During the mycotoxin immunoassay(s), there would be one or more washing steps using buffer +/- detergent (Tween 20). It was therefore of interest to see whether the interfering species identified in wheat/chilli would be removed by washing, or whether they would adsorb and be firmly bound to the surface of the SPCEs.

In the first experiment, SPCEs were exposed in a pH 7.0 buffer solution containing wheat or chilli extracts, for 30 minutes (thus simulating the immunoassay competition step). The SPCEs were then washed with PBS alone (no detergent) and subjected to LSV in pH 10 buffer. The resulting voltammograms are shown in Fig 2.15.

After 30 min incubation, then a PBS wash, SPCEs exposed to wheat extract still gave peaks at +0.4 V and +0.7 V, whereas Chilli gives smaller peak at +0.65 V. Thus, the chilli interferent washed off more readily than wheat interferent(s), suggesting that wheat interferent(s) are more readily/more firmly adsorbed onto the SPCEs than chilli interferents.

In the second experiment, the same procedure was adopted, but the washing step included 0.1% Tween 20 (in PBS). Voltammograms are shown in Fig 2.16. In this case, SPCEs exposed to wheat still showed peaks at +0.4 V and +0.7 V. Those exposed to chilli now gave negligible current increases compared to the blanks (sensors incubated in buffer alone).

The conclusion from these experiments was therefore that the chilli interferent, although present at relatively high concentration, does not appear to absorb onto the SPCEs and washes off more readily than wheat interferent(s). In contrast, the wheat interferent(s) are more firmly absorbed than Chilli interferents. In spite of its presence, however, the relatively high oxidation potential of the wheat interferents (+0.4 and 0.7 V) relative to that known for 1-naphthol (the product of the immunoassay; Ep = +0.17 V) means that the species found in wheat will probably not affect the immunoassay, since the peak responses will be separated sufficiently to allow resolution for analytical purposes.

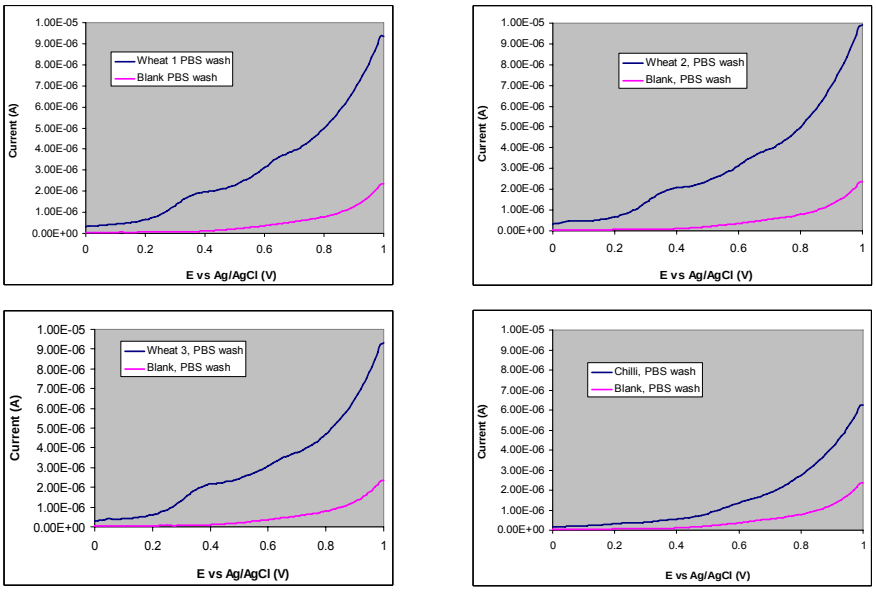

Fig. 2.15. Voltammograms obtained for SPCEs after incubation in wheat or chilli extract, followed by washing in PBS.

Immunosensors and immunoassays

The following section describes the results of experiments carried out to develop and optimise electrochemical immunoassays for aflatoxins, ochratoxin A and deoxynivalenol (DON).

The assays were based on an indirect competition assay using an immobilised capture antibody: competition between free antigen and biotin-labelled antigen was followed by the addition of streptavidin-labeled enzyme (alkaline phosphatase), then addition of substrate solution (1-naphthyl phosphate for the electrochemical assay). The formation of the product 1-naphthol, was then detected electrochemically. A schematic representation of the assay format is shown in Fig 2. 17; in this case the mycotoxin shown is aflatoxin B1 (AFB1).

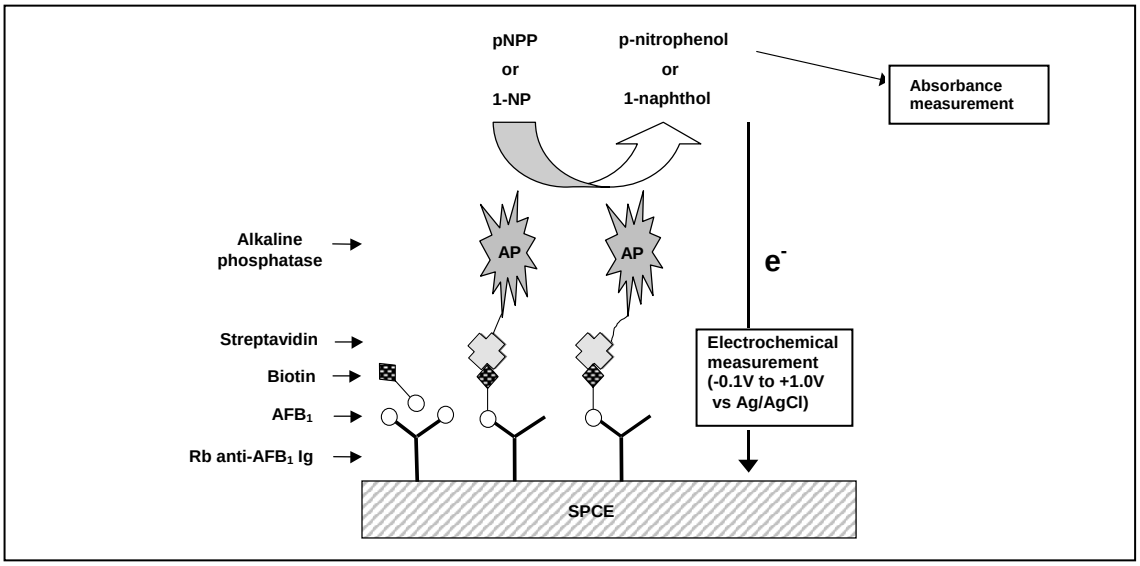

Fig. 2.17. Schematic diagram of mycotoxin immunoassay

Aflatoxins

Testing AFB1 immunoassay reagents by ELISA

Enzyme-linked immunosorbent assay (ELISA) on 96-well plates was used to test the aflatoxin reagents for binding. The first antibody to be tested was the anti-aflatoxin B1 mouse monoclonal antibody, AT-B1 (as ascites fluid) from Sigma. This was used in conjunction with a rabbit IgG anti-mouse capture antibody; this approach has been used previously by ourselves and others and serves to orientate the monoclonal antibody to maximise binding of its antigen. The procedure was as follows:
Medium-protein-binding 96-well ELISA plates (Greiner Labortecknik Ltd., Glos., UK) were coated overnight at 4^0C with 50 μl of anti-AFB1 serum diluted 1/100 in PBS. After rinsing with PBS, wells were blocked with 200 μl of the appropriate blocker in PBS overnight at 4^oC. Wells were rinsed with PBS, then 100 μl of appropriate AFB1 dilutions in 10% methanol/PBS were added per well and plates were shaken at room temperature (RT) for 30 min. Fifty microlitres of AFB1-biotin conjugate diluted 1/600000 in PBS were then added and incubated with shaking for a further 30 min at RT. Wells were washed 4X with PBS/T, then 2X with PBS, before addition of 50 μl streptavidin-AP (1/500 in PBS) per well for 30 min at RT with shaking. After a final series of washing (5X PBS/T, 2X Tris-HCl, pH 9.9), 145 μl of pNPP substrate solution were added per well and plates were incubated for 90 min at RT. The resulting colour development was measured by absorbance at 405 nm using an Anthos plate reader. Absorbance values were used to calculate the percentage of potential antibody binding sites for free AFB1 remaining occupied by biotinylated AFB1; this percentage binding value was plotted against free AFB1 concentration. The percentage value (of A/A0) was derived from: (A - Asat)/(A0 - Asat) x 100 , where Asat = absorbance value when fully saturated by free antigen and A0 = absorbance value in absence of free antigen.

An antibody loading study in which the mAb was titrated with various fixed loadings of rIgG resulted in reasonable titration curves (Fig 2.18A). However, the absorbance values were at a maximum of 0.180, with a background signal of 0.140. It was evident that although absorbance increased with increasing rIgG loading between 14 and 56 μg/ml, at the lowest rIgG loading (7 μg/ml) the absorbance values were at their highest. This phenomenon, and the relatively high background signal, indicated that there was some non-specific binding of the streptavidin-alkaline phosphatase (SA-ALP) conjugate. Fig 2.18B shows the normalised responses after subtraction of values obtained for assays performed in the absence of the biotinylated AFB1. This serves to emphasise the low absorbance maximum of 0.04 units.

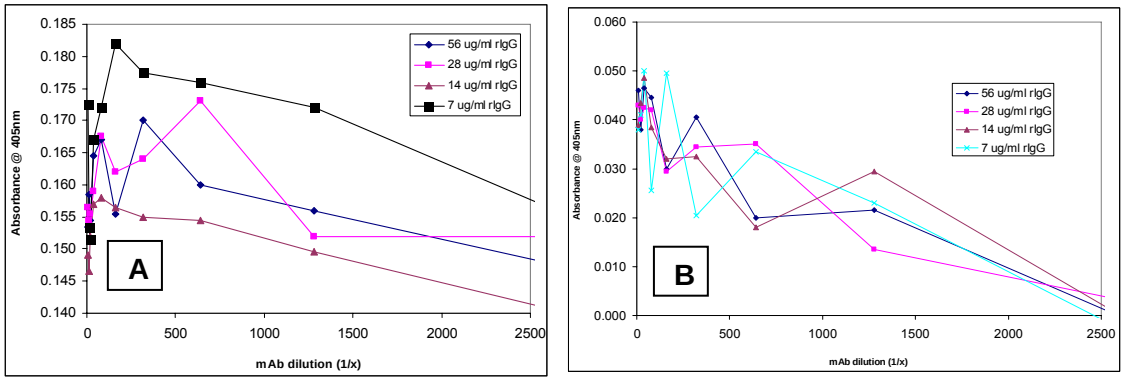

Fig. 2.18. ELISA assay for aflatoxin B1: titration of mAb AF-B1 with varying rIgG loadings; no blocker. Assay results obtained (A) in presence or (B) after subtraction of values in absence of biotinylated aflatoxin B1.

The effect of introducing a blocking step was next investigated by adding a solution of 1% polyvinyl alcohol (PVA) after the rIgG step. The resulting titrations are shown in Fig 2.19.

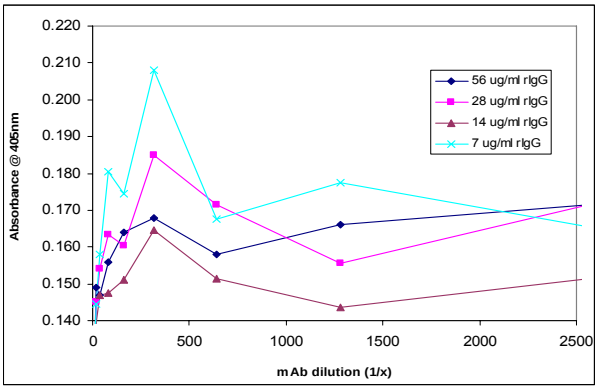

Fig. 2.19. AFB1 ELISA results using PVA blocking step.

There was no improvement in the absorbance signal, or reduction in the background response when using the blocking step. Further experiments in the absence of the rIgG capture layer, using the mAb alone, failed to show any enhancement of specific binding; in fact, as the mAb was diluted, the absorbance signal increase, confirming that SA-ALP was binding non-specifically to the microwells. The best specific signal from the above tests was obtained using a loading of 7 μg/ml rIgG with a dilution of 1/160 of the mAb. Using these conditions, a titration of free aflatoxin B1 was attempted by ELISA. However, the resulting calibration plot was not useable (Fig 2.20).

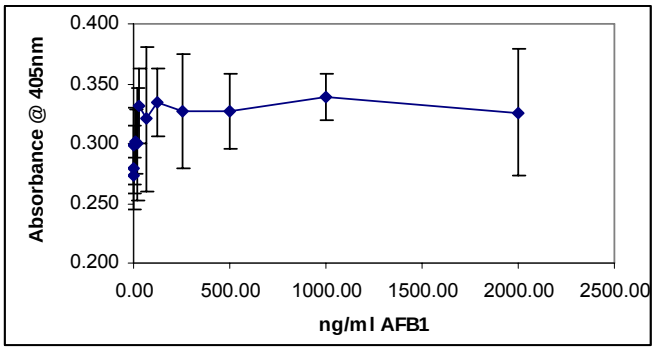

Fig. 2.20. ELISA for AFB1 using mAb AF-B1 with rIgG capture antibody.

An alternative anti-AFB1 antibody was therefore tested. This was the IgG fraction of rabbit anti-aflatoxin B1 serum from Sigma-Aldrich. This polyclonal reagent was tested alone (ie. in the absence of a capture antibody) since this approach is commonly used in commercial ELISA systems. In this assay, a blocking step was included using a 3% BSA solution in PBS.

The initial titration of the antibody with fixed concentrations of biotinylated AFB1 and SA-ALP resulted in a good titration plot (see Fig 2.21), indicating that the antibody was binding the biotinylated reagent specifically. A dilution of 1/100 of the antibody was selected for further study.

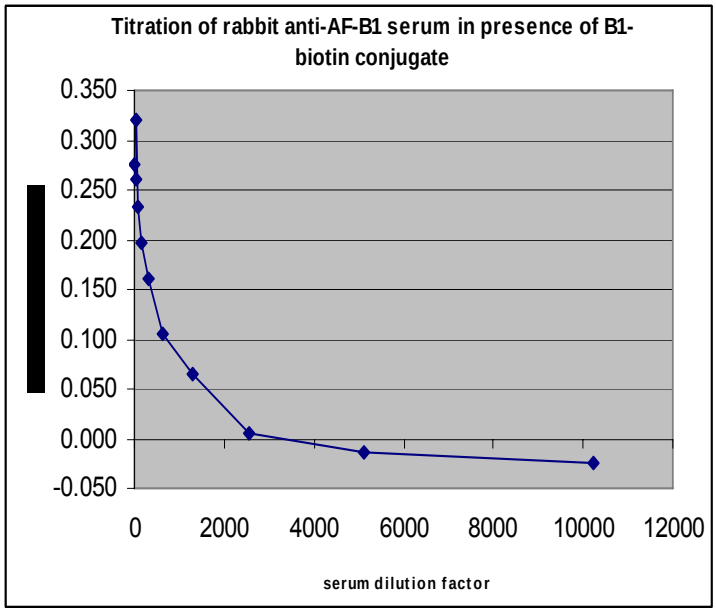

Fig. 2.21. Titration of polyclonal anti-AFB1 rabbit serum (IgG fraction) by ELISA using fixed concentrations of biotinylated AFB1 and SA-ALP.

Using the optimum dilution of capture antibody, in combination with fixed concentrations of biotinylated AFB1 (1/600000 as recommended by the suppliers, Tepnel Biosystems) and SA-ALP (1/500), a calibration plot of free AFB1 was performed by ELISA. Fig 2.22 shows the result and demonstrates that a very sensitive calibration plot was obtained in the concentration range between 0.08 and 0.6 ng/ml, using these semi-optimised conditions. The ELISA in 96-well plates showed a background absorbance of around 0.1 units.

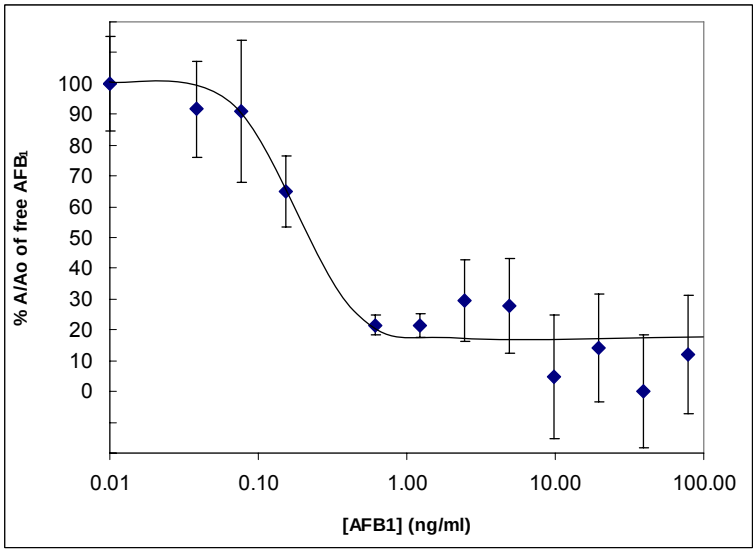

Fig. 2.22. Calibration plot for AFB1 by ELISA using rabbit anti-aflatoxin serum as capture antibody

Effect of blocking agents: SPCEs versus ELISA plates

In order to select a blocking agent suitable for use in an AFB1 immunoassay on SPCEs, experiments were undertaken to investigate the non-specific binding of immunoassay reagents on ELISA plates and on SPCEs. At this stage, SPCEs were printed on polyester substrate. Uncoated ELISA plates or SPCEs were used for the following experiments: Several different blocking agents were tested using various steps of either the ELISA protocol (see above) or using the same reagent concentrations in the colorimetric immunoassay on SPCEs. The protocol for the SPCEs was as follows: the surface of the working electrode was coated, by passive adsorption, with a solution of anti-AFB1 serum diluted in PBS. This solution was applied either manually using a 1-10 μl micropipette (Barky Instruments International, Folkestone, UK) or automatically, using the BioDot instrument, to SPCEs which had been pre-cut into combs of 12 sensors. After overnight incubation in a moist box at 4^{o}C, SPCEs were rinsed with PBS, then placed into microwells containing 345 μl of blocking solution (PBS containing appropriate blocking agent) and incubated overnight at 4^{o}C. SPCEs were rinsed with PBS, and then placed into microwells containing 200 μl of AFB1 standard solutions in 10% methanol/PBS for 30 min at RT with shaking. One hundred microlitres of biotinylated AFB1 in PBS were then added to each well and incubation continued for a further 30 min, shaking at RT. SPCEs were washed X4 with PBS/T, 2X with PBS, then placed into microwells containing 250 μl of streptavidin-AP diluted in PBS. After incubation for 30 min, shaking at RT, the SPCE strips were finally washed X5 in PBS/T, X2 in 0.1M Tris-HCl buffer, pH 10, then placed into microwells for exposure to substrate solution. For each blocker, the ELISA or the immunoassay were performed for replicate wells or sensors in the absence of free AFB1.

Fig 2.23a shows the effect of various blocking agents on bare ELISA plates following addition of 1/500 streptavidin-AP and indicates that the most efficient blockers are BSA, casein, casein hydrolysate, Marvel and gelatine (200 Bloom), all of which performed equally well and were capable of reducing the non-specific binding by up to 92%. In order to examine the effect of blockers on SPCEs, the same blockers were first tested using polyester strips without any screen-printed electrodes on their surface.

This test would give an indication of the ability of blockers to prevent non-specific binding of the streptavidin-AP reagent to the SPCE backing (ie. the reverse face to the screen-printed electrodes) which would be exposed during the immunoassay when carried out in microwells. Fig 2.23b shows that there was a high level of non-specific binding in the absence of a blocker. The most efficient blocker was gelatine (75% blocking efficiency) followed by BSA, then PVA, casein and Marvel.

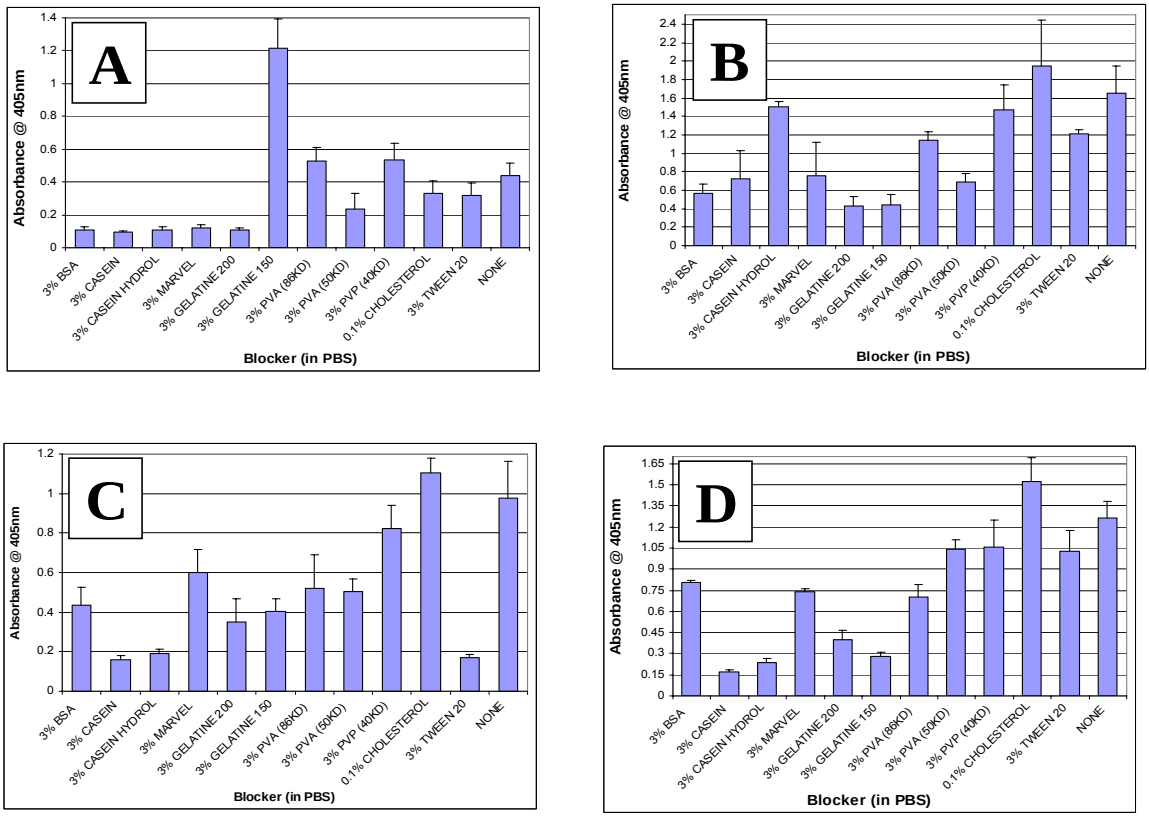

Fig. 2.23. Effect of various blocking agents on absorbance readings after incubation of (A) bare ELISA plate wells (B) polyester backing card strips (C) SPCE working/Ag/AgCl dielectric surface with streptavidin-AP, or (D) SPCE working/Ag/AgCL/dielectric surface with streptavidin-AP followed by biotinylated AFB1. Bars are mean values +SD for n=4 replicate measurements.

The colorimetric assay was then performed in a way which would examine the effect of blockers on the non-specific binding of streptavidin-AP to the working surface only of the sensors. Bare SPCEs were blocked as before in microwells, but the subsequent incubation step was performed by adding reagent (streptavidin-AP) in 80 μl volumes onto the surface of sensors which were laid flat, so that working electrode, Ag/AgCl electrodes, and dielectric layer, but not the reverse face, were coated. Fig 2.23c shows that, compared with the binding in the absence of blocker, casein was the most efficient agent (85% blocking efficiency), and followed closely by Tween 20 and casein hydrolysate. All of the other agents gave poor blocking efficiency (< 65%). This experiment was repeated, this time exposing the working surface of the sensors to both the 1/600000 biotinylated AFB1 and 1/500 streptavidin-AP steps of the assay. Again, casein was the most efficient blocking agent (86% efficient) (Fig 2.23d).

Testing casein blocker on SPCEs

Since casein appeared to be the most promising candidate blocker for the SPCEs, it was next tested in the complete colorimetric immunoassay on SPCEs. BSA and Tween 20 were also tested in this experiment. SPCEs were coated first with 1/100 anti-AFB1 serum, and then blocked, before all the subsequent steps of the colorimetric assay were performed. The results (Fig 2.24) showed that, as was the case for the SPCE working surface (Fig 2.23 c & d), casein proved to be a more efficient blocker than BSA, or Tween 20. It was evident that the blocking efficiency for casein was less than that seen on the working surface alone (Fig 2.23d) and was more similar to that seen when the polyester card alone had been tested (Fig 2.23b). This was most likely due to the contribution of para-nitrophenol being generated from enzyme non-specifically bound to the reverse side of the SPCE which was poorly blocked by the casein. However, since in the electrochemical immunoassay, the working electrode will only be able to detect product (1-naphthol) which lies within its local diffusion layer, the presence of a (relatively) low concentration of product generated from the rear of the sensor by non-specifically adsorbed streptavidin-AP is unlikely to adversely influence/add significantly to the electrochemical response seen at the working electrode.

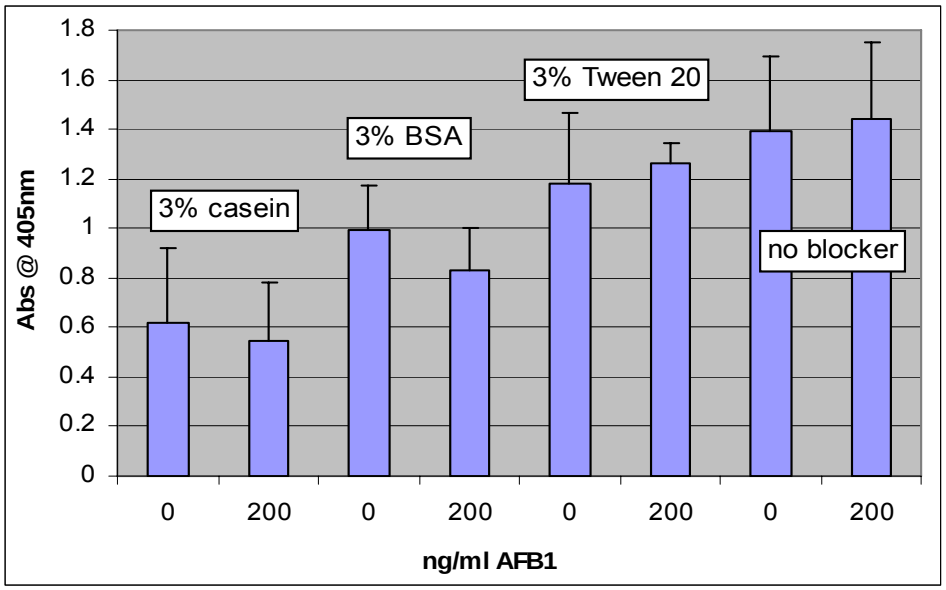

Fig. 2.24. Absorbance values obtained for colorimetric immunoassay performed on SPCE biosensors exposed to 0 or 200 ng/ml of free AFB1 and blocked previously with casein, BSA, Tween 20, or unblocked. Bars show mean + SD for N = 3 repeat measurements.

Electrochemical Immunoassay for AFB1 on SPCEs.

Effect of casein blocker on electrochemical immunoassay response
The same SPCEs which had been tested colorimetrically (Fig 2.24) were next placed into wells containing 1-NP substrate solution and subjected to the voltammetric measurement procedure, linear sweep voltammetry (LSV). Those SPCEs blocked with casein produced lower peak currents than the other groups and significantly gave the largest current difference (500 nA) between solutions without free AFB1 compared to 200 ng/ml of AFB1. This current value was nearly twice that seen for the unblocked sensors (270 nA). Although a background current of 1800 nA still existed in the presence of 200 ng/ml free AFB1, provided this was consistent, it would be possible to use this system to measure AFB1 quantitatively.

Method of antibody deposition onto SPCEs

The volume of antibody solution applied to the SPCE surface was of the order of 2μl. The optimum volume proved to be 1.8 μl, derived experimentally using the BioDot instrument; the nearest approximation achieveable by hand was 2 μl. This volume ensured coverage of the entire working area without spread over onto the dielectric surface. The antibody solution was applied either manually with a micropipette, or automatically using the BioDot dispenser. Table 5 shows the mean current responses and precision values for replicate immunosensors coated with antibody using these approaches and tested in the electrochemical immunoassay. In the case of direct deposition onto non pre-wet electrodes, the best precision achieved was 11.9% using the BioDot. However, the expected decrease in current response due to a high concentration of free AFB1 was not seen, suggesting that surface coverage with antibody was inconsistent. In contrast, when the working electrodes were pre-wet with deionised water prior to BioDot deposition, the spread of solution over the working electrode improved visibly and the precision improved to 6.6%. Further improvements will be anticipated by introduction of a humidifying chamber during antibody deposition in future experiments.

Table 2.5. Mean and CV values for current responses (n = 5) obtained from immunosensors fabricated using different methods of antibody deposition.

Deposition method	ng/ml AFB_1	Mean Peak current (nA)	CV(%)
2ul by hand, not pre-wet	0 1000	1705 1255	14.3 32.8
1.8ul, BioDot, not pre-wet	0 1000	2644 2872	15.5 11.9
1.8ul, BioDot, pre-wet	0 1000	2616 1750	14.8 6.6

Method used for preparing SPCE array combs.

A comparison was made between two different methods used for cutting polyester-based SPCEs into a 12-electrode array "comb" shape for use as sensors in 96-well microtitre plates. Combs were fashioned from the polyester substrate either using scissors, or using a PVC saw to cut out the required shape. The resulting combs were coated with antibody (1.8 ml of antibody onto the working electrode using the BioDot Instrument - see previous section) then subjected to the full immunoassay for AFB1 after competition with either none, or 1000 ng/ml of free AFB1. When using scissors, it was difficult to avoid distorting the substrate, whereas use of the PVC saw led to the production of small particles of PVC which were liable to adhere to the working electrode surface. Fig 2.25 shows that mean current responses at 0 ng/ml AFB1 were slightly lower for SPCEs prepared using scissors than those using the PVC saw, and that precision was worse (19.1% CV) when using scissors than when using the PVC saw (CV = 8% for the 1/100 antibody loading). For the 1/100 antibody loading, CVs for sensors exposed to 1000 ng/ml AFB1 were more similar for the two groups, being 20.2% (scissors) and 16.6% (PVC saw). Immunosensors coated with higher antibody loadings (1/50 and 1/25 dilutions) were also tested using the SPCEs prepared with the PVC saw. Precision values were similar for these groups, apart from the 1/25 loading with 1000ng/ml AFB1 which showed extremely good reproducibility (CV = 1.6%).

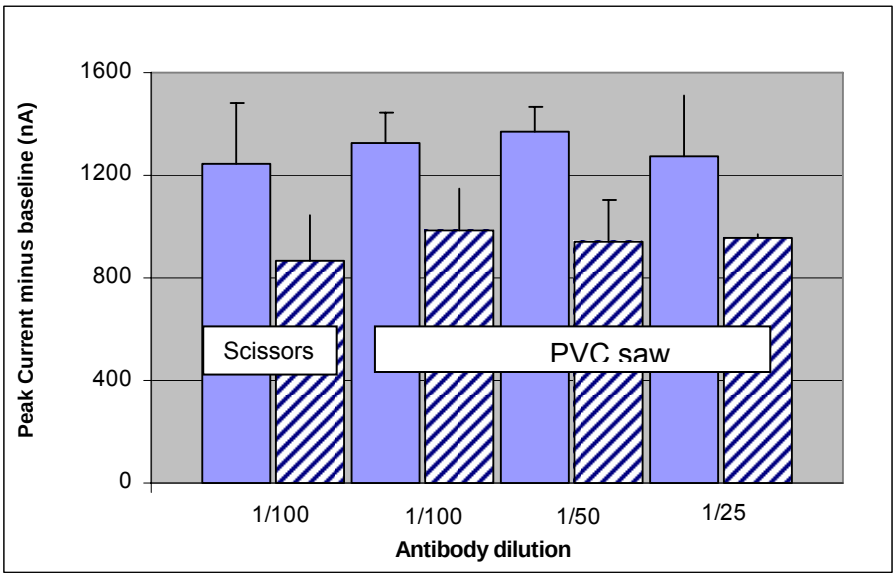

Fig. 2.25. Bar graph showing mean current responses (+SD) for n=6 SPCEs/group prepared using scissors or a PVC saw and used as immunosensors with 0 (solid bars) or 1000 (hatched bars) ng/ml AFB1.

The conclusion from this study was that there was a marginal advantage in using the PVC saw over scissors to cut out comb shapes from the polyester SPCE sheets. However, both methods resulted in precision values of around 20% which would be too high for acceptability in a final sensor device. An improved method of preparing sensor combs would therefore be required. A third method of preparing the combs was therefore investigated; in this case, the region of polyester between adjacent electrodes was outlined using a scalpel; the blank region of polyester could then be snapped out from the rest of the card. Although this approach was very time-consuming and required

extreme care, it eliminated the distortion of the polyester seen when using scissors. This approach was used for subsequent experiments on polyester SPCEs (see below).

Calibration plot for electrochemical immunoassay on SPCEs using casein blocker

A series of AFB1 standards was prepared for calibration studies over the concentration range 0.3 to 39 ng/ml. These were tested using the full electrochemical immunoassay procedure with SPCEs (polyester, prepared using a scalpel) coated with 1/100 dilution of antibody and blocked with 3% casein/PBS. The resulting voltammograms (Fig 2.26A) showed an oxidation peak for 1-naphthol at an Ep of +190 mV versus the Ag/AgCl reference electrode, which decreased with increasing concentration of free AFB1 according to the calibration plot shown in Fig 2.26B. The working range of the immunosensor was therefore between 0.15 and 2.5 ng/ml, with a detection limit of around 0.15 ng/ml (ppb). In a repeat experiment, the reproducibility (coefficient of variation) of the sensor for n = 3 measurements was 6.9%, 7.9% and 8.3% for free AFB1 concentrations of 0, 0.78 and 3.12 ng/ml respectively. Note that this precision was improved compared to sensors prepared using methods other than the scalpel - see above).

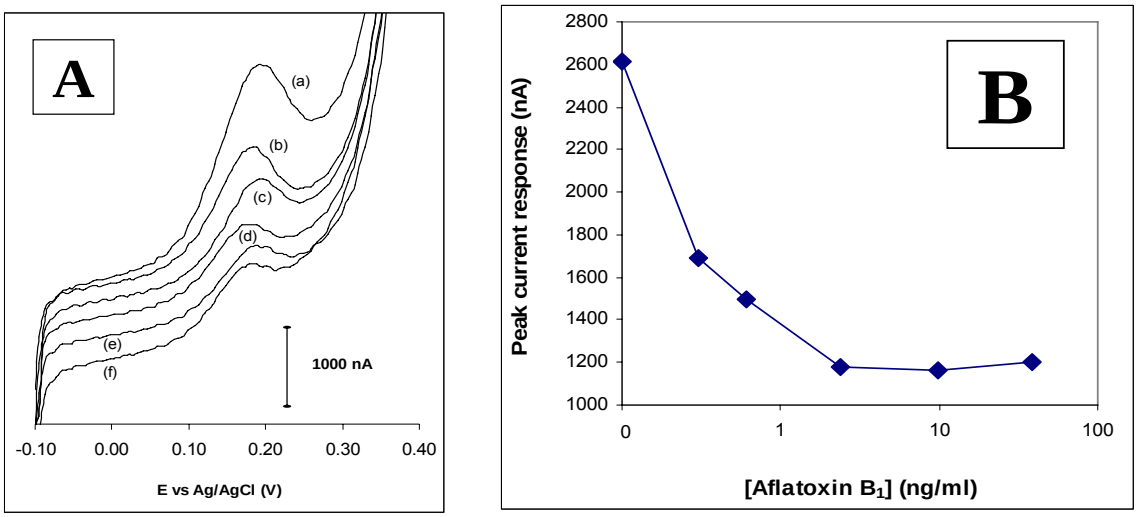

Fig. 2.26. (A) Voltammograms corresponding to (a) 0, (b) 0.3, (c) 0.6, (d) 2.4, (e) 9.7 and (f) 39 ng/ml free AFB1. (B) Calibration plot for AFB1 using electrochemical immunoassay.

Optimisation of reagent concentrations for AFB1 electroimmunoassay using casein blocker.

The above calibration plot for the electrochemical AFB1 immunoassay was performed using an antibody loading based on a colorimetric titration with a BSA blocker solution. Thus, for a final assay protocol, it would be necessary to obtain an antibody titration using an electrochemical measurement step. Also, the hitherto used concentrations of SA-ALP and biotinylated AFB1 were based on suppliers' suggested dilutions and were therefore only semi-optimised for the assay. It was therefore desirable to re-optimise each reagent in order to obtain a final assay protocol for best detection of AFB1 using the electrochemical immunoassay.

Rabbit anti-AFB1 serum

A titration of rabbit serum is shown in Fig 2.27. The dilution of biotinylated AFB1 was fixed at 1/600000, whereas the SA-ALP dilution was varied between 1/250 and 1/5000. It was necessary to use a dilution of no greater than 1/250 SA-ALP to obtain a reasonable current response. There was a clear hook effect in the presence of high antibody loading. Therefore the optimum loading from this experiment was deduced to be 1/300 (Log_2 300 = 8.23).

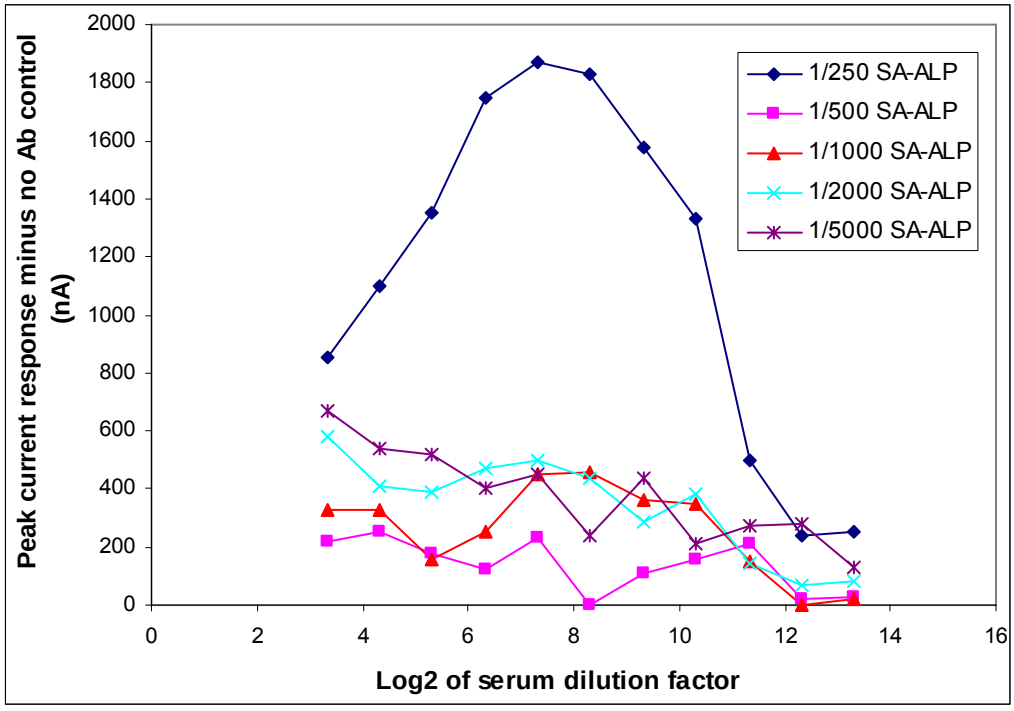

Fig. 2.27. Titration of antibody loading on SPCEs used in AFB1 electrochemical immunoassay in absence of free AFB1. Biotinylated AFB1 = 1/600000.

SA-ALP

From Fig 2.27 it was apparent that the best response was obtained for SA-ALP at a dilution of 1/250 and that the response was much reduced, even with half as much SA-ALP. Fig 2.28 shows a plot obtained from a titration of SA-ALP in the same AFB1 electrochemical immunoassay, but using sensors coated with the optimised dilution of antibody (1/300). Peak current response increased with increasing SA-ALP concentration (Fig 2.28). Working dilutions of 1/150 (Log2 150 = 7.23) and 1/500 (Log2 500 = 8.96) were selected for further investigation.

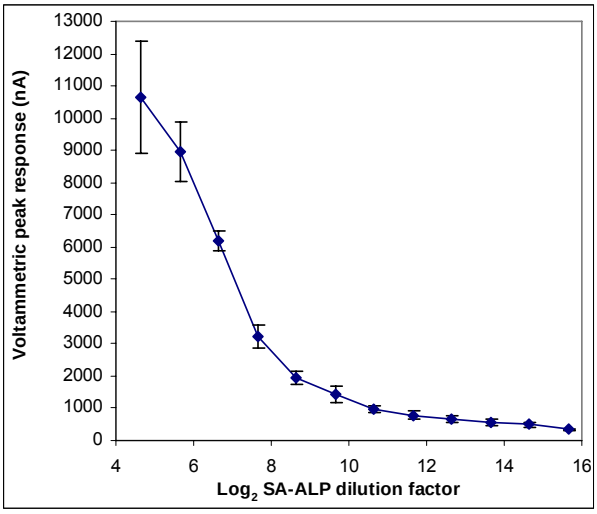

Fig. 2.28. Titration of SA-ALP in electrochemical AFB1 assay. Antibody loading = 1/300. Biotinylated AFB1 = 1/600000.
Each point represents the mean + SD for n= 3 repeat sensors.

B1-biotin.

Titration results for the B1-biotin conjugate in the presence of the selected SA-ALP dilutions are shown in Fig 2.29. Based on these plots, B1-biotin dilutions close to the top of the linear regions were selected for use in calibration studies. The selected dilutions were 1/4000,000 (with 1/150 SA-ALP) and 1/600,000 (with 1/500 SA-ALP).

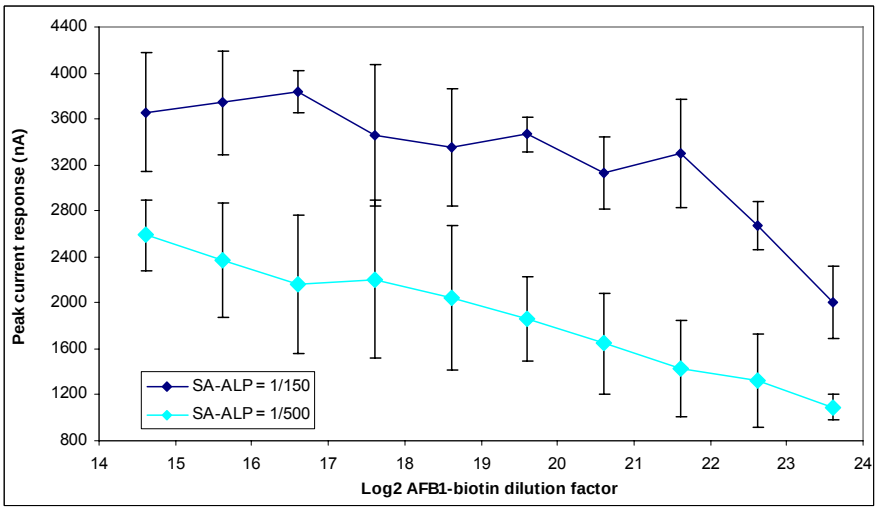

Fig. 2.29. Titration of B1-biotin conjugate with selected SA-ALP dilutions. Antibody dilution = 1/300. Each point represents the mean +SD for n=3 repeat sensors.

Calibration plot.

Calibration plots were obtained using the two sets of reagent concentrations arrived at as described above, using free AFB1 dilutions prepared in PBS/10% methanol over the concentration range 0.8 - 5000 ng/ml.

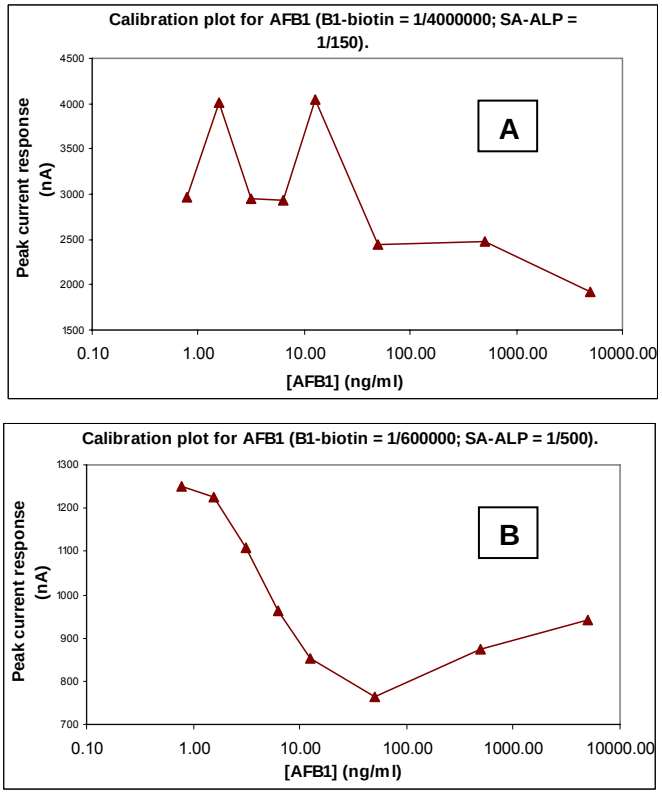

Fig. 2.30. Electrochemical immunoassay calibration plots obtained using two sets of reagent concentrations as indicated.

The calibration plots, in which each point represents the mean value from two repeat sensors, are shown in Fig 2.30. When using the first set of conditions (Fig 2.30A), a poor calibration plot was obtained which showed a tendency towards a hook effect at low AFB1 concentrations. When using the second set of conditions (Fig 2.30B), a sigmoidal plot was obtained over the concentration range of interest. At high AFB1 concentrations, an increase in current response, rather than the expected decrease, was observed. Although in practice, real grain samples would be unlikely to contain levels of AFB1 over 100 ng/ml, this anomaly would be the subject of further investigation. Representative voltammograms, together with the calibration plot over the concentration range of interest for grain analysis, are shown in Fig 2. 31. The working range for this plot was 0.8 to 50 mg/ml, with a detection limit of approximately 2 ng/ml.

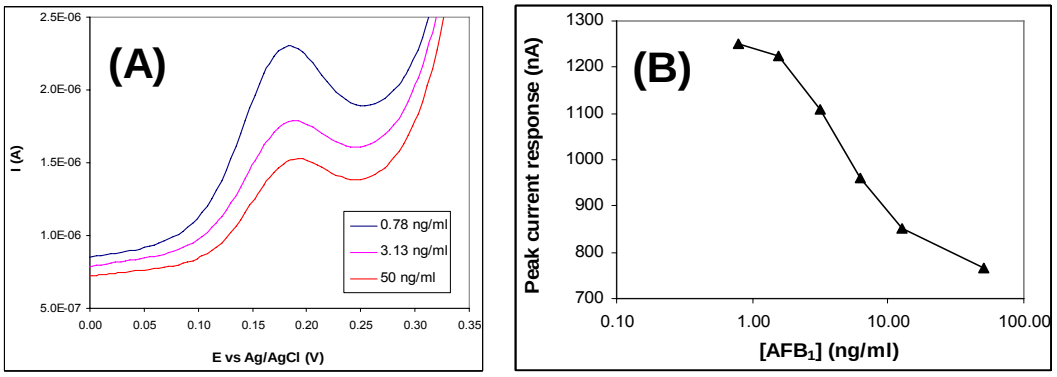

Fig. 2.31. Electrochemical immunoassay for AFB1 (A) voltammograms and (B) calibration plot for AFB1 in phosphate buffer solution.

Effect of AFB1 solvent type on electrochemical immunoassay.

Based on previous work in our laboratory, we were aware that the SPCEs could tolerate methanol at up to around 10% without deleterious effects to their electrochemical behaviour. In developing an assay for mycotoxin in grain extracts, it would be necessary to resuspend the extracted grain in a solvent, with methanol being a suitable choice (N.Byrd, CCFRA, personal communication). Hence, a 10% methanol/PBS solution had been used for all studies to this point.

The calibration plot obtained above (Fig 2.31) showed the sigmoidal shape characteristic of an immunoassay. In order for this plot to be useable in assaying real AFB1-containing samples, it would be desirable for the assay to be as robust as possible and to have a precision of less than 10% CV over the concentration range of interest. The previous investigation revealed that at high concentrations of free AFB1, there was an increase, rather than a decrease in the analytical signal. A possible explanation for this effect was that at high concentrations, AFB1 might be insoluble or form micelle-like structures and therefore fail to compete against the labelled toxin for antibody binding. It therefore seemed worthwhile to investigate some alternative solvents for their effect on the performance of the electrochemical immunoassay.

The first experiment involved testing the effect of using alternative solvents on the electrochemical immunoassay response in the absence of a competitor (free AFB1) and in the presence of a fixed concentration of competitor (50 ng/ml AFB1). Five experimental groups were elected as follows, with AFB1 being prepared in each of the following solvents at 0 and 50 ng/ml: Gp 1: PBS only, Gp2: 10% MeOH/PBS, Gp3: 1% MeOH/PBS, Gp4: 10% dimethyl sulfoxide (DMSO)/PBS and Gp5, 10% acetonitrile (CH_3CN)/PBS. The immunoassay was conducted as before, using a 3% casein/PBS blocking step. Immunosensors were therefore immersed in microwells containing these competitor solutions for 30 min, prior to the addition of AFB1-biotin solution. The experiment would therefore test the effect of the various solvents on the competitive interaction and on the antibody's ability to bind the conjugate. Current responses were recorded for n = 3 sensors for each group. The results are shown in Fig 2.32.

Fig. 2.32. Bar graph showing mean (n =3) current response +SD for five experimental groups after tests of 0 and 50 ng/ml AFB1 as competitor using various solvents for preparation.

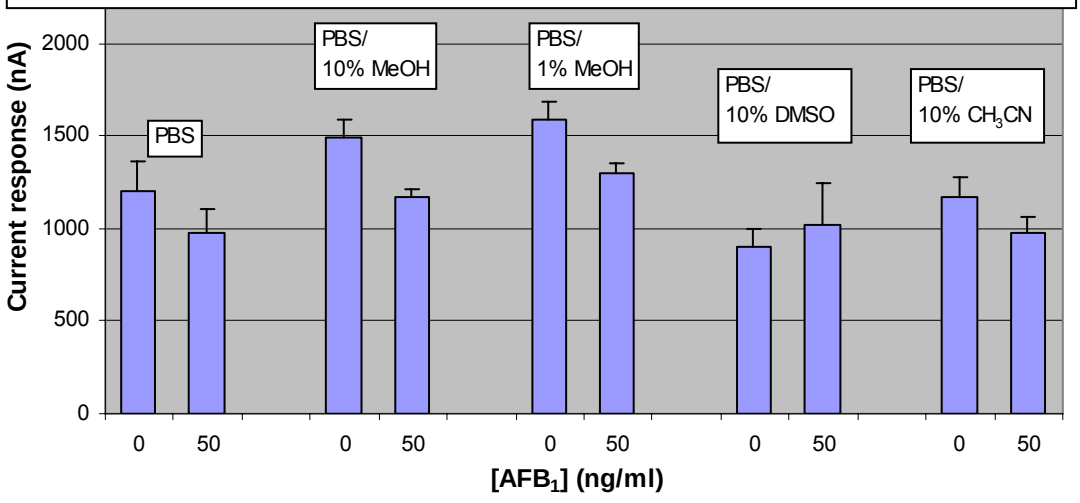

Comparison of the current responses obtained in the absence of AFB1 competitor (0ng/ml) showed that the highest currents were obtained after exposure to the solvents containing methanol, followed by the CH_3CN-containing solvent which showed no significant difference from PBS alone. The inclusion of DMSO appeared to be detrimental to the current response. In the presence of 50 ng/ml of competitor, the control (PBS only) showed a reduction of only 200 nA compared to the blank. The best reduction was obtained for the 10% MeOH/PBS solvent (at 300 nA), followed by 1% MeOH/PBS and then 10% CH_3CN/PBS. The presence of DMSO appeared to perturb the assay and did not show competition. The conclusion from this experiment was that the 10% MeOH/PBS solution appeared to be the preferred combination solvent for the assay.

The second experiment involved performing a calibration plot for AFB1 over the concentration range 0 to 625 ng/ml using as diluents for free AFB1, the solvent groups: (1) PBS alone, (2) 10% MeOH/PBS and (3) 10% CH_3CN/PBS. The results are shown in Figs 2.33 - 2.35. In each case, an increased current response was observed at high concentrations of free AFB1. This effect was most pronounced for the CH_3CN/PBS diluent (Fig 2.32), but still occurred for the other two solvents at concentrations greater than 100 ng/ml.

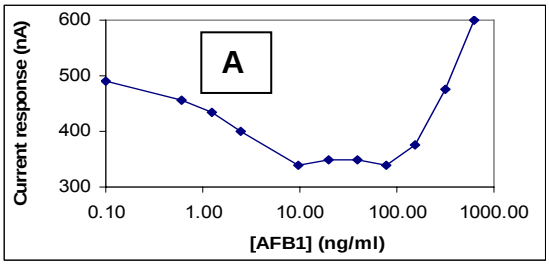

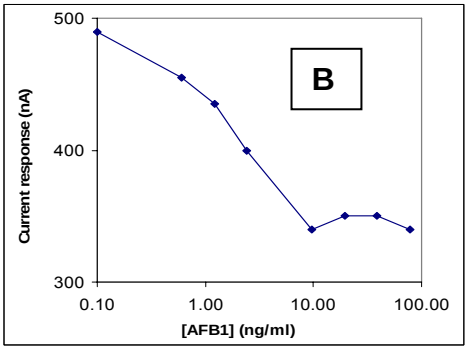

Fig. 2.33. Calibration plot for AFB1 diluted in PBS only. (A) 0 - 625 ng/ml (B) 0 - 78 ng/ml

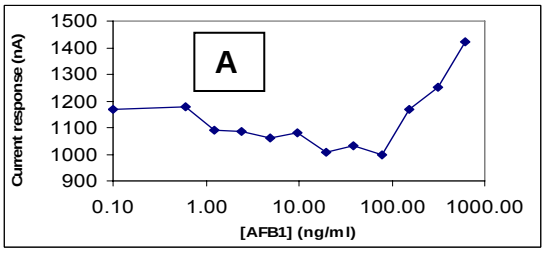

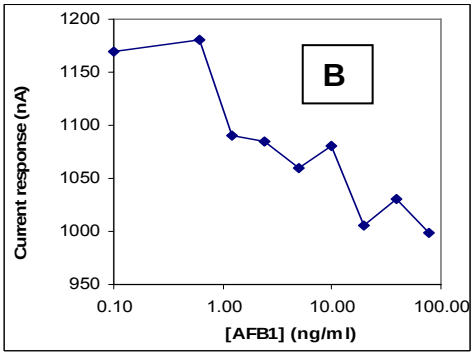

Fig. 2.34. Calibration plot for AFB1 diluted in 10% methanol/PBS. (A) 0 - 625 ng/ml
(B) 0 - 78 ng/ml.

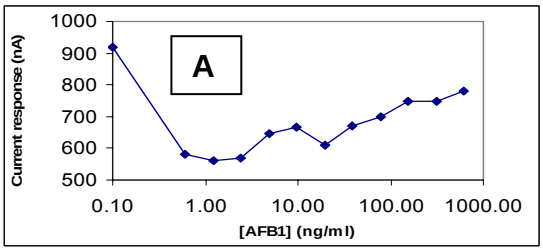

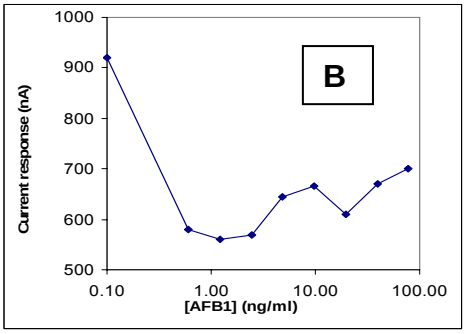

Fig. 2.35. Calibration plot for AFB1 diluted in 10% CH_3CN/PBS. (A) 0 - 625 ng/ml
(B) 0 - 78 ng/ml.

When calibration plots are compared over the lower concentration range (0 - 78 ng/ml; see Figs 2.33B, 2.34B & 2.35B), the most precise plot was obtained in PBS alone (Fig 2.33B). In the presence of 10% methanol (Fig 2.34B), a reasonable but noisier plot was also obtained. In the presence of CH_3CN, a steeper plot was obtained, with a limited working range of 0 - 2.4 ng/ml. In conclusion, PBS alone, although giving a good calibration plot, could not be used, since grain extracts would of necessity be extracted into methanol. 10% methanol/PBS would therefore remain the solvent of choice for further experiments at present.

AFB1 assay using ceramic sensor combs.

The previous studies on the AFB1 assay had used sensors prepared using SPCEs printed on polyester. In order to develop the assay for use in an automated way, it would be necessary to translate the assay onto to ceramic sensors for operation in the Uniscan automated 96-well instrument.

An antibody loading of 1/300, established on the polyester SPCEs, was used to coat arrays of 12 SPCEs printed on ceramic substrate. At this stage, the coating was performed manually in a 2μl volume of PBS. After overnight storage at 4°C, the sensors were used in the AFB1 assay, performed manually by immersion of the combs into reagent solutions contained within wells of a 96-well microtitre plate. A 3% casein/PBS blocking step was used as before, and the measurement step was by linear sweep voltammetry using the PG580 potentiostat. Calibration plots were obtained for AFB1 standards prepared in PBS/10%methanol over the concentration range 0 - 625 ng/ml. Various combinations of reagent conditions were investigated. The plots obtained for a fixed dilution of SA-ALP (1/500) and various dilutions of biotinylated AFB1 are shown in Fig 2.36. From this plot, a dilution of 1/1000 was selected for further studies. The working range based on this plot extended over the concentration range from 0 up to 325 ng/ml.

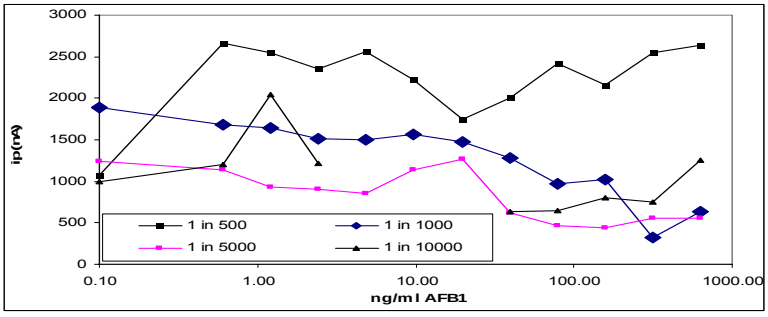

Fig. 2.36.

Calibration plots obtained for AFB1 in buffer using ceramic sensors/manual assay/LSV measurement. Each plot represents a different dilution of biotinylated AFB1 conjugate. SA-ALP was used at 1/500.

Cross-reactivities of AFB1 ceramic comb sensors.

Ultimately with a view to developing a neural network for interpretation of the data output from a series of different sensors, it was of interest to investigate the ability of the AFB1 sensors to detect aflatoxin species besides AFB1. Using the optimised reagent conditions (previous section), a series of calibration plots was obtained using, as the free mycotoxin, serial doubling dilutions of AFB1, AFB2, AFG1 or AFG2. Hence the assays would determine the ability of each of these mycotoxins to compete with the biotinylated AFB1 for binding to the anti-AFB1 antibody. The calibration plots resulting from these assays are shown in Fig 2.37. A slight hook effect was observed for the AFB1 plot between 0 and 1ng/ml AFB1. However, comparing the degree of competition for each plot between 1.2 and 10 ng/ml, it was possible to rank the aflatoxin sensor in order of cross-reactivity with the aflatoxins in the order: AFB1>AFG1>AFB2>AFG2 (AFG2 effectively shows no cross-reactivity with the antibody).

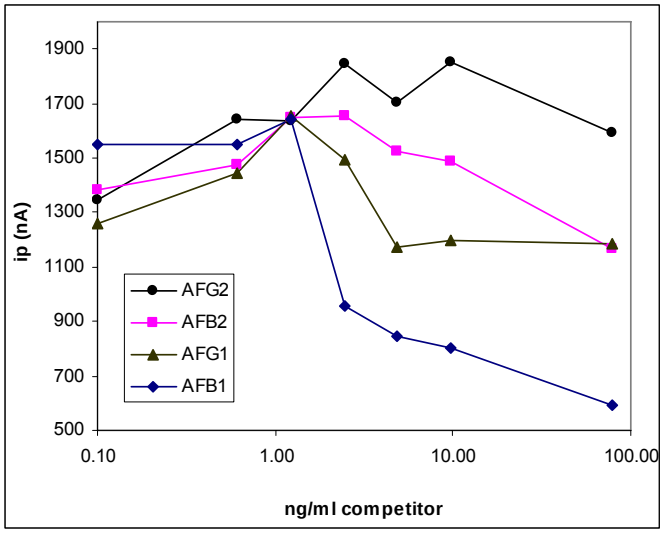

Fig. 2.37.

Calibration plots for different aflatoxins using AFB1 assay.

This rank order agrees with the cross-reactivities stated in the literature for this antibody. This experiment therefore indicates that the electrochemical immunoassay for AFB1 generates sensible data which could be adapted for incorporation into a neural network system involving several sensors (based on different capture antibodies) showing different cross-reactivity profiles. Such a system could be used in an attempt to quantify various different aflatoxins/other mycotoxins within a mixture.

Conclusions for aflatoxin B1

The ability to fabricate screen-printed immunosensors in an array format and to use these in a competitive electrochemical immunoassay conducted in combination with 96-well microtitre plate wells has been demonstrated in principle. In the case of the AFB1 assay, the SPCE array was printed onto polyester substrate and the assay was performed using manual reagent application and wash steps, finishing with a measurement step which used linear sweep voltammetry. The very low achievable detection limit of 0.15 ng/ml obtained for AFB1 is compatible with the requirements of

the Food Industry and therefore holds promise for further studies which will be undertaken to test and validate the assay using real samples from grain extracts. The study using a single analyte forms the basis of further studies which will undertake to develop electrochemical immunoassays for additional mycotoxins, with the ultimate aim of developing an automated instrument capable of making simultaneous determinations of multiple mycotoxin analytes. Sensors based on an anti-aflatoxin B1 antibody have been demonstrated which are based on SPCEs printed on ceramic 12-electrode comb arrays which are compatible with operation using an automated 96-well assay platform/potentiostat. The demonstration that such sensors show predictable cross-reactivities with a range of other aflatoxin species lays the foundation for further work to develop an automated system which may ultimately benefit from mathematical data analysis involving a neural network system which can interrogate a sample matrix and quantify its constituent individual analytes.

Ochratoxin A (OTA)

Testing OTA immunoassay reagents by ELISA or electrochemical immunoassay.

A rabbit anti-ochratoxin A (OTA) reagent from Tepnel Biosystems was tested for its ability to work as a capture antibody for a competitive OTA immunoassay in an ELISA assay. Microtitre plates were coated with increasing dilutions of antibody (from 1/10 to 1/10240). Following a blocking step with 3% casein/PBS, 100 μl of PBS/10% methanol was added to each well to simulate the addition of free OTA. After a 30 min incubation period, this was followed by the addition of 50 μl of biotinylated OTA in PBS for 30 min. Plates were then washed, before the addition of streptavidin-ALP conjugate (1/500) for 30 mins. After a final wash, each well received 145 μl of pNPP substrate solution and the absorbance of the solutions at 405 nm was measured after 90 min. One plate was incubated with OTA-biotin and one was incubated in its absence. Results (Fig 2.38) showed that there no correlation between antibody dilution and absorbance, and that there was no increased signal in the presence of biotinylated OTA compared to its absence. These data indicated that this unpurified rabbit serum did not induce specific binding of biotinylated OTA and would therefore not be suitable for use in the electrochemical immunoassay on SPCEs.

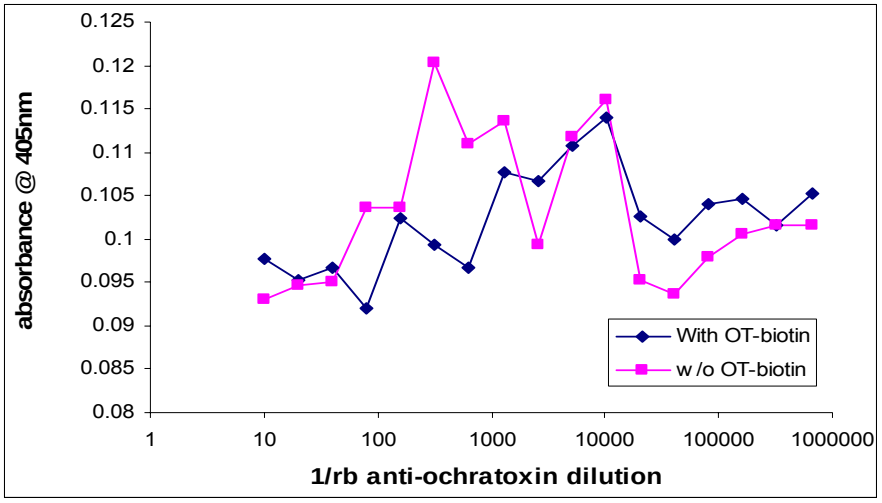

Fig. 2.38. ELISA data for titrated rabbit anti-OTA capture antibody in presence or absence of biotinylated OTA conjugate.

A second reagent, supplied by Tepnel biosystems, was a rabbit anti-OTA antibody which had been purified using Protein A. This reagent was tested directly using SPCEs for its ability to bind biotinylated OTA. SPCEs printed on polyester were coated manually with 2 μl volumes of anti-OTA antibody in increasing doubling dilutions from 1/10 to 1/10240. After overnight incubation at 4 degrees C, the SPCE surfaces were blocked by immersion in a solution of 3% casein/PBS overnight. After rinsing, they were placed into microwells containing 200μl PBS/10% methanol (to simulate free OTA) for 30 min at RT, after which time a further 100 μl were added, containing biotinylated OTA (at 1/250, 1/500, 1/5000 or 1/50000) for 30 min at RT. After washing, SPCEs were placed into wells containing SA-ALP conjugate (1/250), before final washing in preparation for electrochemistry. The measurement step then consisted of a 5 min incubation in wells containing 2 mg/ml 1-naphthyl phosphate in Tris-HCl buffer, pH 10, 10 mM $MgCl_2$, followed by linear sweep voltammetry from -0.1 V to +1.0 V at 100 mV/s scan rate. Fig 2.39 shows the titrations resulting from the voltammetric peak current responses. Clearly current responses corresponding to specific binding of biotinylated OTA by the antibody were obtained. The best titration of antibody was observed with biotinylated OTA at a 1/500 dilution. The experiment was repeated, this time using SA-ALP at 1/150 (data not shown). Again, titration of antibody was observed. Overall, the best titration was observed using biotinylated OTA at 1/500 and SA-ALP at 1/250. From the resulting antibody titration (Fig 2.39), the most appropriate choice of antibody dilution for subsequent calibration studies was 1/160, this being the dilution which gave a response just less than equal to saturation (Fig 2.39).

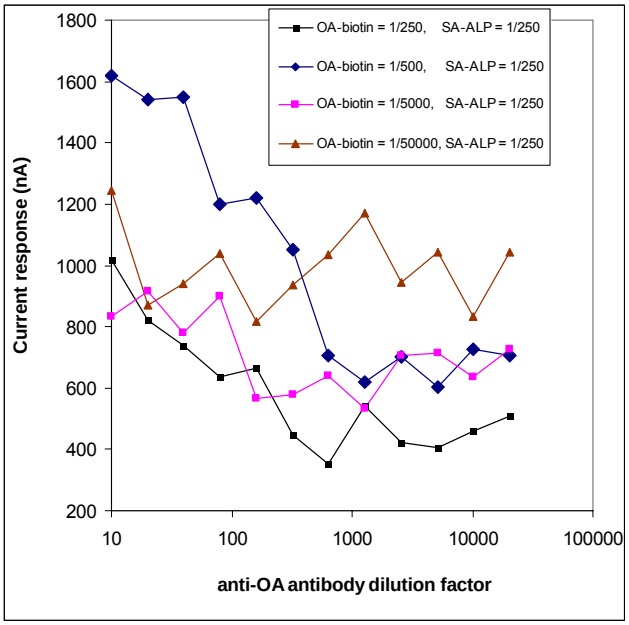

Fig. 2.39. Titration of anti-OTA antibody (protein A-purified) by electrochemical immunoassay using various dilutions of biotinylated OTA. SA-ALP dilution = 1/250.

Electrochemical Immunoassay for OTA on SPCEs.

Combs of 12 SPCEs (on polyester) were coated manually with 2μl of rabbit anti-OTA (Protein A-purified) antibody in PBS and left overnight at 4°C. After being rinsed and blocked overnight with 3% casein/PBS, the sensors were exposed in microwell plates, as described above, to free OTA over the concentration range 0 - 625 ng/ml, then to added biotinylated OTA conjugate (1/500). After washing and exposure to SA-ALP (1/250 or 1/500), then a final wash, electrochemical measurements were made using LSV as described above. The resulting calibration plots are shown in Fig 2.40. Clearly, although at low free OTA concentrations a reasonable plot was obtained, using 1/250 SA-ALP (Fig 2.40A), there were problems at concentrations above 5 ng/ml. By using less SA-ALP (Fig 2.40B), it was possible to obtain a calibration plot approaching a better working range which extended out to 625 ng/ml; however, there was still some anomalous behaviour from individual sensors at high concentrations (above 5 ng/ml) of free OTA.

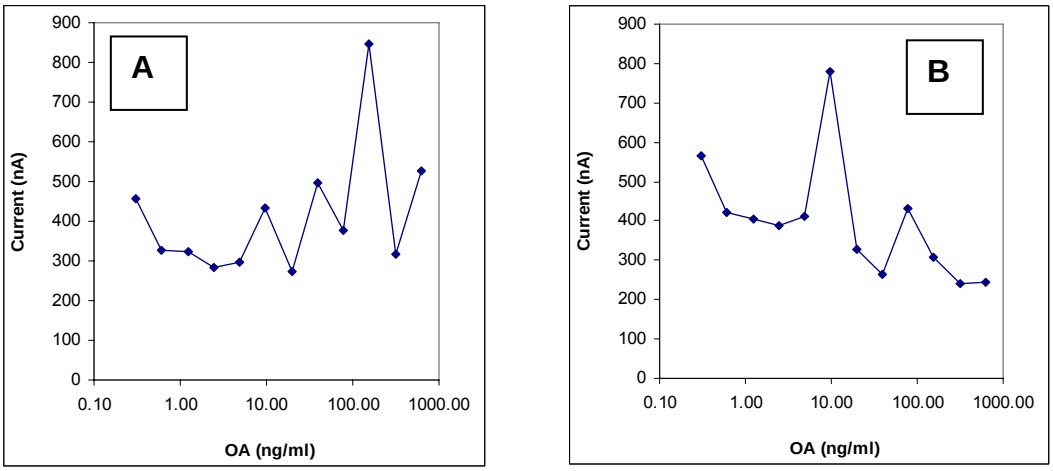

Fig. 2.40. Calibration plots obtained for OTA by electrochemical immunoassay using biotinylated OTA at 1/500. SA-ALP dilution = (A) 1/250 or (B) 1/500. Each point obtained from a single sensor.

Biotin wash

Under optimised reagent conditions (previous section), the OTA electrochemical immunoassay behaved well at low free OTA concentrations (0 - 4.8 ng/ml), but showed anomalous behaviour at higher concentrations. One possibility was that, in spite of the casein blocker, SA-ALP was binding non-specifically to the electrode surface, or to protein, resulting in high levels of anomalous enzyme activity. One option to control this phenomenon was to introduce a wash step with D-biotin in order to compete off any loosely-bound SA-ALP during the final washing phase, immediately before the substrate incubation and measurement steps. The plots shown in Fig 2.41 demonstrate that the biotin wash does appear to lower the high signals obtained at high concentrations of free OTA. It is also apparent that signals at the lower concentrations are reduced, so that the calibration plot is only useable at best between 0 and 1 ng/ml. Although this experiment suggests that non-specific binding can be improved using a biotin wash, the improvement is not sufficiently dramatic to justify including an extra step in the experimental protocol of the immunoassay.

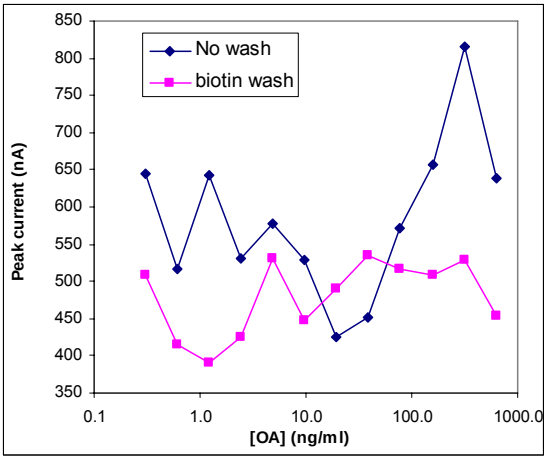

Fig. 2.41. OTA calibration plot with or without final wash with D-biotin.

OTA assay using higher antibody loading.

Selection of a 1/160 dilution of anti-OTA antibody in experiments so far was based on the use of a sub-saturating antibody coating on the SPCEs (see Fig 2. 39). In view of the high signals obtained in calibration plots at high concentrations of free OTA, it was of interest to examine the effect of using a higher antibody loading in a calibration plot. From the antibody titration (Fig 2.39), it appeared that there was no danger of a hook effect at high antibody loading, so a reasonable calibration plot could be anticipated. A plot resulting from an OTA assay using an antibody loading of 1/30 dilution, followed by a 3% casein block and assay as before, is shown in Fig 2.42A. Although this plot is noisy, it does exhibit the correct overall trend expected for a competitive assay.

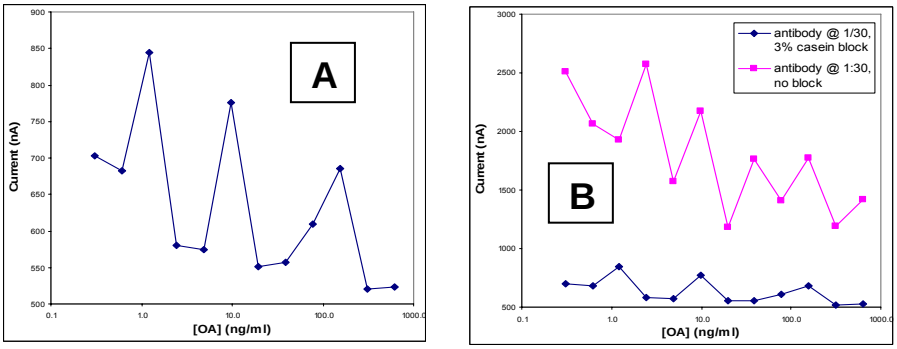

Fig. 2.42. Calibration plots for OTA at high antibody loading (A) in the presence and (B) in the presence or absence of a casein blocking step.

OTA assay without blocking step.

In the previous work with aflatoxin A, and so far with OTA, the use of a casein blocking step had been used to lower non-specific binding of SA-ALP to the SPCE surface. The use of a blocking step meant an extra step during the assay process and would mean that sensors must be blocked at some stage after antibody coating. It was important to see the effect of omitting the blocking step on the OTA immunoassay. Fig 2.42B shows the calibration plot resulting from an OTA immunoassay using a 1/30 antibody loading, in which the blocking step was omitted. It is apparent that the size of the current responses increases dramatically without the blocking step, indicating that casein was preventing some electron transfer from naphthol to the SPCE surface. Moreover, the shape of the calibration plot in the absence of blocker is reasonable, particularly between 0 and 1.2 ng/ml. This result indicates that it may be possible to omit a blocking step and still obtain a satisfactory OTA calibration.

Effect of adding free OTA and biotinylated OTA as a mixture.

The overall aim of this work was to develop an electrochemical immunoassay for OTA which could be adapted to automation whilst keeping the number of assay steps to a minimum. Rather than adding the free OTA for 30 min prior to the biotinylated OTA, it was of interest to add these two solutions simultaneously in a single 30 min incubation step. Fig 2.43 shows a calibration plot resulting from such an experiment. The working range, in this case 0 - 20 ng/ml, is similar to that obtained using separate incubation steps (Figs 2.40 and 2.41), although the plot still suffers from the high current responses seen at higher concentrations. The antibody loading was 1/30. There was no blocking step.

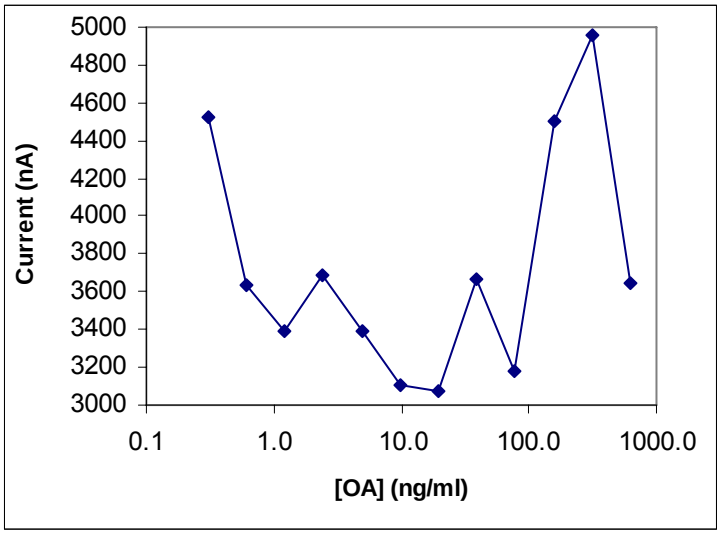

Fig. 2.43.

Calibration plot obtained using simultaneous incubation of free and biotinylated OTA as a mixture

Effect of including Tween in OTA calibration standards.

At this stage, it appeared that an OTA immunoassay may be feasible using a simple one-step antibody loading, without a casein blocking step, followed by a competition step involving a single incubation of a combined mixture of free and biotinylated OTA. However, at best as seen in Fig 2.43, the resulting calibration plot(s) still suffered from noise and anomalous behaviour at high concentrations of free OTA (above 20 ng/ml). A possible explanation for the high signals at high OTA concentrations was solubility effects at threshold levels leading to aggregate formation of the free OTA and therefore making it unable to compete against the biotin-labelled species, leading to increasing, rather than decreasing signals. In order to investigate this possibility, it was of interest to test the immunoassay performance using free OTA which was prepared in the presence of Tween 20 or Tween 80, both of which have detergent action. Dilutions of free OTA were prepared in 10% methanol/PBS as before, or in the same solvent with added Tween 20 or Tween 80 at 0.1% v/v. The resulting calibration plots obtained from these dilutions in the electrochemical immunoassay are shown in Fig 2.44. In the absence of Tween, the calibration showed the usual anomaly at high OTA concentrations (Fig 2.44A). In the presence of Tween 20 (Fig 2.44B), although a useable region was evident from 0 - 5 ng/ml, the plot was still very noisy at higher concentrations. In the presence of Tween 80 (Fig 2.44C) , there was now a pronounced hook effect at low concentration, but the detergent appeared to have improved the behaviour at the higher concentrations, and overall, the plot appeared more as anticipated for a competitive immunoassay.

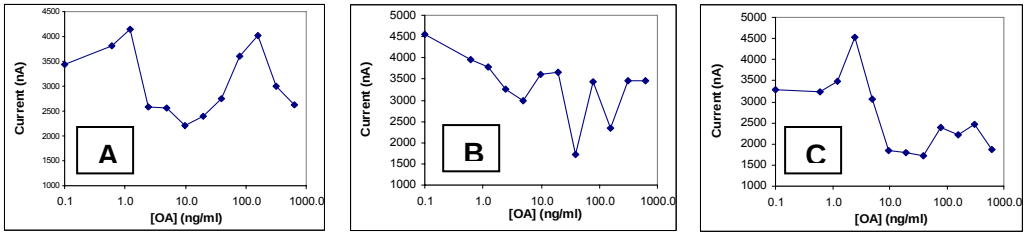

Fig. 2.44. OTA electrochemical immunoassay calibration plots obtained using free OTA diluted in 10% MeOH/PBS alone (A) or the presence of (B) 0.1% Tween 20 or (C) 0.1% Tween 80.

A further experiment was then conducted, this time reducing the concentration of biotinylated OTA by fivefold to a dilution of 1/2500. Once again, the best plot was obtained for the plot in which Tween 80 was included in the diluent. This plot is shown in Fig 2. 45, where it is apparent that the hook effect at low concentrations evidenced only by a single point and at higher concentrations the plot shows reasonable behaviour up to100 ng/ml.

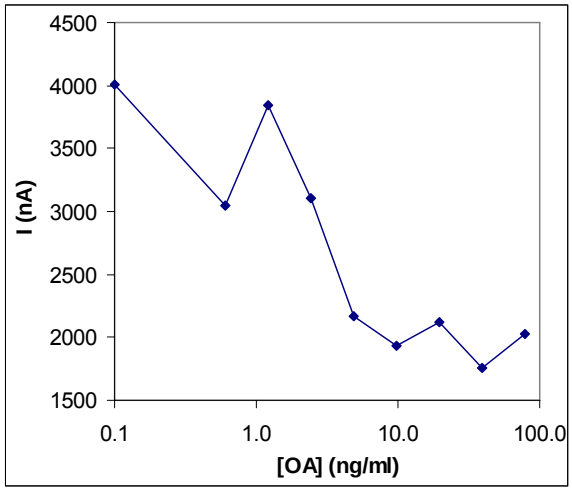

Fig. 2.45. OTA calibration plot in presence of 0.1% Tween 80, using biotinylated OTA at 1/2500.

Optimisation of percentage methanol for electrochemical OTA immunoassay.

The OTA assay would be required to tolerate the presence of methanol, since this was to be the solvent for resuspension of wheat extracts for real sample testing. To this point, dilutions of free OTA were prepared in PBS containing 10% methanol. Since 200 □l volumes of these dilutions were added to 100 μl volumes of biotinylated OTA, the resulting methanol percentage in the wells was 7%. This percentage had not been fully optimised, so an experiment was performed in which OTA calibration standards were prepared in PBS containing 0, 10, 20, 40 or 80% methanol. These led to final concentrations in the microwells of 0, 7, 13, 26.6 and 53% methanol in PBS. Fig 2.46 shows the calibration plots obtained for these various assays. The best curves were seen for dilutions prepared in 20% or 80% methanol. Hence, these percentages were selected for further investigation using wheat extracts containing OTA.

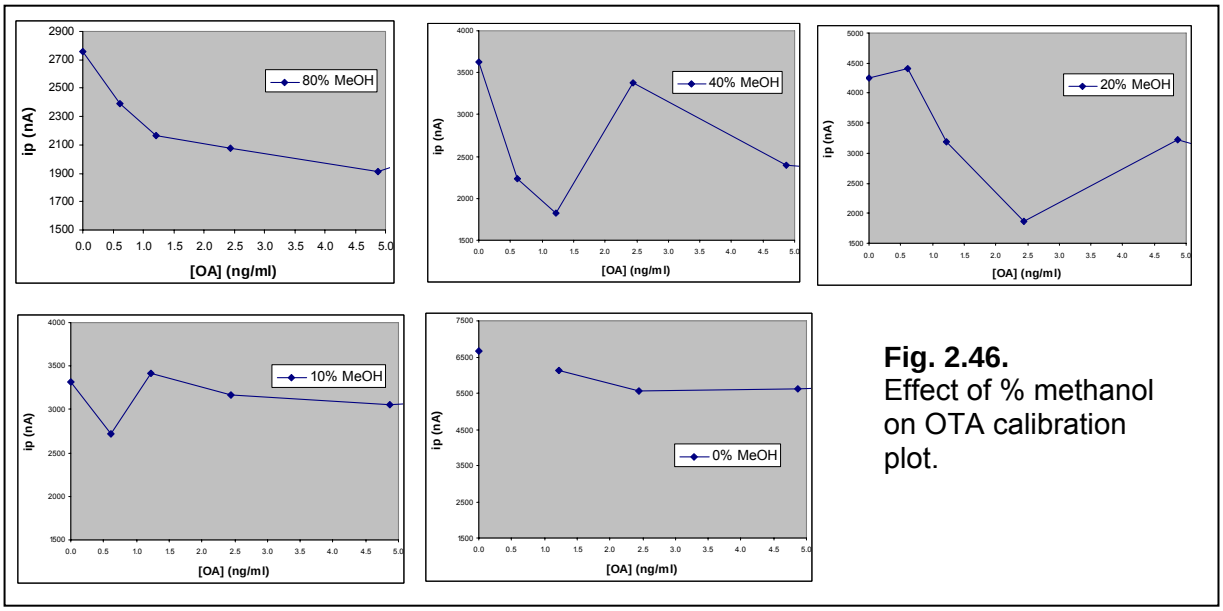

Fig. 2.46. Effect of % methanol on OTA calibration plot.

Electrochemical OTA immunoassay using spiked wheat extract.

OTA standards were prepared in the presence or absence of wheat (extracted and supplied by CCFRA) as follows:

Presence of wheat:

5g wheat extract into 1ml MeOH
200 μl of this added to 800 μl containing appropriate % MeOH in PBS/0.1% Tween 80, to give either 20% or 80% in this solution. (Dilution of original 1ml of MeOH is now 1/5; so 5 g now in 5 ml).
100 μl of this now added to 100 μl of OA standards in 20% or 80% MeOH/PBS/0.1%Tween 80.
So 5g sample is now in 10 μl. Therefore 1ml is from 0.5g.
200 μl of this sample then added to wells containing 100 μl of OA-biotin solution in PBS.

Absence of wheat

Prepared PBS/0.1% Tween 80 containing 20 or 80 % MeOH, without wheat.
100 μl of this now added to 100 μl of OA standards in 20% or 80% MeOH/PBS/0.1% Tween 80.
200 μl of this sample then added to wells containing 100 μl of OA-biotin solution in PBS.

Voltammetry of OTA sensors exposed to solutions in the presence/absence of wheat.

In order to determine whether the presence of wheat would introduce any interfering electrochemical signals into the immunoassay, antibody-coated SPCEs were subjected to the full immunoassay on solutions containing no free OTA in the presence or absence of wheat in 20 or 80% methanol/PBS/0.1% Tween 80. As a measurement step, the sensors were subjected to linear sweep voltammetry after 5 min incubation in the substrate buffer (Tris-HCl, pH 10/10mM $MgCl_2$), containing 1-naphthyl phosphate. Fig 2.47 shows the resulting voltammograms. The left-hand panel (A) shows that after exposure to a 20% methanol solution, there was an enhancement of the usual peak current response due to oxidation of the enzymatic product, 1-napthol, at +200 mV. At higher potentials, there was evidence of a minor oxidizing species in the wheat at around +400 mV. Fig 2.47B shows that, in contrast, sensors exposed to wheat in the presence of an 80% methanol/PBS solution exhibit a dominant second peak at an Ep of around +400 mV, with little enhancement of the analytical 1-naphthol peak. In both cases, the interfering peak occurs at a more positive potential than the analytical signal for 1-naphthol, and so is not likely to interfere with the 1-naphthol reading. However, the dominance and broadness of the second peak in 80% methanol means that it may overlap with the 1-naphthol signal. This potential problem does not appear likely using a 20% methanol/PBS solution for preparing the free OTA/wheat samples.

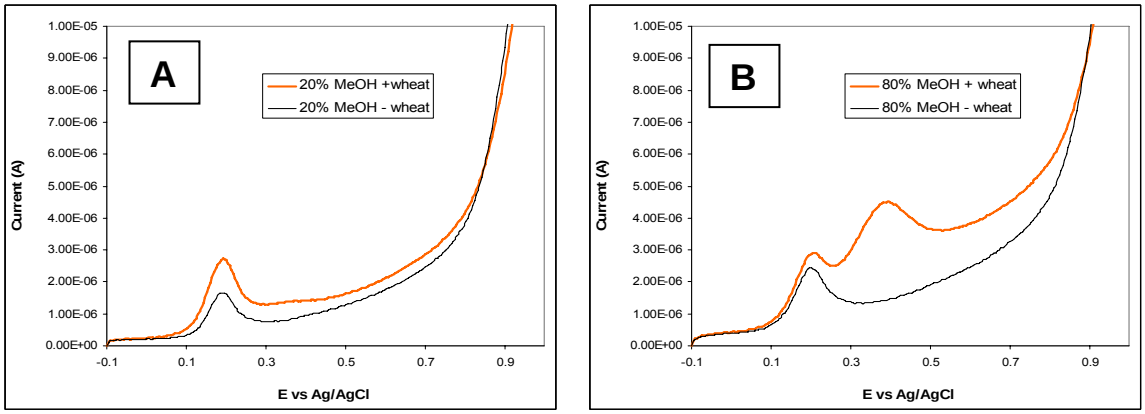

Fig. 2.47. Voltammograms of OTA sensors after exposure to solutions with/without wheat extract. (A) solutions containing 20% MeOH/PBS (B) solutions containing 80% MeOH/PBS.

Testing for matrix effect from wheat using electrochemical OTA assay.

Calibration plots were obtained for free OTA in the presence or absence of wheat at concentrations from 0 - 4.8 ng/ml prepared in 20% or 80% methanol/PBS/0/1% Tween 80 solutions. The resulting calibration plots are shown in Fig 2.48. Both plots demonstrate that there is a positive current matrix effect due to the presence of the wheat, compared to sensors tested in its absence. Clearly the best plot was obtained using the 20% methanol/PBS/0.1% Tween 80 solution as diluent for the OTA.

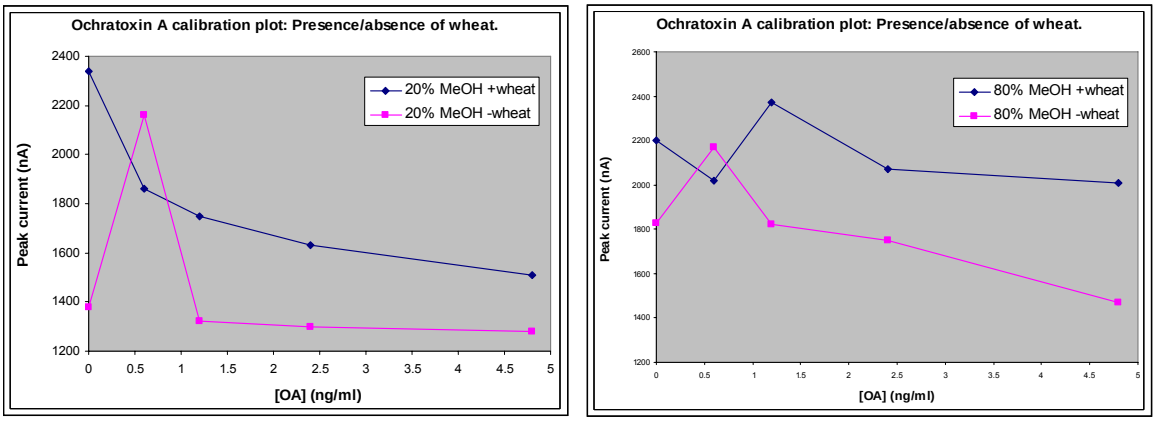

Fig. 2.48. OTA calibration plots obtained in presence or absence of wheat using 20% or 80% methanol as solvent.

Using these optimised conditions, a further series of calibration plots over the OTA concentration range 0 -19.5 ng/ml was obtained in spiked wheat extract, on four separate 12-electrode combs (10 electrodes per comb were used) printed on polyester, as shown in Fig 2.49. With the exception of Comb C, reasonably repeatable calibration plots were obtained, with CVs of less than 10% for the majority of concentrations. Comb A produced the best plot which gave a useful working range between 0 and 5 ng/ml OTA.

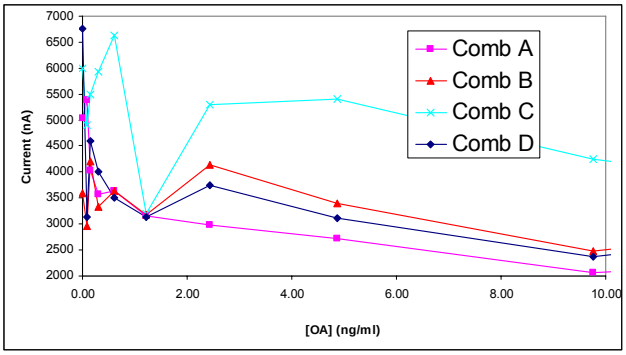

ng/ml OA	CV%
19.5	16.7
9.8	9.4
4.9	10.9
2.4	16.2
1.2	0.7
0.6	2.0
0.3	9.2
0.2	6.7
0.1	35.2
0.0	30.8

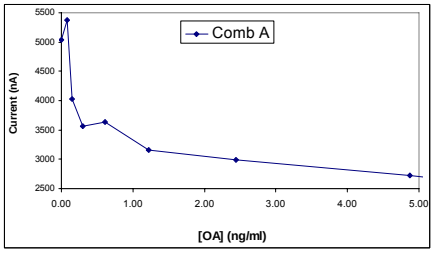

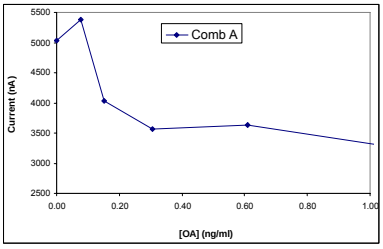

Fig. 2.49. OTA calibration plots obtained using four 12-electrode combs, expanded plots for Comb A, and Table showing coefficient of variation at each concentration

Inclusion of AET stabiliser solution

In order to facilitate long-term storage of antibody-coated electrodes, the inclusion of a stabiliser solution from A.E.T. was proposed. Three stabiliser solutions were provided: P2, P15, P16. Before selecting a suitable stabiliser, it was necessary to investigate each one for any electrochemical activity which might interfere with the performance of the OTA sensors. The three stabilisers were prepared at dilutions of 1/10 to 1/1000 in 0.1M TRIS/HCl buffer, pH 10. These solutions were then tested voltammetrically with bare SPCEs. The voltammograms are shown in Fig 2.50.

P2 contained electroactive material, whereas P15 and P16 appear to be electroinactive. However, the peak potential for P2 was at the relatively high potential of +0.7V and since oxidation of P2 began above +300mV, it was concluded that this should not present a problem for sensors based on measurements using 1-naphthyl phosphate, where the oxidation peak for 1-naphthol occurs at +170 mV vs Ag/AgCl. Similar voltammograms were obtained for each stabiliser solution following application of 2 ml dried onto the SPCE surface, followed by voltammetry.

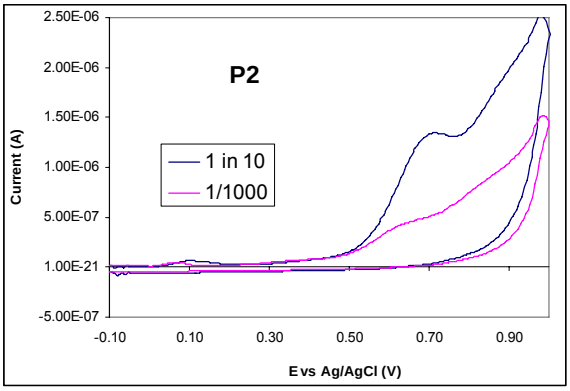

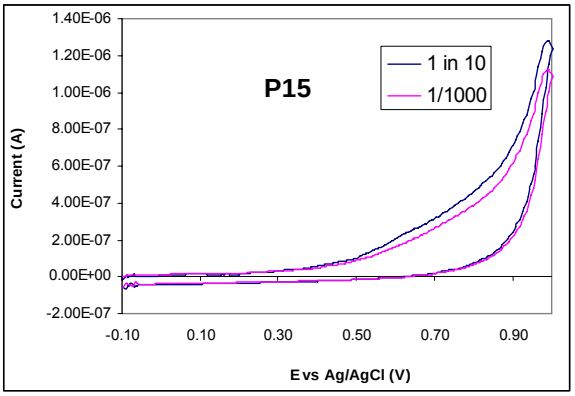

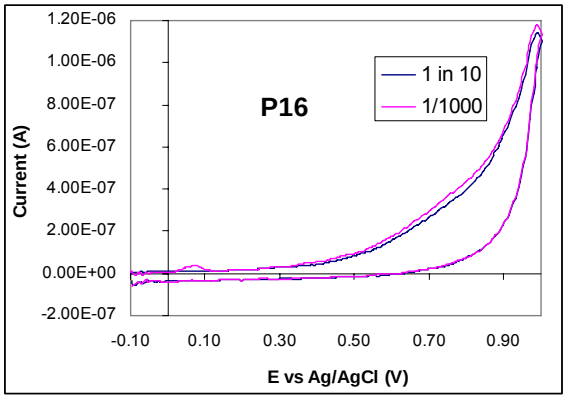

Fig 2.50.

Voltammograms obtained using bare SPCEs for dilutions of AET stabilisers solutions prepared in buffer.

It was noteworthy that the P2 stabiliser exerted a slight acidic effect when added to pH10 buffer (changed to 9.8), whereas P15 and P16 showed negligible change.

Of the stabilisers tested, P2 was recommended as being most suitable for stabilising antibodies. P2 was therefore selected for further studies/incorporation into biosensors.

OTA assay on comb of 12 SPCEs - precision using manual operation.

SPCEs printed on ceramic substrate were coated with anti-OTA antibody diluted in a 50:50 solution of P2 stabiliser:PBS. The method is summarised below:

- **SPCEs are GEM mycotoxin electrodes prepared in combs of 12 and printed on polyester or ceramic substrate.**
- **Prepare biosensors by depositing rabbit anti-OTA (Protein A-cut, Tepnel Biosystems) onto SPCE working area.**
- **Antibody is diluted 1/30 in 50:50 PBS:AET P2 stabiliser; place this solution in plate for aspiration by Biojet.**
- **Snap out individual comb from substrate.**
- **Place comb on BioDot platform at RH = 60%.**
- **Dispense 1.8μl per electrode using BioDot program "mycotoxin ceramic double line dispense 1.8μl per sensor."**
- **Sensors are dried in dessicator (silica gel). After 30 min drying, place biosensors in dessicator at 4°C until use.**

These sensors were then tested for reproducibility using the OTA electrochemical immunoassay as summarised below:

Electrochemical assay
Prepare dilutions of OTA in 20% MeOH/PBS/0.1%Tween 80.
Prepare 1/2500 dilution of OTA-biotin conjugate (Tepnel Biosystems) in PBS.
Add 100μl of 1/2500 OTA-biotin solution per well of a 96 well plate.
Add 200μl of appropriate OTA dilution per well. (Total well volume = 300 μl)
Insert biosensor combs into wells
Shake, 30 min, RT.
Wash combs 4X PBS/T, 2X PBS.
Add 250 μl of 1/500 SA-ALP conjugate in PBS/well.
Insert combs.
Shake, 30 min, RT.
Wash 5X PBS/T, 2X 0.1M Tris-HCl, pH 10
Insert sensors into wells containing 300 μl 2mg/ml 1-naphthyl phosphate in 0.1M Tris-HCl, pH10/10mM $MgCl_2$.

After 5 min at open circuit voltage, apply linear sweep voltammetry (-0.1V - +1.0V; 100 mV/s) using individual PG580 potentiostat.
Measure anodic peak height.

Results were obtained for 12 repeat sensors with no free OTA (ie. maximum current response) and showed the following coefficients of variation:
DAY 1 15.4%
DAY 5 15.3%

OTA assay on comb of 12 SPCEs - precision using automated measurement.

Two combs of (ceramic)sensors were tested. The OTA assay was performed as above using the ceramic, stabilised immunosensors, but the measurement step was performed using chronoamperometry (from open circuit voltage to +0.5V) rather than LSV. In one case, the chronoamperometry was performed manually, as above, by inserting electrodes into wells and applying substrate solution manually, measuring each sensor individually and sequentially. For the second comb, the sensor array was inserted into the automated Uniscan instrument and chronoamperometry was applied simultaneously to all 12 sensors.

Results for coefficient of variation on current responses taken at 5s were as follows:

Comb 1 - MANUAL MEASUREMENT: 15.0%
Comb 2 - AUTOMATED MEASUREMENT: 4.6%

This result demonstrated the advantage of being able to perform all measurements simultaneously. It also demonstrated that it was possible to obtain good precision for 12 identical immunosensors, treated in the same was through the entire immunoassay, using chronoamperometry as the measurement step rather than LSV.

OTA assay on comb of 12 SPCEs - calibration plot using automated measurement.

A series of OTA calibration standards was prepared in 20% Methanol/PBS/0.1% Tween 80 at concentrations of 0, 0.3, 0.6, 1.2, 2.4 and 4.8 ng/ml. These were tested with ceramic sensors using the full OTA assay, performed manually apart from the measurement step which was conducted as above by chronoamperometry using the autoinstrument. Various dilutions of SA-ALP were investigated, including 1/500, 1/1000 and 1/5000; biotinylated OTA was tested at dilutions of 1/2500 and 1/5000. Current responses were recorded for sensors measured in 1-NP and in buffer alone (blanks) so that the influence of surface-bound proteins/surface area changes could be assessed. The best calibration plot is depicted in Fig 2.51. The calibration plot measured in 1-NP gives a working range between 0 and 2.4 ng/ml, with no evidence of a hook effect. The blank responses are reasonably consistent across the concentration range, but there are some differences in the response obtained; subtraction of the blanks does lead to a more sensitive plot. This result indicates that there may be a case for including a blank sensor for each sample.

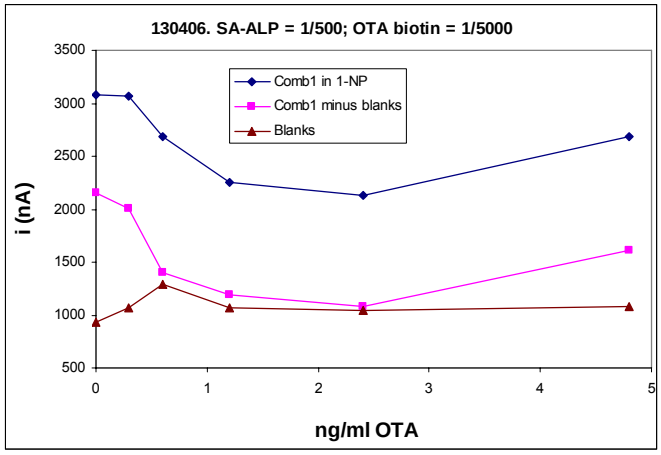

Fig. 2.51.

Calibration plot for OTA in buffer using ceramic/stabilised sensors, manual assay and automated measurement step.

OTA assay in wheat - calibration plot using automated measurement.

Using the best reagent conditions arrived at in the previous section, a series of OTA standards was prepared in wheat extract. The concentration of wheat in the 200 ml of OTA standard was 1g/ml or 1g/10ml. The OTA assays were preformed manually, using ceramic sensors, with an automated chronoamperometric measurement step, as described above. Three replicate calibration plots obtained using the 1g/10ml OTA standards are shown in Fig 2.52.

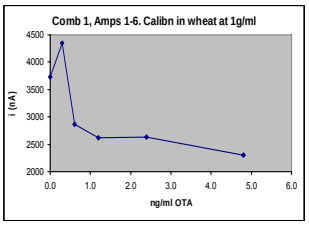

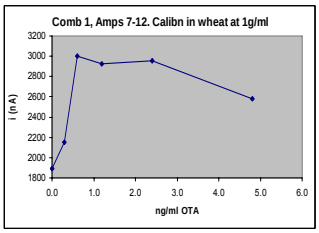

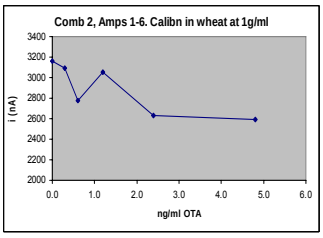

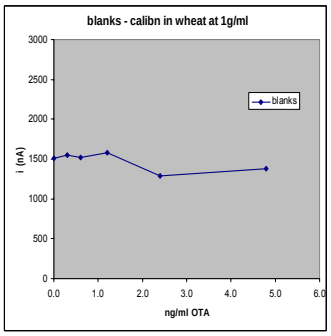

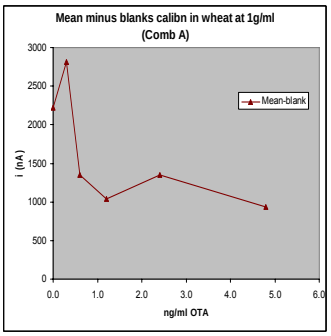

Fig. 2.52.

OTA calibration plots obtained in spiked wheat at 1g/ml using manual assay/automated measurement.

Clearly there is considerable variation between the plots. The blank responses showed little variation across the calibration range. The bottom right panel shows the blank-corrected plot for one of the plots. Although there is a hook effect at low free OTA concentration, the plot shows otherwise reasonable behaviour.

Fig 2.53 shows plots of the mean and standard error data for results obtained using wheat at 1g/ml or 1g/10ml equivalent (using ceramic sensor combs). CVs for both sets of data ranged from around 3% up to 12%, with the exception of the lowest concentrations in the 1g/ml plot where CV values of 34% were obtained. In both cases, the occurrence of a hook effect at low concentration suggested that further optimisation of reagent conditions for wheat analysis may be required.

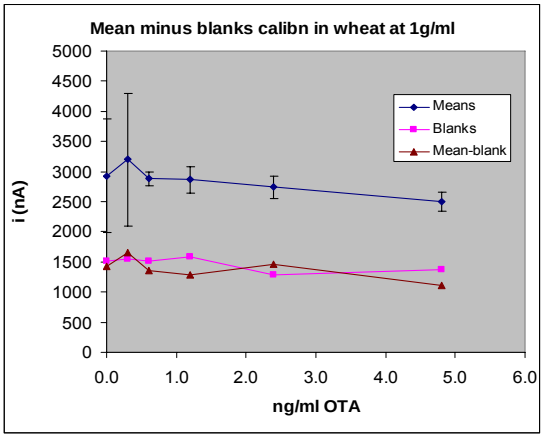

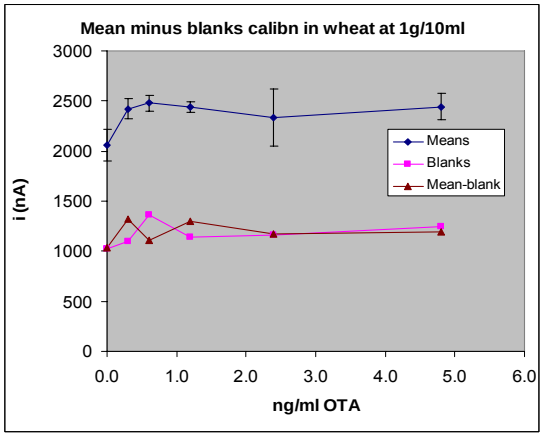

Fig. 2.53. Calibration plots obtained for OTA standards spiked into wheat at 1g/ml or 1g/10ml equivalent. Manual assay using automated chronoamperometric measurement step.

OTA assay in wheat - calibration plot using fully automated assay.

All steps in the OTA were next performed automatically using the Uniscan Instrument (described in Section 3.2 and Appendix 1). Five Rows of a 96-well microtitre plate were utilised as illustrated in Fig 2.13 (Section 3.2). The contents of Row 1 were: 100 μl biotinylated OTA (in PBS) + 200 μl containing OTA standard and wheat extract in 20% methanol/PBS/0.1% Tween 80. Each well contained 0.1g wheat in the 200 μl volume. The concentration of free OTA standards in the 200 μl volume covered the range 0 – 4.8 ng/ml. These concentrations could be expressed directly in ppb of OTA in wheat equivalent by applying a multiplication factor of 2.

A comb of 12 ceramic immunosensors (prepared using anti-OTA antibody plus P2 stabiliser) was mounted in the gantry of the automated instrument, and the whole experimental set-up was configured as illustrated in Table 1. From this point onwards, the entire assay proceeded in an automated fashion and culminated in a series of 12 chronoamperometric datasets for each of the 12 potentiostats, one corresponding to the current response of each sensor on the comb. The duration of the assay was 77 mins for a comb of 12 sensors. The resulting calibration plot obtained for sample and respective blank wells is shown in Fig 2.54. In this plot, the blank signals were very similar across the concentration range, suggesting that a blank subtraction may not be necessary to obtain the best plot. The plot obtained for the sensors in substrate solution is shown on an expanded scale in Fig 2.55.

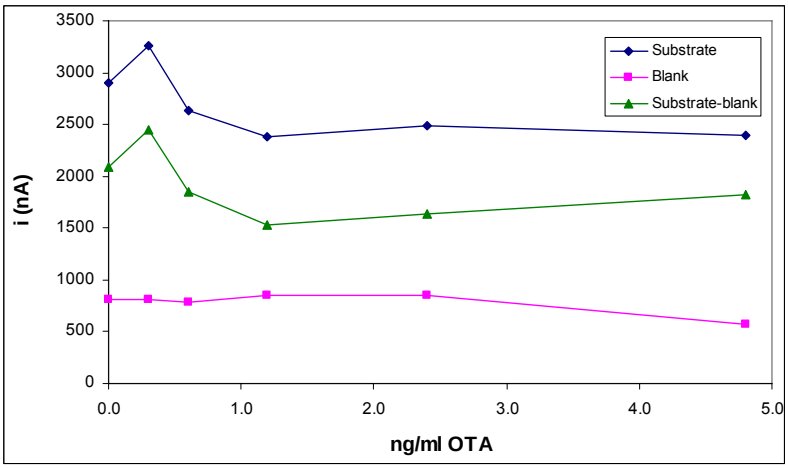

Fig. 2.54. Calibration plots obtained for OTA in wheat + blanks using fully automated instrument.

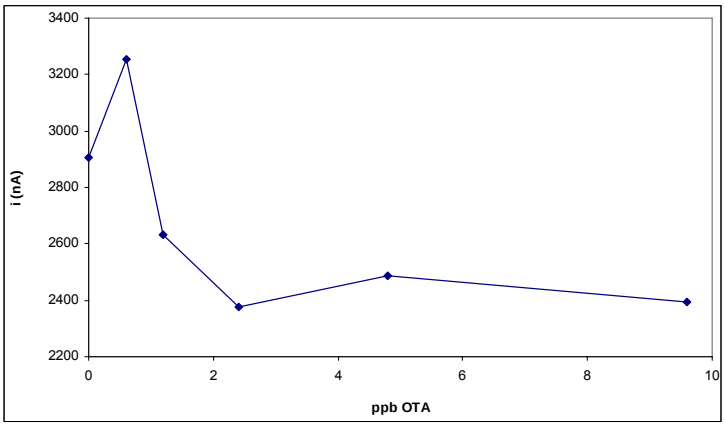

Fig. 2.55. Calibration plots obtained for OTA in wheat using fully automated instrument. Values expressed in ng/g wheat (ppb).

Concentrations of OTA are expressed in ng OTA/g wheat (ie. ppb). Thus, the working range of the assay appeared to be between 0.6 and 2.4 ppb. Further optimisation is required to remove the hook effect which limits the effective working range available at present.

A fresh set of OTA immunosensors was prepared, this time using three different antibody loadings: 1/30, 1/60 and 1/120 in order to perform a repeat of the above experiment, and to investigate the effect of antibody loading on curve shape. Wheat extract was spiked as previously and the electrochemical immunoassay was performed using the autoinstrumet to yield calibration plots as shown in Fig 2.56. At this stage the sensors had been prepared and stored at 4^0C for 4 days. The 1/60 antibody loading (Fig 2.56B) did lengthen the working range of the assay compared to the 1/30 loading (Fig 2.56A), whereas the 1/120 loading (Fig 2.56C) had little effect. However, the curve shape for the 1/30 loading in this case showed no hook effect and a useable plot with a working range from 0 - 2.4 ppb. Although this range extends to below the required detection limit of 3-5 ppb for OTA in processed and raw cereals/spices, a simple dilution or extraction into a larger volume would make this curve suitable for use on real samples.

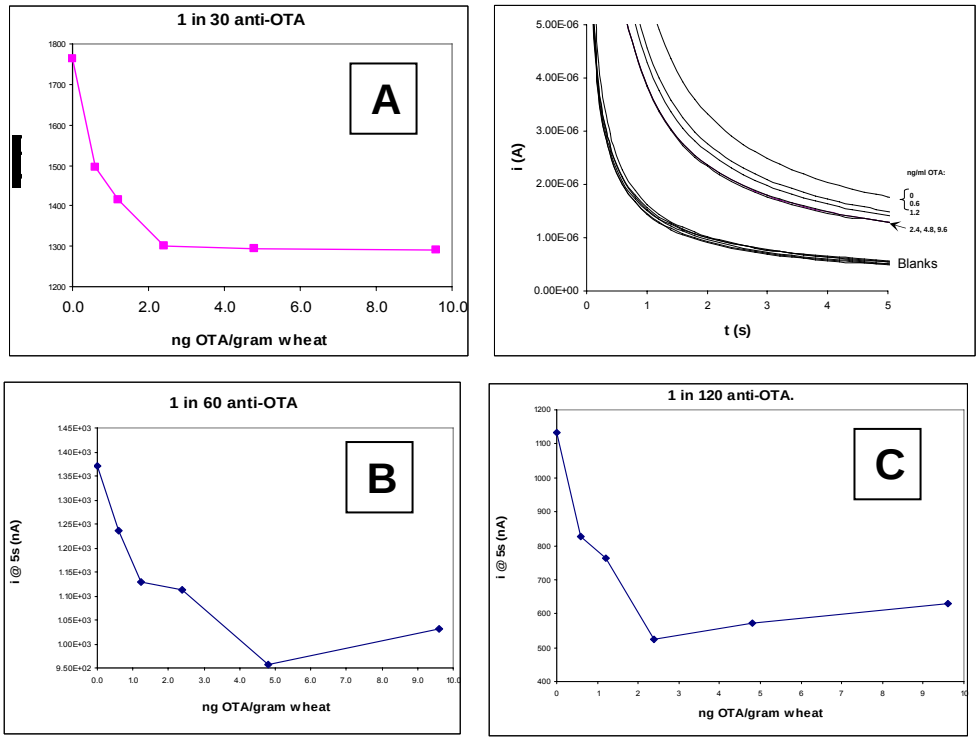

Fig. 2.56. Calibration plots of wheat spiked with OTA obtained using automated instrument. Antibody loadings on immunosensors were: (A) 1/30, (B) 1/60 and (C) 1/120. Top right panel shows chronoamperograms for plot (A).

OTA assay in wheat - further calibration plots on spiked wheat extract

Spiked wheat samples from CCFRA were tested for the presence of OTA using the automated instrument and immunosensors coated with 1/30 anti-OTA-pus-stabiliser (same batch as in previous experiment, now 6 days old). Wheat extract was divided into six aliquots and spiked with OTA over the concentration range 0 - 6.1 ppb. These solutions were tested in duplicate on two combs of 12 sensors. Results for the first comb are shown in Table 2.6 and Fig 2.57. The plot, based on the average current response for two sensors (Fig 2.57), shows a similar shape to that obtained previously (Fig 2.56A), when combs were 4 days old. Interestingly, the data appear to fall into two separate series of current responses, one for even, and one for the odd-numbered sensors on the comb.

Biosensor	ppb OTA	nA
1	6.1	2159
2		1157
3	3.1	1872
4		1137
5	1.2	1821
6		1134
7	0.6	1848
8		1289
9	0.05	1996
10		1468
11	0	2803
12		2506

Table 2.6. Current responses for OTA-spiked wheat on a 12-sensor comb array.

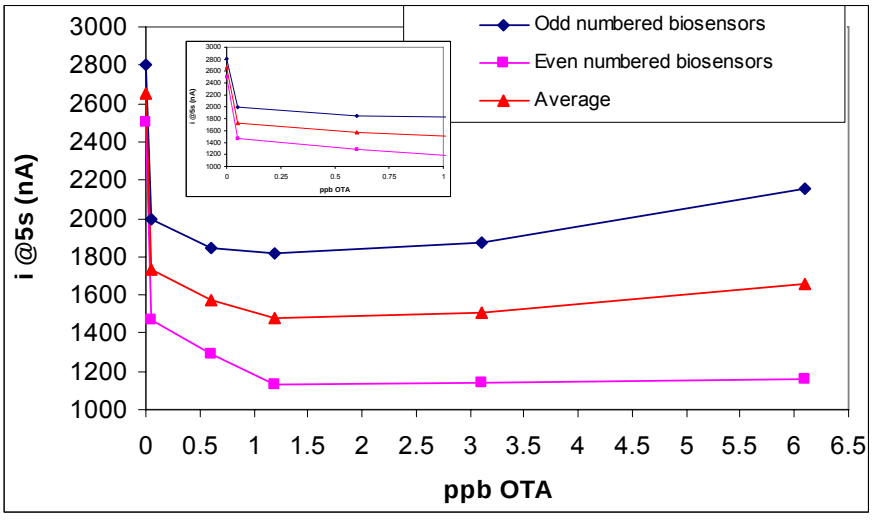

Fig. 2.57. Calibration plot using data obtained from OTA-spiked wheat on a single 12-sensor comb array.

In the case of a second comb of immunosensors, prepared and stored identically to the first, the calibration plot showed a hook effect at low free OTA concentration (Fig 2.58), and current responses continued to decrease at OTA concentrations above 1.2 ppb. Clearly this variation in behaviour between combs of sensors was a cause for concern.

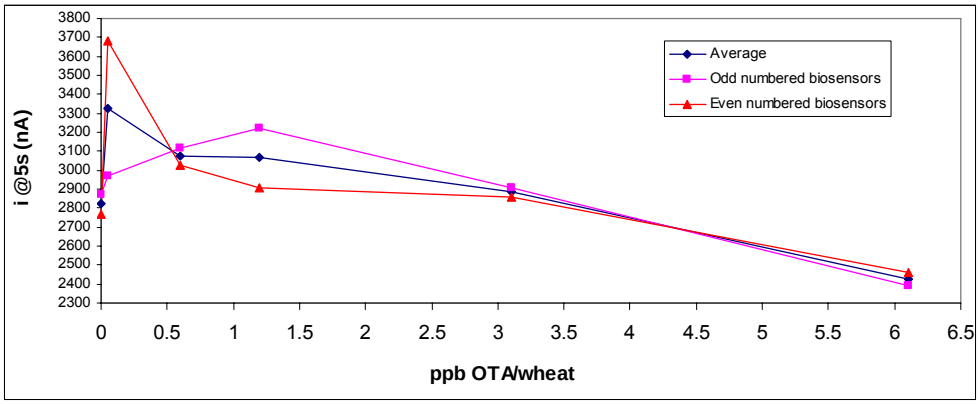

Fig. 2.58. OTA calibration plot for spiked wheat extract using a second comb of immunosensors.

OTA assay in wheat - precision tests on combs of OTA immunosensors.

A fresh batch of OTA immunosensors was prepared on 17-07-06 as previously (1/30 anti-OTA-plus P2 stabiliser). Wheat extract spiked with 2.5 ppb of OTA was applied to all 12 sensors on a single comb and the assay was run using the autoinstrument. Data are shown in Fig 2.59 (amperograms, CV values and individual current responses at 5s). The CV at 5s was 8.0%. There was no obvious trend in size of response across the comb, but this size of variation meant that there was a standard deviation of 297 nA for a mean signal of 3697 nA.

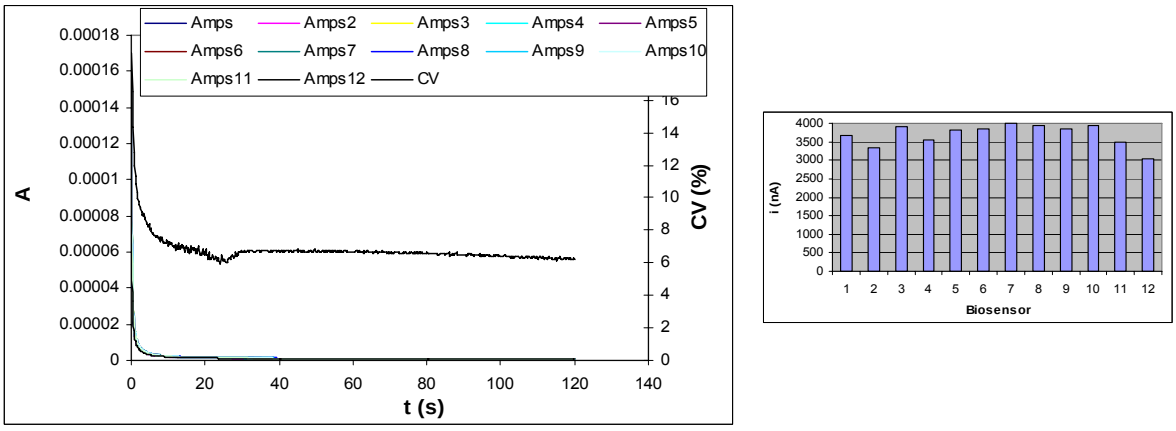

Fig. 2.59. Chronoamperograms, CV values and individual current responses for 12 OTA sensors on a single ceramic comb, responding to 2.5 ppb OTA-spiked wheat.

A second comb of sensors, this time for a batch of sensors prepared identically, but now 19 days old, gave a CV of 10%. The mean current response for this second comb was 2524 nA, compared to 3697 nA for the comb from the other batch of sensors. Clearly the variation both in mean current responses between batches and in coefficients of variation for sensors within individual combs was greater than acceptable.

Given the relatively high background currents found in this assay, and the fact that the working current range is between 500 and 1000 nA, an acceptable standard deviation would be less than 100 nA. For a mean current response of 3000 nA, this equates to a desirable intra-comb CV of 3.3% for 12 sensors.

A further experiment was conducted on OTA sensors prepared on 17-05-06 which were 2 days old. Four combs of 12 sensors were tested using wheat extract, this time spiked with 1ppb OTA. The CV values and mean current responses obtained for these combs are shown in Table 2.7. Within this batch of sensors, the mean current response for 4 combs was 2301nA, with a standard deviation of 189nA, giving a CV of 8.2% from comb-to-comb. The intra-comb variation however, for 12 sensors, ranged from 11.1% to 21.3%.

Comb number	Mean current response (n=12), nA	Coefficient of variation (%)
1	2416	11.1
2	2353	13.8
3	2021	21.3
4	2414	14.9

Table 2.7.

CV values and mean current responses for 12 OTA sensors on each of four ceramic combs, responding to 2.5 ppb OTA-spiked wheat.

Further tests on the batch of sensors prepared on 28-04-06, now aged 26 days, and tested on OTA-spiked wheat at 1ppb, revealed intra-comb CVs of 6.8, 12.1 and 8.1%. The mean current response was 2375 nA.

A calibration plot using the same batch of sensors, now 27 days old, was obtained using wheat spiked with OTA over the concentration range 0 - 2.4ppb. The resulting calibration plot is shown in Fig 2.60.

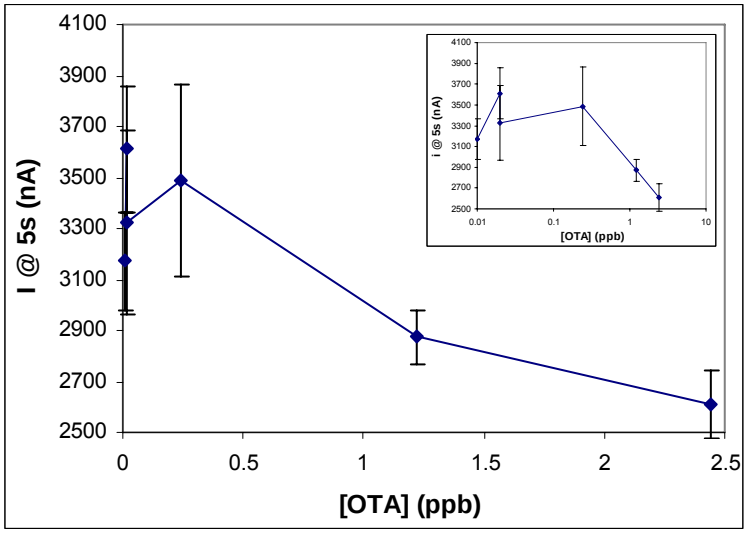

Fig. 2.60. Calibration plot obtained for OTA-spiked wheat extracts tested using ceramic sensors and fully automated electrochemical immunoassay. (Insert uses linear-log plot to expand the low-free-OTA region).

Data for Fig 2.60 are given in Table 2.9 below. The CVs for replicate sensors fell within the range 3.7% to 10.8%. This indicated that it was possible to obtain good precision within a comb. However, clearly it was also possible to obtain greater than 10% variation within any comb; also there was a difference in the mean current responses obtained for the same spiked extract when tested using two separate combs (compare the 0.02 ppb results on combs 1 & 2: 7.8% variation).

ppb		mean nA	SD	CV (%)
0.01	(comb 1)	3171	195.2	6.2
0.02	(comb 1)	3610	244.6	6.8
0.02	(comb 2)	3327	360.2	10.8
0.24	(comb 2)	3487	375.6	10.8
1.22	(comb 4)	2874	105.0	3.7
2.44	(comb 4)	2609	136.2	5.2

Table 2.9. Current responses, SD and CV data for OTA assay performed using autoinstrument. Data are taken from three different sensor combs as indicated.

This result indicated that although the overall behaviour of the sensors gave a calibration plot showing good overall shape (particularly in the 1 - 2.5 ppb region), there was a requirement for improved reproducibility at the lower OTA concentrations.

A new batch of OTA immunosensors was prepared on 20-06-06, using a new batch of SPCEs printed on ceramic substrate; the printing of the dielectric layer had been modified to improve the appearance of the printing in terms of the spread of the ink over the ceramic layer in order to minimise the occurrence of pinholes which were a possible source of imprecision. By eye, these sensors appeared to be of improved quality; also altered registration of the printed layers facilitated ease of comb preparation by improving the ability to "snap" out the defined comb shape from the printed sheet. When tested for reproducibility, these bare electrodes showed excellent precision (see Section 2.2). On DAY 1 after preparation, OTA immunosensors were tested for reproducibility by being run through the entire OTA immunoassay in the absence of free OTA. Coefficients of variation for two separate combs were: COMB 1: 327% for n=12, dropping to 8.3% for n=10 electrodes; COMB 2: 6.2% for n = 12 electrodes. Interestingly, the behaviour of the current response with time for this batch of sensors differed from previous batches in that precision improved with time of sampling. So, for instance, at 5s, precision was 10.2%, at 30s it was 7.1% and at 100s it was 6.2% for comb 2.

When tested in the same way on DAY 5 after preparation (storage at 4^{o}C, dessicated), precision again improved with time of sampling. So, for COMB1, CVs were 8.9%, 5.3% and 3.5% at times 5, 30 and 100s for n=11 sensors (25.9% for n=12 sensors). A second comb gave a CV of 7.2% at 100s (n=12 sensors).

An examination of the mean current responses for each of these combs showed a CV of 7.5% for mean current responses measured at 5s. The size of current response obtained correlated with the particular comb (R^2=0.86) rather than the day of testing (age of sensor; R^2=0.03).

Taken together with data from the previous batches of sensors, these results indicated that bare electrodes showed good precision on each comb of electrodes tested, and that precision after antibody coating (even by BioDotting) and immunoassay performance dropped to around 7% to 10% CV for replicate sensors/combs. In itself, this was a reasonable finding, given the number of manipulations/assay steps involved. However, as discussed above, the required precision for a useable assay, given the size of the background current responses in the OTA assay, would be around 3%.

A calibration plot for OTA-spiked wheat was performed using this batch of sensors. However, the plot (Fig 2.61) showed a very pronounced hook effect at low OTA concentration, even after blank-correction (subtraction of a blank sensor signal at each OTA concentration). The reason for this effect is unknown, given that all known assay parameters were the same as those used for the plots obtained in Figs 2.57 and 2.60. The only variable was the identity of the wheat extract; to implicate the wheat would infer that wheat encourages a higher density of biotinylated OTA to bind antibody, causing steric hindrance of SA-ALP enzyme at low free OTA concentration and a consequent hook effect. The alternative solution is that the antibody loading, and other reagent concentrations which were optimised for the previous ceramic sensors, now needed re-optimising for the latest batch of SPCEs.

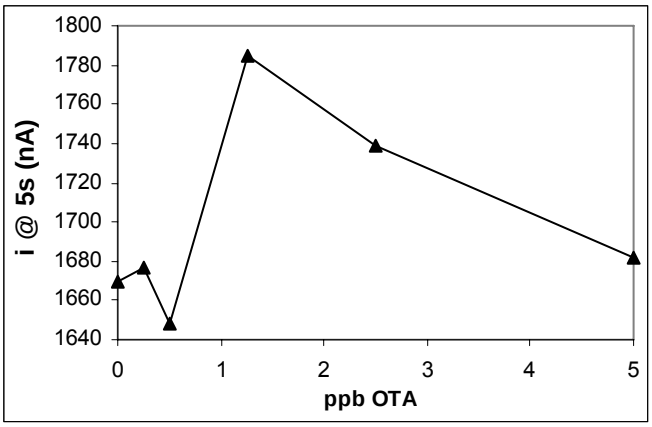

Fig. 2.61. Calibration plot for fully-automated OTA assay using sensors prepared on 20/06/06. The same plot shape was observed taking currents at 5s, 30s or 100s.

In previous studies on progesterone sensors we had used carbonate buffer, pH9.6 (CB) as the coating buffer with good success. For the next studies, sensor combs were therefore coated with antibody diluted in CB rather than PBS. Stabiliser was not included at this stage.

Re-optimisation of the antibody loading on this batch of sensor combs gave a linear drop in current response with falling antibody loading (not shown). However, in order to achieve this kind of plot it was necessary to use a higher concentration of biotinylated OTA and SA-ALP than with the previous sensors. Thus, when combined with biotinylated OTA at 1/500 and SA-ALP at 1/150 dilutions, an antibody titration was obtained which indicated that the best choice of antibody loading would be 1/30, thus agreeing with the previous loading experiments above. It seems possible that variation in the dielectric layer and/or surface charge/hydrophobicity from one batch of SPCEs to the next could lead to the requirement for different concentrations of labelled reagents in order to achieve the optimal binding/signalling behaviour.

Using the newly-optimised reagent concentrations, a calibration plot was obtained for OTA in buffer solution (ie. OTA diluted in 20%MeOH/PBS/0.1%Tween 80 as before), performing the assay manually (including casein block) with a LSV measurement step. The resulting plot is shown in Fig 2.62. This plot showed reasonable behaviour at low OTA concentration, and a working range between 1.2 and 2.5 ng/ml OTA.

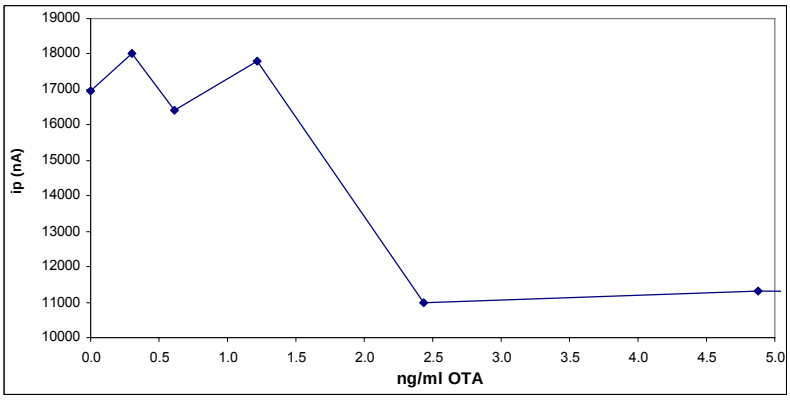

Fig. 2.62. OTA calibration plot in buffer for 20/06/06 ceramic comb immunosensors using manual assay/LSV measurement step.

Using the same reagent conditions, a calibration plot was then obtained in OTA-spiked wheat performing the assay manually (including casein block) with a LSV measurement step. The resulting plot is shown in Fig 2.63 for one ceramic immunosensor comb. This plot showed excellent behaviour throughout the calibration range from 0 - 39 ng/ml OTA.

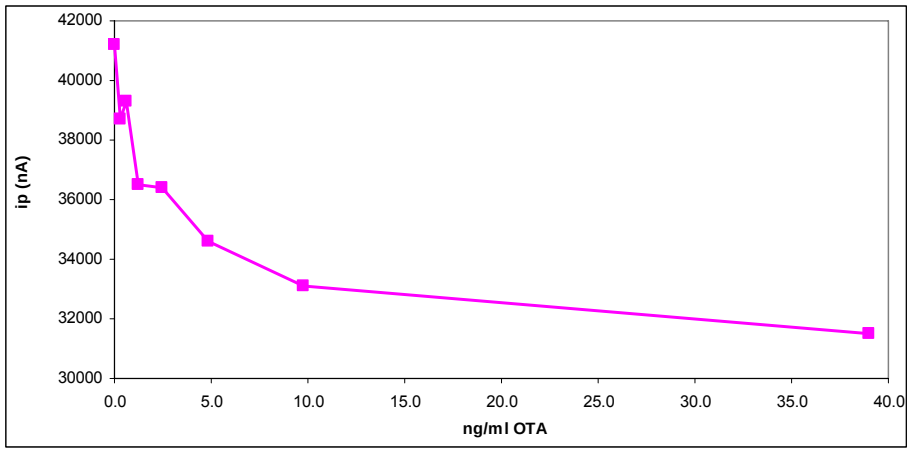

Fig. 2.63.

OTA calibration plot for OTA-spiked wheat using manual assay/LSV measurement step.

Conclusions for OTA

This section of the Report has described a series of experiments which have been conducted with the ultimate aim of developing an electrochemical immunoassay for Ochratoxin A which can be operated in an automated fashion and can be used to determine the concentration of this mycotoxin in a food matrix such as wheat. Through an iterative process, these experiments have succeeded in producing a functioning immunoassay with a working range suitable for determining levels of OTA usually found in wheat. Initially, the immunosensors were fabricated from polyester and then were screen-printed onto ceramic substrate with improved robustness and the potential for automated operation. This part of the project has succeeded in producing an assay which when operated manually, with a linear sweep measurement step, can produce excellent data on individual combs of electrode sensors (eg. Fig 2.63). There is no doubt, however, that levels of precision between and even within individual combs of immunosensors do not at present meet acceptable requirements for a robust and reproducible assay, even when sensors are prepared with antibody stabiliser.

Regarding automation, the Uniscan instrument is capable of operating in a robust manner and shows flexibility in terms of its programmability. However, the experiments undertaken on real wheat samples have highlighted the limitations of the chronoamperometric measurement step. Even if blank sensors were included for every test sample (thus reducing the number of samples tested), any variation in performance of individual sensors would compromise the data obtained using a blank subtraction. The most reliable data appear to be obtained using a scanning waveform such as linear sweep (or differential pulse) voltammetry. Each sensor then has its own baseline from which to read the analytical response.

Deoxynivalenol (DON)

Testing antibody, DON-biotin and SA-ALP reagents by ELISA.

Using antibodies directly as capture antibodies.

Two candidate antibody reagents, R177 and R178 (both rabbit sera from IFR, Norwich) were to be tested for their ability to bind biotinylated DON (Tepnel Biosystems Ltd). An ELISA assay in 96-well microtitre plates was set up in order to be able to try out various combinations of antibody, biotinylated DON and streptavidin-alkaline phosphatase (SA-ALP) reagents to test for DON-specific binding and to arrive at an optimised set of conditions. The assay was performed in a competitive manner in a similar way to the previous AFB1 and OTA assays described above. ELISA wells were coated with dilutions of R177 or R178 antibody in carbonate buffer, pH 9.6 and incubated overnight at 4^{o}C overnight. After being rinsed with PBS, wells were blocked with a solution of 3% BSA/PBS for 2h at room temperature (RT). Fifty microlitre volumes of biotinylated DON, together with 200 μl per well of 20%MeOH/PBS/Tween80 (to simulate a free DON-containing sample) were then added for 60 min. After being washed, wells received 100μl of SA-ALP for 30 min. Finally, wells were washed before 150 ml of pNPP solution was added per well. After waiting 60-90 min for colour development due to enzymatic production of p-nitrophenol, the absorbance of each well was measured at 405nm using a plate reader.

In this initial experiment, neither the R177 nor the R178 antibody showed any specific binding of DON-biotin. Fig 2.64 shows that there was a hint of specific binding using R177and 1/1000 DON-biotin (with 1/1000 SA-ALP) but that responses in the absence or presence of 1/100 DON-biotin were almost equivalent to this (low absorbance) level. Consequently, it appeared that a direct capture by the anti-DON antibodies would not generate specific binding of DON-biotin.

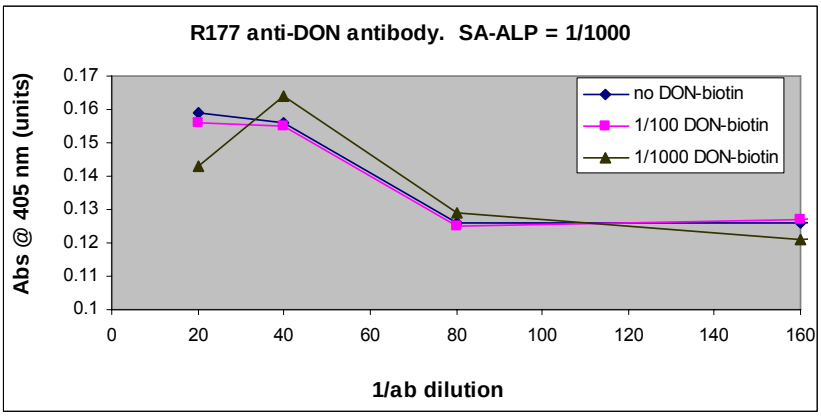

Fig. 2.64.

Titration of anti-DON antibody, R177 used directly as capture antibody in ELISA assay.

Using antibodies via a primary capture antibody layer.

It is well-known that the orientation of an antibody on an ELISA plate can be influenced by using a primary capture layer (antibody or Protein A) which is specific for the constant regions of the heavy-chain regions of the antibody structure. In this way, the likelihood of orientating the antibody with its antigen-binding regions facing away from the substrate is improved and the antigen-binding enhanced.

Thus, a second ELISA was set up for DON, this time incorporating a first step in which a mouse anti-rabbit IgG reagent (over the concentration range 0.25-2.5 micrograms/well) was laid down overnight as a capture layer for the rabbit anti-DON antibody, R177. The rest of the assay was performed as before. Various dilutions of the DON-biotin reagent were tested; the SA-ALP dilution was fixed at 1/500. The results of this experiment showed clear evidence that specific binding of DON-biotin correlated with increasing concentration of DON-biotin and that a titration of the R177 antibody was occurring. Fig 2.65 illustrates this phenomenon by showing a plot of data obtained for an assay performed using the mouse capture antibody at a concentration of 2.5 μg/well. The occurrence of a hook effect is evident at R177 a dilution below 1/160 suggests that this dilution, or a slightly greater one, would be suitable for further experiments.

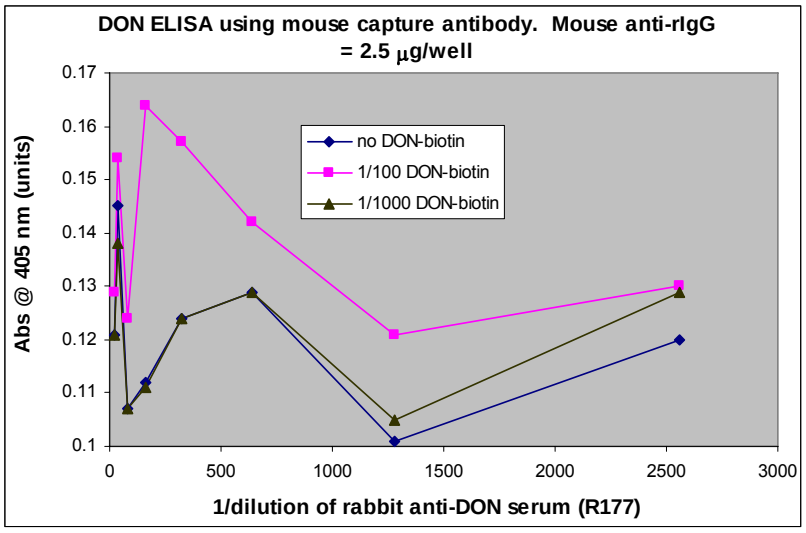

Fig. 2.65.

DON ELISA using mouse anti-rabbit capture antibody layer.

In a second attempt to improve the DON ELISA by using a primary capture antibody, the mouse anti-rabbit IgG reagent was substituted by a goat anti-rabbit IgG reagent. The above experiment(s) were repeated. Once again, evidence for specific binding of DON-biotin occurred, being most impressive again in the case of wells which had received 2.5 μg/well of the goat antibody. Fig 2.66 illustrates the data obtained. In this case, there was slight evidence for a hook effect at a dilution of R177 of 1/20 only.

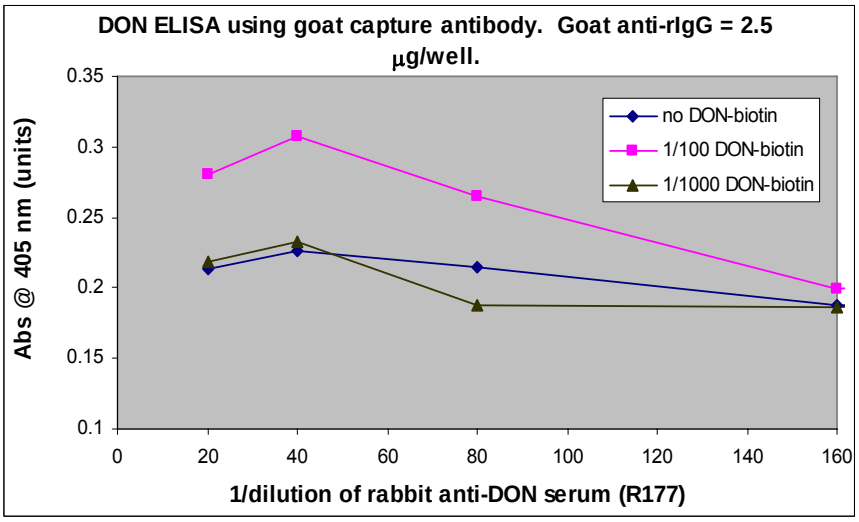

Fig. 2.66.

DON ELISA using goat anti-rabbit capture antibody layer.

In summary, it appears that when used in conjunction with a primary capture antibody, the R177 rabbit anti-DON serum may be a suitable reagent for use in developing an electrochemical immunoassay for DON. The choice of the mouse or goat anti-rabbit IgG reagent would be a compromise between the likelihood of observing a hook effect in the final sensor, and the amount of R177 reagent required to produce a given number of sensors. Thus, the goat antibody shows less evidence of a hook, but may be required at a dilution of around 1/50 to produce the required sensitivity of signal. Really, both reagents should be tested empirically for performance in DON calibration plots in combination with the R177 antibody.

Conclusions for DON.

The results reported in this section indicate that work on the DON electrochemical immunoassay is clearly at a preliminary stage of development. However, the finding that the R177 antibody will bind DON-biotin specifically when used in conjunction with a capture antibody is a significant step towards further development. The R178 antibody remains to be tested, and then the next step will be to prepare immunosensors by coating SPCEs with capture antibody-then-R177/8. The necessity for this two-antibody approach will require the introduction of a new way of incorporating a stabiliser into the immunosensors, ie. a single-step coating process will not be possible; instead, the capture antibody will need to be coated, followed by a second step in which the R177/8 is applied, together with a stabiliser which with the aim of creating a sensor with a long shelf-life.

Overall Conclusions

The work summarised in this Report has achieved the following goals:

1) Fabrication of screen-printed carbon electrode (SPCE) arrays printed on both polyester and ceramic substrate.
2) The development and testing of an automated 96-well plate platform and 12-channel potentiostat for performing automated immunoassays/enzyme assays using SPCEs on ceramic substrate. This instrument operates in chronoamperometric mode.
3) The development of a prototype electrochemical immunoassay for Aflatoxin A which succeeds in manual operation in buffer solution. Sensors fabricated/tested on polyester combs.
4) The generation of aflatoxin cross-reactivity data which is consistent with that obtained using other immunoassay methods.
5) The development of a prototype electrochemical immunoassay for OTA which is successful in manual operation in buffer and wheat and has been tried in automated mode. Sensors fabricated/tested on ceramic combs. This work has identified the requirement for an instrument which can use a scanning electrochemical waveform as the measurement step, rather than a chronoamperometric mode.
6) The identification of candidate reagents for development of an electrochemical immunoassay for DON and the necessity for a primary capture antibody.

This work has led to integration of electrochemistry and immunoassay technology into an automated platform which, with further development, can be exploited for use in both immuno- and enzyme-assay formats in combination with screen-printed electrode/biosensor/immunosensor arrays. This platform has the potential for rapid sampling and generation of data suitable for neural net processing in a laboratory or “off-site” locations.

Section 3. Instrument development

Introduction

The Mycotoxins will be measured by the amperometric reaction of a sensor. The sensor comprises a small screen printed substrate which is chemically modified to produce an amperometric response to Mycotoxins. The amperometric response of the sensor is stimulated and measured by a potentiostat. The proposed system will be multi channel, such that several sensors may be measured simultaneously. The measurement requires that the sensors be exposed to different solutions at various stages of the measurement procedure. These requirements have led to the concept of an instrument which is based on a multi-well plate and a sensor array which is able to be immersed in different rows of the well-plate as required.

System Overview

The system physical components will comprise the mechanics illustrated in the conceptual drawing (Fig 3.1) together with an electronics rack and a standard Windows based PC. The PC will run a bespoke software application to control the hardware and manage the measured data. Furthermore, an internal system check will verify the system is functioning correctly. Further to issue 1.01 of this document it has been suggested that the system mechanics should have a lid to maintain a dust free environment within the multi-well plate area.

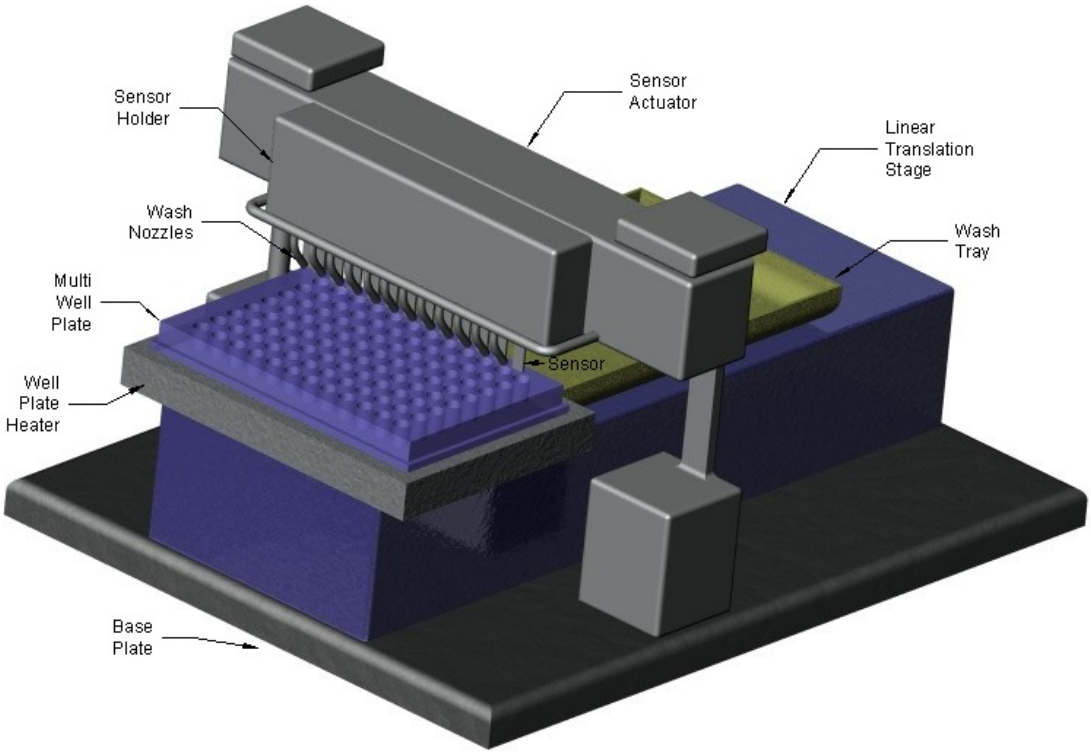

Figure 3.1 Conceptual drawing of the system mechanics

Measurement Procedure

The instrument will be required to implement the measurement procedure defined in this section.

The procedure assumes that the washing of the sensors is performed in a separate row of the well plate. This method would have a considerable advantage in a commercial version of the instrument where a pre-prepared well plate with a tear of lid could be supplied as a consumable. Because this washing approach is unproven the instrument will also incorporate washing nozzles which could perform a more conventional washing process.

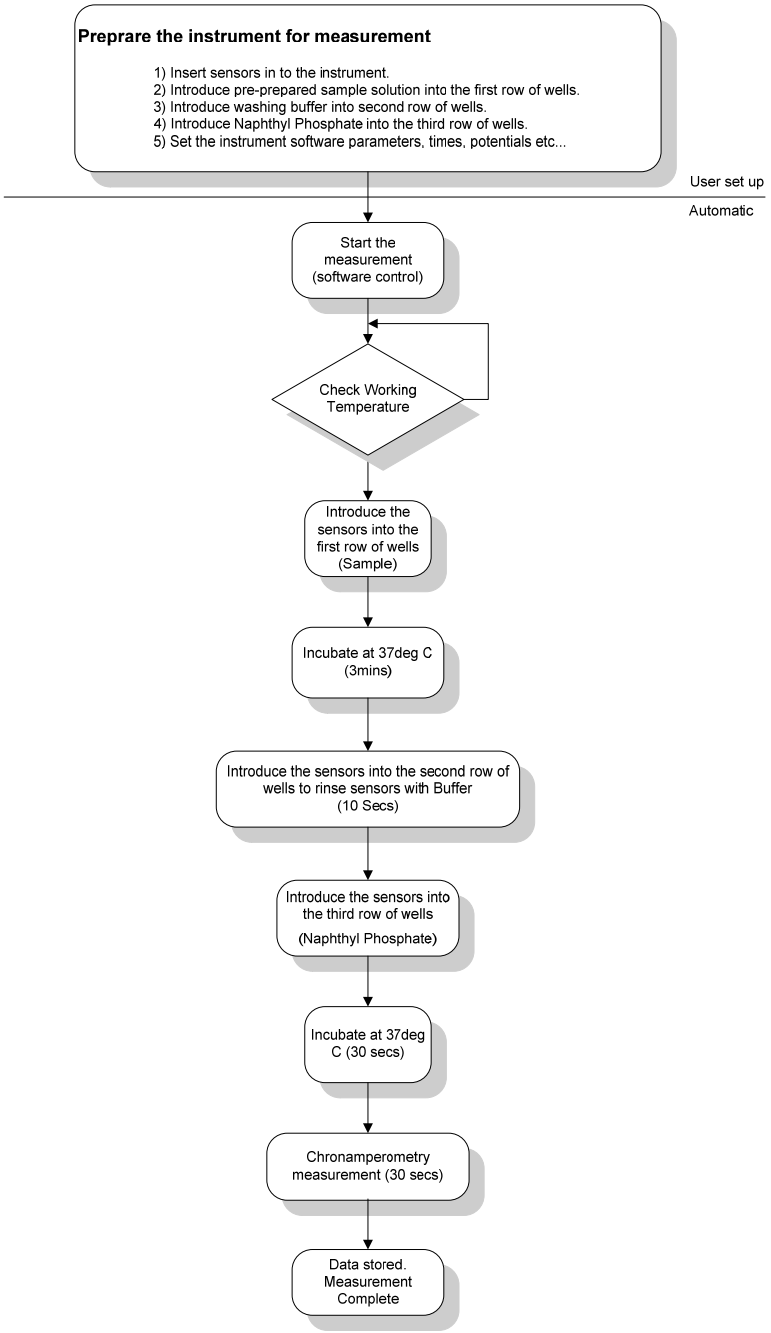

System Components

The major components of the system are specified here:-

Sensor – A screen printed Mycotoxin sensitive amperometric sensor. The system will accommodate up to 12 sensors at one time in a 1 x 12 array. Figure 3.2 below shows the sensor detail:-

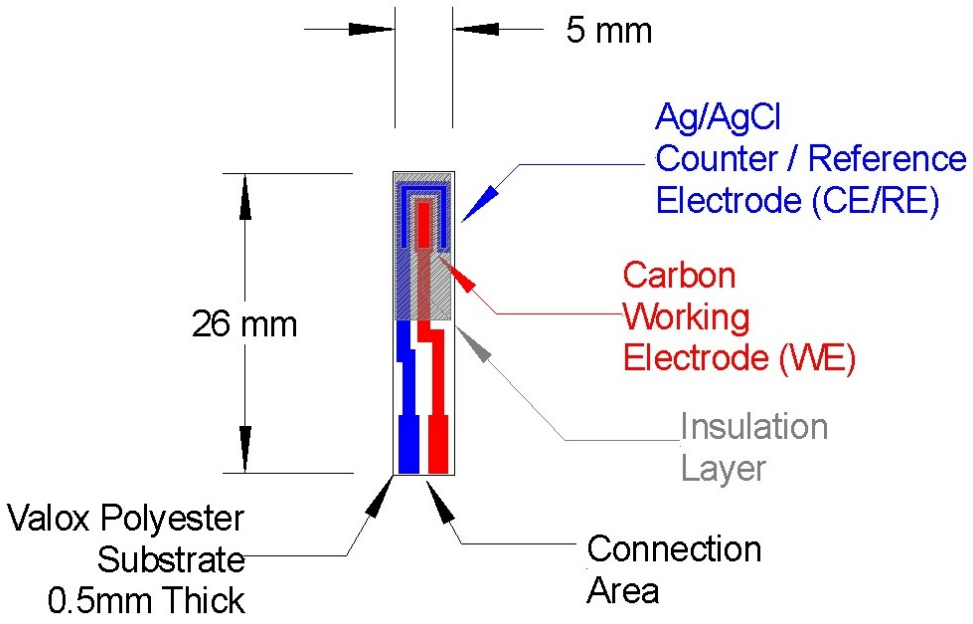

Figure 3.2 Sensor General Arrangement

Sensor Holder – An easily removable holder which will provide the physical mounting required by the array of sensors and the electronic connections required to interface the sensors to the system. The initial holder will accommodate individual sensors, though it is envisaged that the system will accommodate an array of sensors on a single “comb” shaped substrate in a commercial version.

Multi Channel Potentiostat – An array of 12 potentiostats which stimulate and measure the response of the sensors.

Each of the Potentiostats will have the following minimum specification:-

Applied Potential Range:	+/- 1.000Volts.
Applied Potential Resolution:	1 mV.
Applied Potential Accuracy:	+/-1 mV.
Measurable Current Range:	+/-30 µA.
Measurable Current Resolution:	1 nA.
Accuracy:	+/-1 nA, +/-0.1% of Reading (whichever is greater).
Measurement Technique:	Chronoamperometry.
Typical Sample Rate:	1 Hz.
Typical Number of samples:	30.

Communication with the controlling computer.

Figure 3.3 Typical Potentiostat Card and Electronics Rack

Electronics Rack – An enclosure containing all the electronic modules. This includes the array of potentiostats and modules to control pumps and solenoids. The rack will host the electronic connections between all the system components.

Multi-Well plate – A standard 96 well (12 x 8) plate used to hold the solutions, into which the sensors are immersed.

Well plate heater – An aluminium tray to hold the Multi-Well plate. The tray will incorporate resistive heaters and a temperature sensor capable of maintaining the Multi-Well plate at a constant temperature of 37 deg centigrade.

Linear translation stage – A motor driven linear translation stage on to which the Well plate heater is mounted. The translation stage will be capable of positioning the Multi-Well plate rows such that the array of 12 sensors may be aligned with any of the 8 rows in the plate. The stage will also provide extended movement to allow a sensor wash to be performed via the nozzles. In this case the waste liquid from the wash will be collected in the wash tray.

Sensor Actuator – A structure which will support the sensor holder above the well plate and by action of a motor, lead-screw and linear bearing, lift the sensors in and out of the well plate wells. This action will be controlled by the personal computer software application.

Sensor Wash nozzles – a series of 12 nozzles which will provide a wash jet on to the sensor, on electrical switching of the wash pump under software control.

Base Plate – The plate on to which the system is constructed.

Wash tray – A tray to catch the waste from the sensor washing process.

Computer / Software – A Windows compatible PC will run a bespoke software application which will provide all the control and data processing for the instrument.

Software Specification

The system software will be a Microsoft® Windows application running on a standard PC. The software will provide the following functionality:-

- Control the hardware, to implement the required measurement procedure.
- Provide user inputs such that the required experiment variables may be altered by the user.
- Display the chronoampermetric data in graphical form on the PC monitor.
- Provide disk file support for saving and opening measurements.
- Provide a facility such that the data may be simply imported to a specific neural-net analysis package.

The Completed Instrument.

Figures 3.4 to 3.6 show the instrument as delivered to UWE complete with linear stage, control electronics, laptop and software.

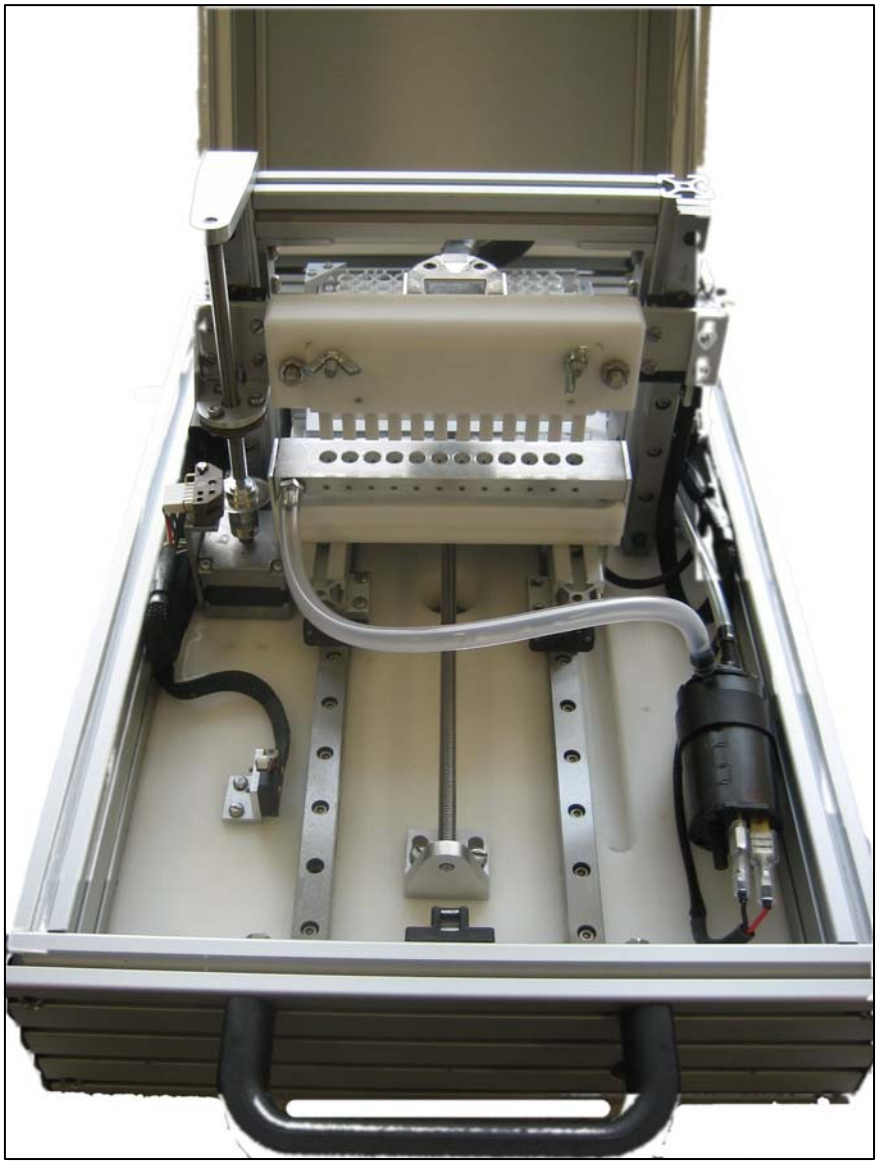

Figure 3.4 Linear Stage plus sensor comb.

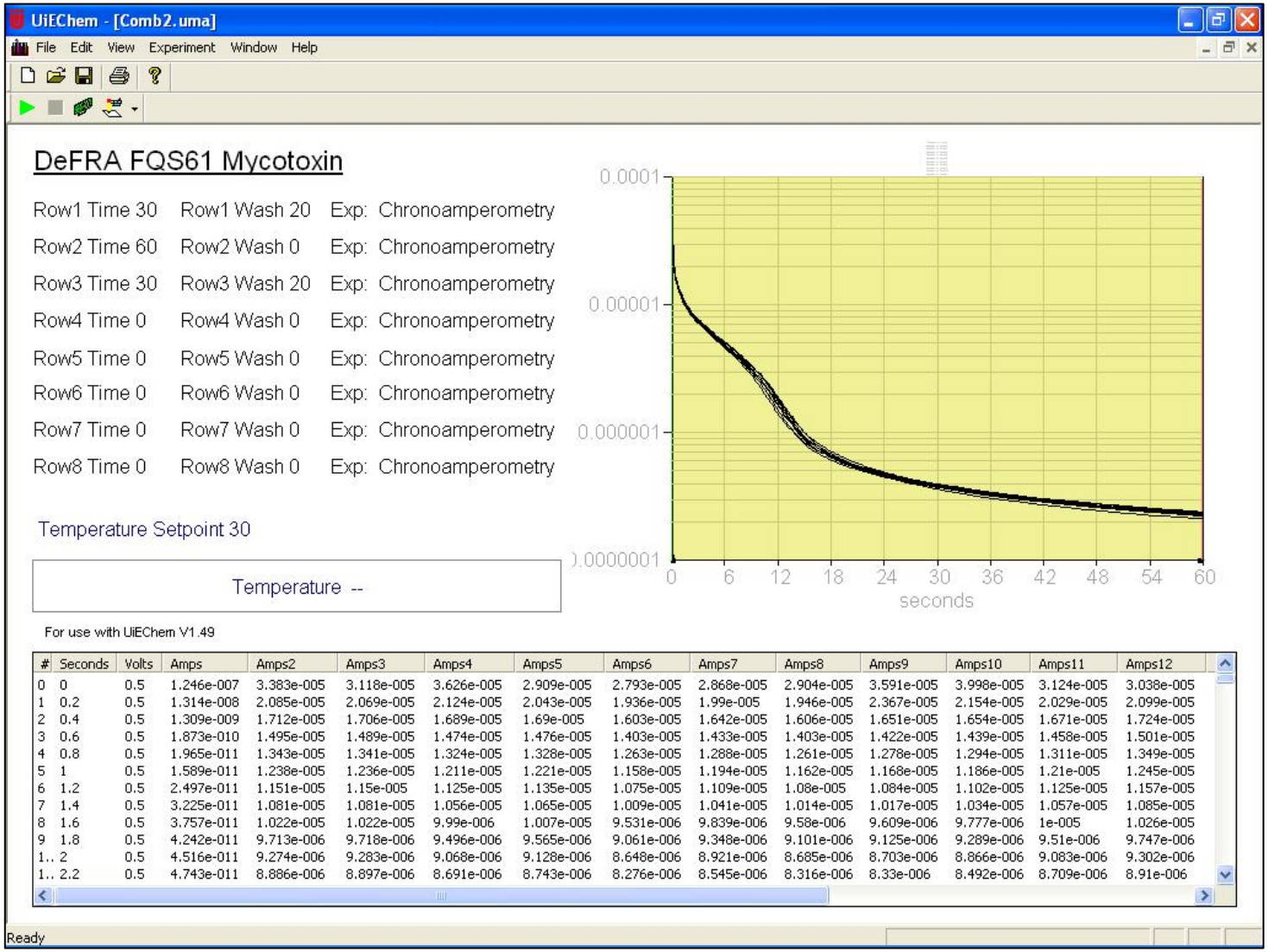

Figure 3.5. Full Instrument with linear stage, twelve way potentiostat rack, control electronics, PC and control software.

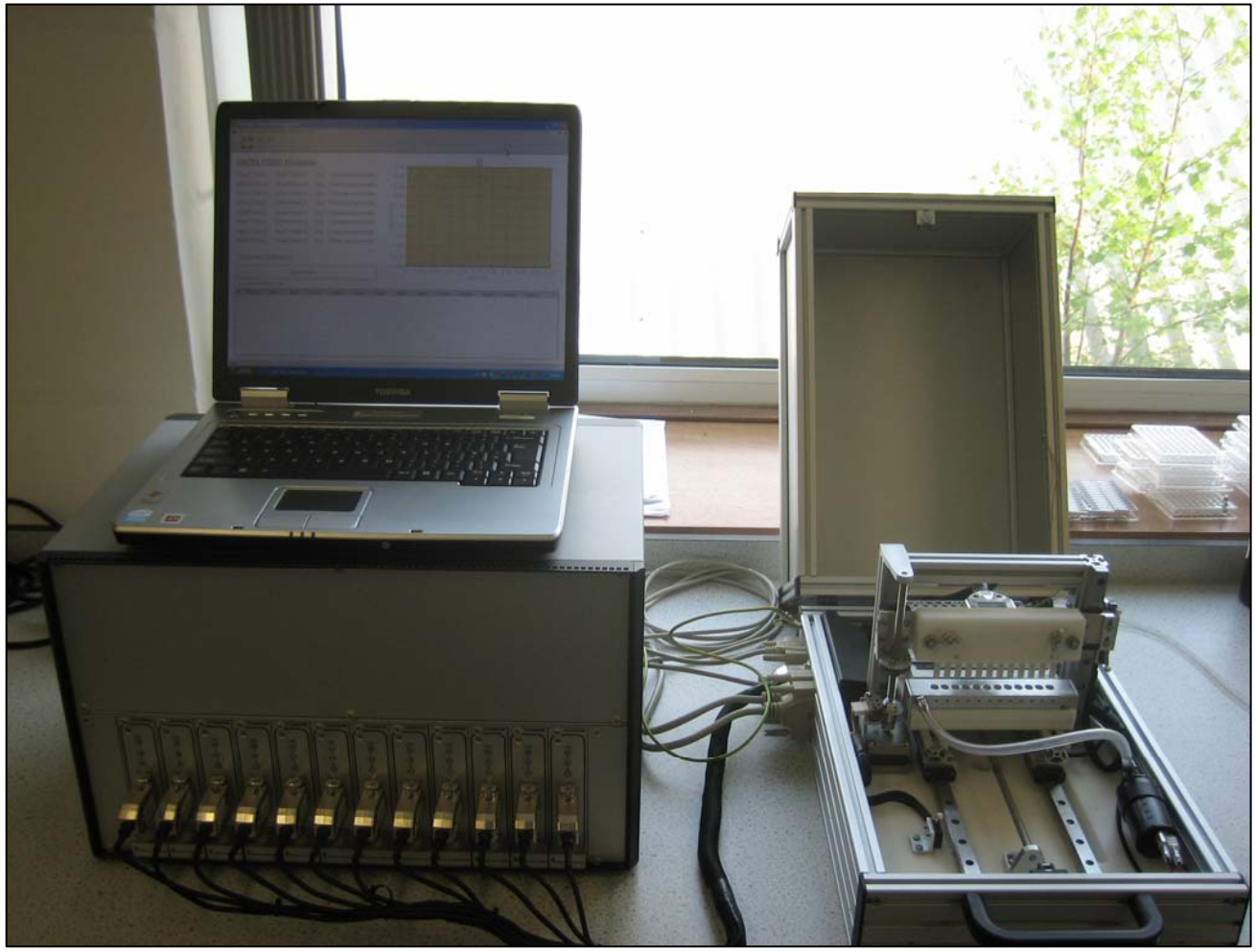

Figure 3.6. The DeFRA FQS61 Mycotoxin macro showing data from a ceramic comb detecting 1-napthol at Uniscan.

Instrument Performance; Dummy Cells.

The instrument was tested on a set of Randles circuits to determine the synchronicity of the switching and the variation of responses seen across the bank of twelve potentiostats. Figure 3.7 below shows the Randles cell used to test the system. This cell produces transients with a time constant of around 10ms and current peaks of ~100nA decaying to a steady state current of ~50 nA. The target measurement of the sensors was of the order of a few hundred nano-amps.

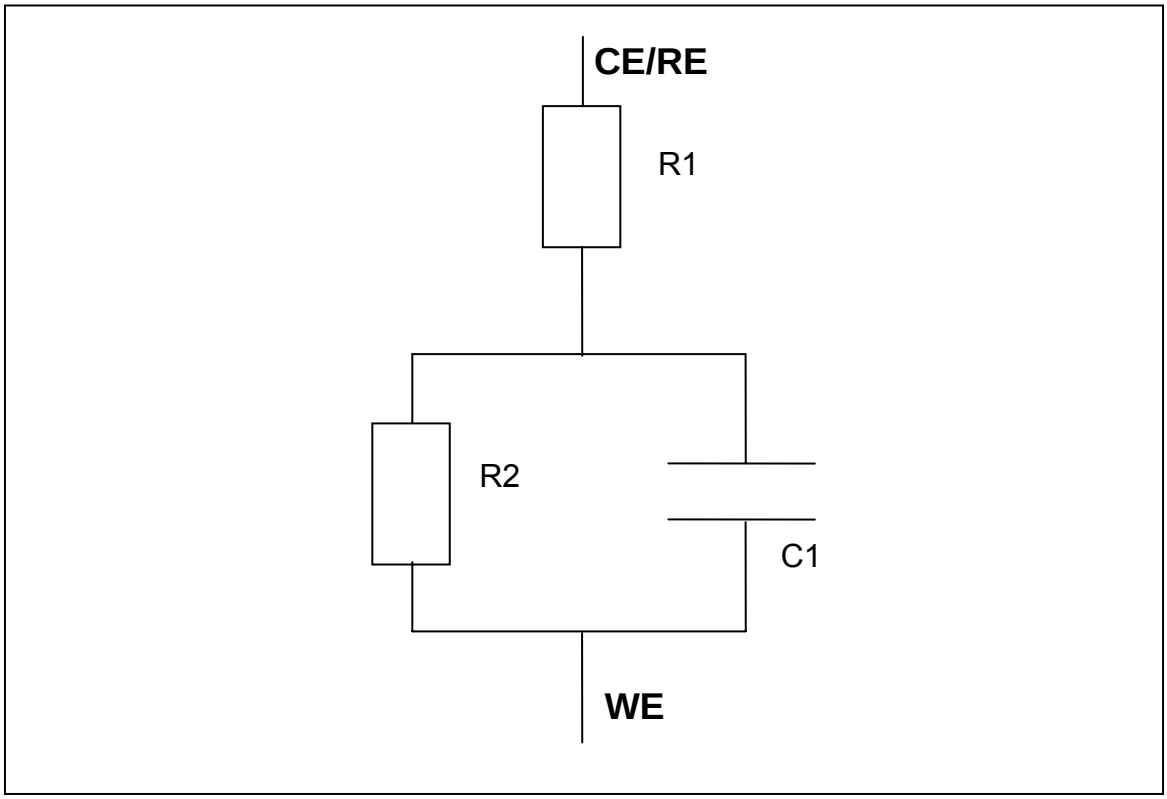

Figure 3.7. A classic Randles cell used for determining the system response to fast transients. Here, R1 = R2 = 10MΩ, C1 = 1nF.

Twelve Randles cells were constructed and the results of the system tests are shown in table 3.1.

Test	Result	Units
Synchronicity of switching across 12 potentiostats.	≤ 250	µs
Repeatability – 12 experiments performed on a single potentiostat with a single Randles cell. †	T: 0.45 S: 0.25	STD % of mean
Variation over 12 dummy cells – measured by a single potentiostat.	T: 1.04 S: 0.54	STD % of mean
Variation across twelve potentiostats – one Randles cell measured by 12 potentiostats.	T: 0.88 S: 0.96	STD % of mean
Variations across twelve potentiostats reading twelve Randles cells run separately.	T: 1.07 S: 0.95	STD % of mean
Variation across twelve potentiostats reading twelve Randles cells run simultaneously using the DeFRA macro.	T: 1.19 S: 1.62	STD % of mean

† T: transient, measured at 10ms after cell is switch on.
S: static DC value, measured over 45ms to 50ms after cell is switched.

Table 3.1. Accuracy and response of the instrument with dummy-cell loads.

Later work required that a Randles cell modelled on the responses of the velox sensors (and later, the ceramic sensors) be prepared. The cell required a peak current of around 60 µA decaying to a DC current of 200 nA in approximately 250 ms. A similar Randles cell was constructed to that shown in figure 3.8 with R1 = 8.57 kΩ, R2 = 2.5 MΩ, and C1 = 30 µF.

This cell required a current measurement over a large dynamic range between 100 µA to 100 nA ranges, depending on the sensor and solution concentration. The potentiostats were upgraded to include an auto-ranging function that automatically switched between the appropriate current ranges as circumstances dictated. A single Randles cell was constructed and used to test the newly upgraded potentiostats. The current trends for all twelve potentiostats and the associated standard deviations of the measurements are shown in figure 3.8 below.

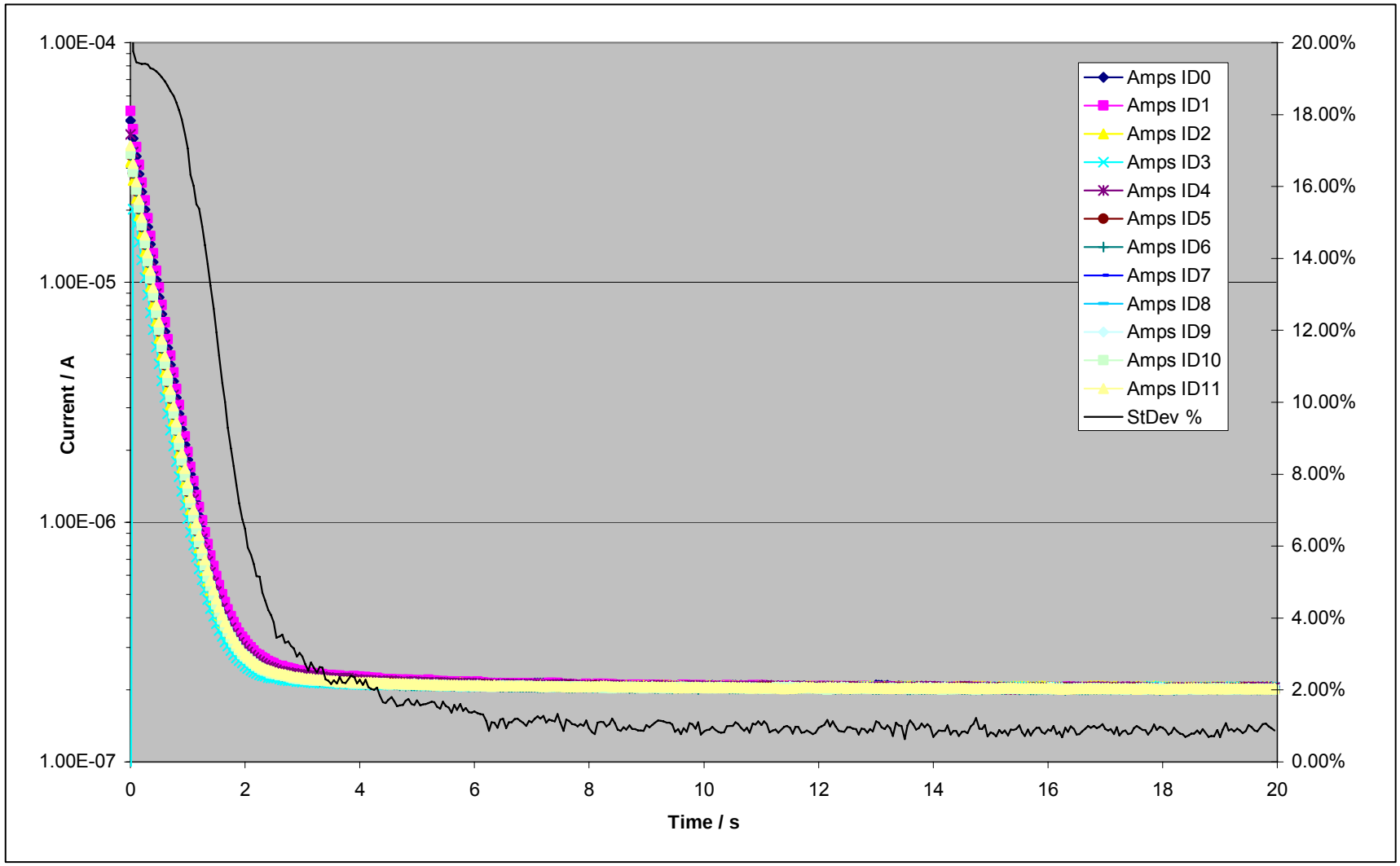

Figure 3.8. Randles cell modelled on sensor responses – 1 cell measured by twelve potentiostats with auto-ranging functionality. The solid trend shows the standard deviation as a % of mean and as a function of time. As can be seen, the minimum error of ~1% can be achieved (according to this model), after approximately a 5 second measurement delay.

Instrument Performance; Velox Substrates.

Table 3.2 shows data for nine consecutive runs of twelve sensors detecting 1-naphtol solution. The first two runs were taken without auto-ranging functionality; the remaining runs were taken with the new functionality.

Run	Sensor No's.	Standard Deviation Resulting
1	1-12	21%
2	13-24	51%
3	25-36	29%
4	37-48	36%
5	49-60	24%
6	61-72	19%
7	73-84	11%
8	85-96	12%
9	97-108	38%

Table 3.2. Percentage standard deviation of mean for Velox substrate sensor runs 1-9.

The first two runs had large standard deviations due to a large distribution of currents and the figures indicate this accurately. What is not apparent from the figures is that runs 3, 4 and 9 have their results adversely affected by either a single or a pair of rogue sensors reporting substantially different values from the other sensors. As these sensors were hand-cut from the Velox sheets and inserted individually into the sensor holder, it is believed that on occasion the sensors were handled unsuitably so that their response was degraded.

Instrument Performance; Ceramic Substrates.

Table 3.3 and figures 3.9 and 3.10 show data for two consecutive runs of twelve-sensor combs detecting 1-naphtol solution. The stage was modified to provide sensor-comb mounting and orientation guides and the data was taken using the auto-range function.

Comb	Sensor No's.	Standard Deviation Resulting
1	1-12	Broke irreparably
2	13-24	9%
3	26-36	4%

Table 3.3. Percentage standard deviation of mean for ceramic substrate sensor combs 1-3. (provided by GEM and AET)

Without the need to manually cut and insert the sensors the accuracy of the reading appears considerably enhanced. One detriment to the ceramic combs was their fragility; out of the three combs supplied, only two were successfully removed from the ceramic sheet. This was partly due to screen-printing overlap from the sensors to the redundant ceramic that was to be removed. However, a definite advantage to using the ceramic substrate beyond the accuracy advantage already stated was that sensor combs would be perfectly aligned when placed in the instrument sensor holder; something that was rarely the case with the Velox substrates. Although the micro-titre plate and positioning system could tolerate a small degree of variation in the sensor locations, there were occasions where the Velox sensors were too badly misaligned for the equipment to run.

Another point to note on the sensor data runs using the ceramic combs is that the initial current spike produced a low standard deviation signal between time = 0 to 5 seconds. A further 40 – 60 seconds are required to pass over the anomalous hump seen centred around 12 seconds.

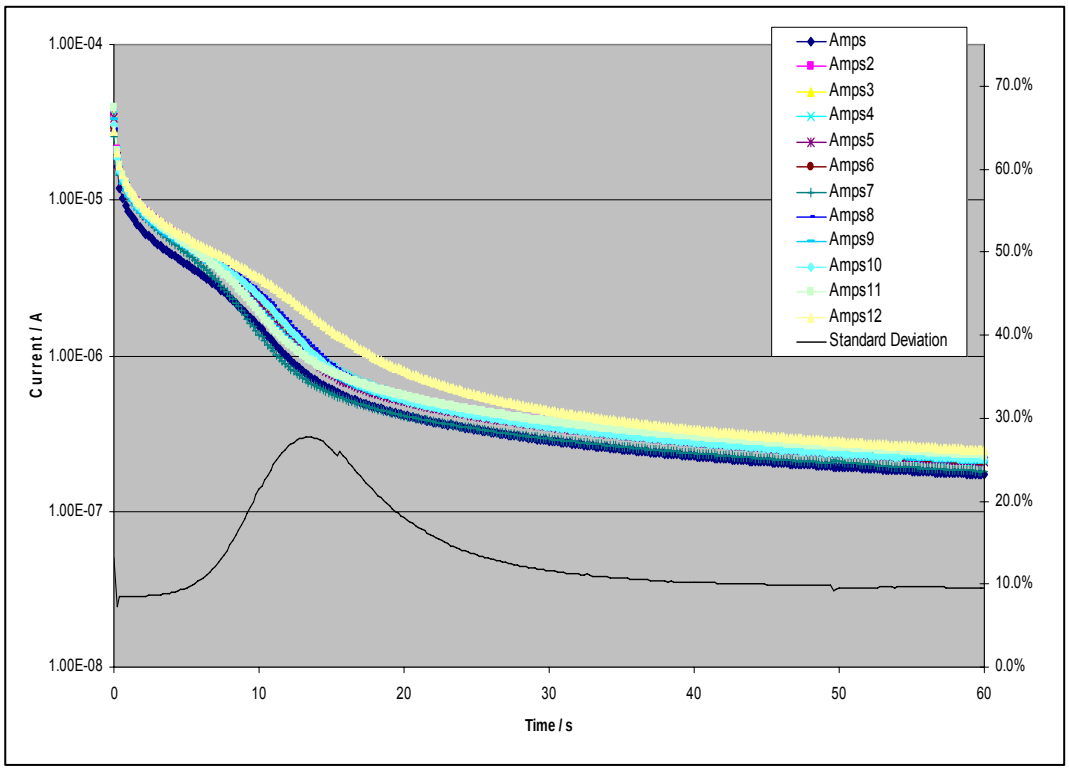

Figure 3.9. Ceramic Sensor comb 1. Current trend and standard deviation vs time.

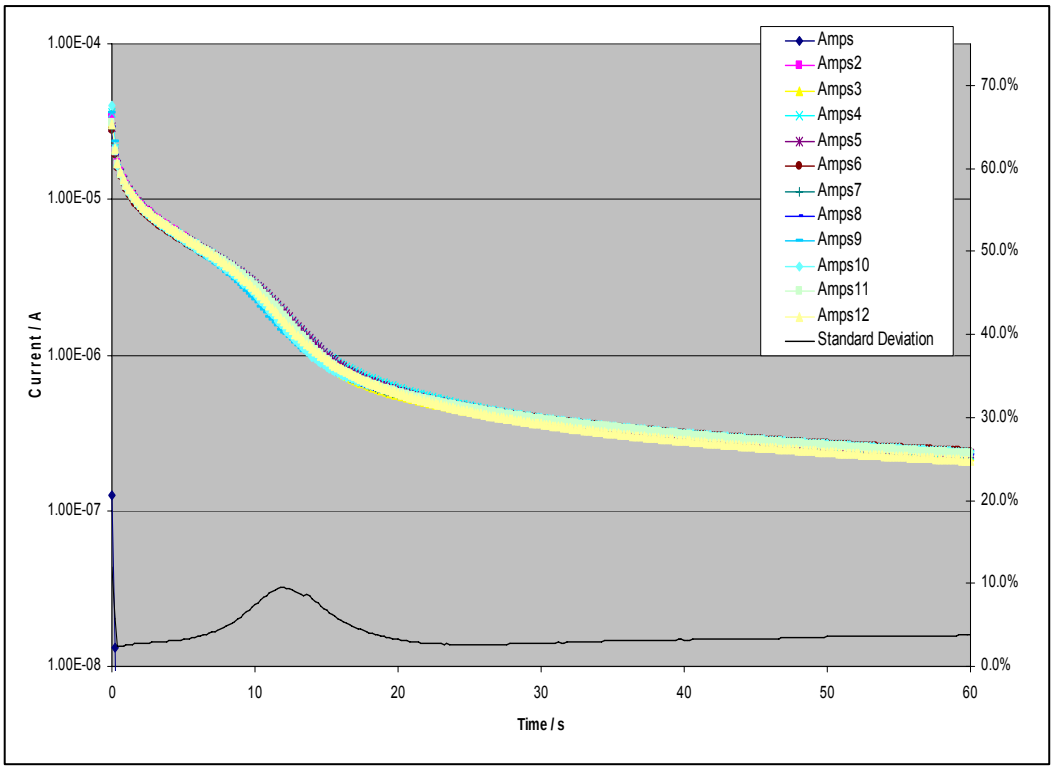

Figure 3.10. Ceramic Sensor comb 2. Current trend and standard deviation vs time.

Neural Net Interface.

A comparison between various market leading and commercial neural network packages was undertaken to gauge the functionality and cost of the packages on offer versus the neural net requirements for FQS61. NeuroSolutions 4.2 was deemed a reasonably priced and flexible system and had demonstrated its usefulness in previous projects. The main requirements for the training of a neural net are:

- calibration curves of analyte concentration versus dedicated sensor response
- calibration curves for cross-reactivity between the various analytes and varying analyte concentrations and the various sensors dedicated to the detection of analytes other than the ones being detected
- inclusion of standard deviation data for sensor response variations on the calibration trends described above
- calibration curves for the blank sensors versus all analyte concentrations

Given the above data, training data can be produced that includes single component, multiple component and noise. Three types of data are commonly produced:

- Training Data Set
- Test Data Set
- Final analysis Data Set

The first element is used to iteratively train the neural network against known values. The second data set is used to test the ‘trained’ network and judge its response to inputs that have not been used in the training process. The test data set is usually the key used to prevent over-training of the network and helps the operator judge when the network is ready. The final data set is another set that has not been seen by the network and will therefore provide a new set of inputs to test the network’s abilities.

After successfully completing the training of a neural network with data generated from calibration plots, data from real sensors detecting know (or spiked) samples can be fed into the system to determine the accuracy of the response and the success of the training. For obvious reasons, the sensor calibration response must be a true representation of the sensors being used including the standard deviation and cross-reactivity parameters.

One of the key points to note in selecting a neural network to perform the data extraction is that there are two extremes that a neural network is either not needed or cannot work. In one extreme there is the case where the sensors are so specific that they do not cross-react with other agents and so do not produce a ‘fingerprint’. In this case, it is more simple and efficient to measure the sensor response and read-off a concentration value directly from the calibration curve. In the other extreme, the sensor responses are so general that they react to all (or many) species with the same magnitude response; obviously there has to be some variation in the response magnitudes of the sensors for a fingerprint to be formed and for the neural network to be used successfully.

In the current system, the data provided to Uniscan details the ochratoxin-A and the aflatoxin-B1 sensor calibration curves (including sensor response variation at each point). To date there is no cross-reactivity data which may well be explainable due to the expected high specificity of the sensors; in essence, reading the concentration from the calibration trend would seem a more suitable method of determining the sample concentration. The origin of this expectation, as the author understands, is that these mycotoxins are classified in different families and thus the cross-reactivity would be small. Having a specific sensor is an obvious advantage; however it does negate the requirement for a neural net. It is also understood that for these reasons, the sensor and sensor interrogation methodology continues to be developed at the time of writing of this report.

It has been mentioned that the need for a neural network would be significantly enhanced if the detection was to look for the difference in the same family of mycotoxins, for example, to look for the difference in aflatoxins B1, B2, G1 and G2. Currently, however, exploitation has placed an emphasis on the production of a vomitoxin (DON) sensor.

Conclusion

All work packages have been completed with the exception of the neural network training. The instrumentation has three main parts; the controlling PC running bespoke software, the potentiostat and electronic control box and finally the linear stage. This provides excitation, measurement and control for up to 12 sensors over 8 individual rows, with variable wash times and temperature control. The system positioning is controlled by stepper motors with position feedback accurate to around 2 μm. The sensor head can take twelve individual 5mm sensors or a single 12-way sensor comb depending on the attachments used.

The software is run on a Windows XP laptop and provides control over the sequencing of the experiment, allows setting of experimental delays and whether or not the sample is perturbed (vibrated). Furthermore, the plate temperature, the potentiostats excitation and cell mode, and the wash times and pressures are all configurable. There is also functionality that will allow individual row settings to be saved for future recall and also allows exporting data to third party software via copy/paste type context menus.

System performance has been assessed by: fast response dummy cells, modelling of sensors' response using further dummy cells to give a specific characteristic signal, and finally by measurement of trends seen in both Velox and ceramic substrate sensors. The dummy cell tests shown that results of around 1% standard deviation (percentage of mean) can be expected from the equipment. The preliminary tests made with the ceramic sensors showed it is possible to achieve 4% standard deviation on sensor readings providing the sensors are handled carefully. Finally, the system was installed at UWE and instruction was given on the use of the FQS61 equipment. Overall, positive and constructive feedback has been given on the instrument relating to both its usefulness and what may be desirable in future iterations of the equipment.

Section 4 Evaluation

The aim of this Work package is to evaluate the prototype instrument and methodology, compare with current methods and investigate possible applications in an industrial context.

Antibody stabilization

Below shows the stability data determined for the anti-aflatoxin B1.
Several of the AET patented stabiliser formulations were screened for their ability to impart stability to the anti-aflatoxin B1 antibody. The anti-aflatoxin B1 was dried down in the presence and absence of the stabiliser formulation. The antibody was then tested optically for its binding affinity to the toxin. The results show (Fig 5.1) that the data line (No ab-P2, brown) and (AB1-P2, pink) had good reactivity of the antibody as determined by the difference in optical density between the zero-antibody control compared to the antibody sample. We can conclude that the stabiliser P2 retains the most antibody binding affinity of the stabilisers tested.

This antibody is stable for at least 5 months at 37°C which is equivalent to 8.5 months at room temperature.

Taking the results from the above study on the anti-aflatoxin B1 antibody, the P2 stabiliser was used as the best candidate for the stabilisation of the anti-ochratoxin antibody.

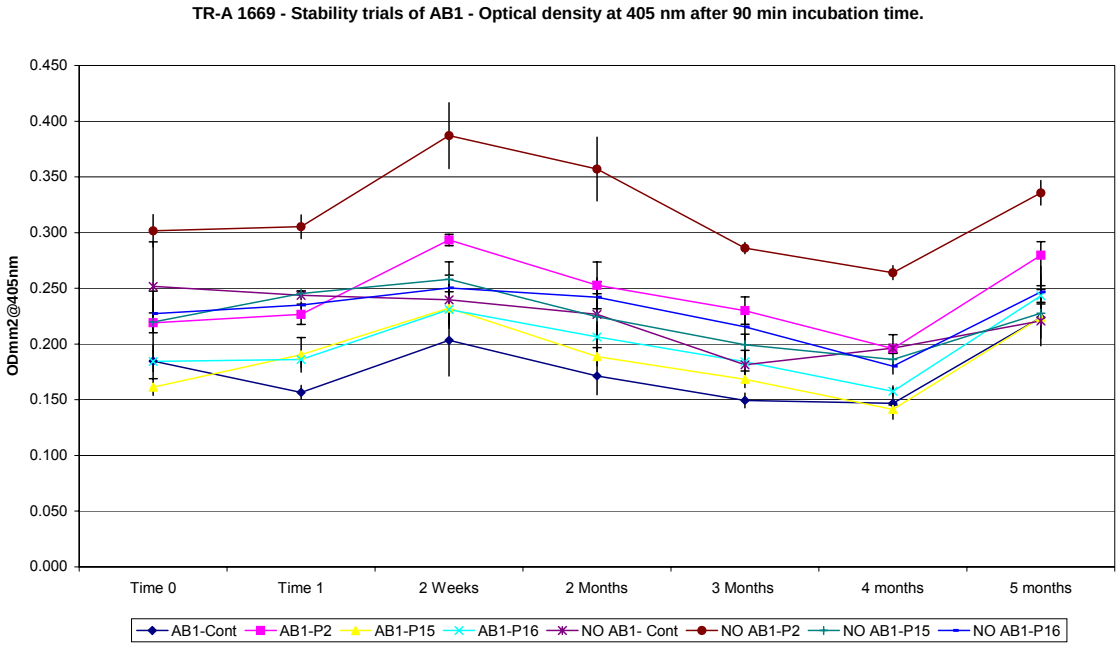

Figure 5.1. Stability studies using different stabilising agents with AB1 antibody. The optical density @ 405 nm was measured at different times, with and without AB1 and with P2 (Q2030317), P15 (Q20303017) and P16 (Q2030317)

The Ochratoxin antibody showed an increase in activity for the first month of testing, arriving to 158.85% after 29 days of incubation at 37ºC, shown in Fig 5.2. After 2 months the activity drops to 107.39%, to level of at 99.58% after 127 days of testing. The increase in activity of the antibody is a phenomenon that was seen before in other assays.

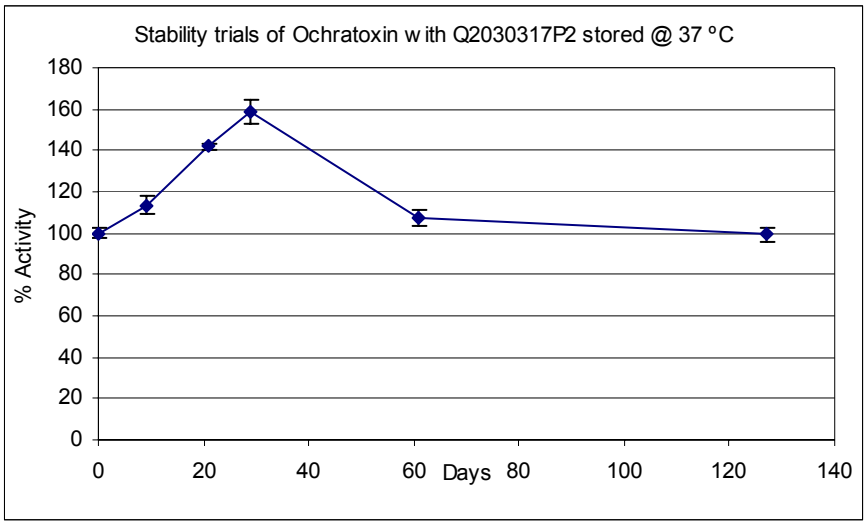

Figure 5.2. Stability studies of ochratoxin antibody

The anti-Ochratoxin antibody shows good stability for 127 days at 37°C. This is equivalent to 213 days or approximately 7 months at room temperature.

We can conclude from this data that both anti-aflatoxin B1 and anti-Ochratoxin antibodies show good stability in excess of 7 months at room temperature using the same AET stabiliser formulation Q2030317P2.

Validation

Evaluation at the end of the project was undertaken using mycotoxin standards (OTA) prepared at levels of interest for the detection of OTA in foods.

Work associated with improving the precision of the assays by fabricating new sensors delayed the end-user work by several months. The instrument has had to stay at UWE rather than be used in-situ in an end-user's laboratory.

OTA assay with real wheat samples tested by end-users.

Representatives from the end-users involved in the FSQ61 project attended at UWE and provided extracts from different samples of wheat which were either blank, or contained OTA at concentrations of 0.6, 1.4, 2.6 ppb. Wheat standards (spiked) were also provided at 0 and 2.4 ppb.

Combs of 12 sensors were prepared as in the previous section, coating with 1/30 anti-OTA antibody in CB without stabiliser. The first comb of sensors was tested against the samples containing 0.6ppb and 2.6ppb OTA; the 0 ppb and 2.4 ppb standards were added into two wells at each end of the comb. The full OTA assay was run using the auto-instrument, and the measurement step was by chronoamperometry. The resulting current responses taken at 5s are shown in Table 5.1.

Table 5.1. Current responses obtained for real wheat samples using OTA sensor comb in auto-instrument

Sensor number	ppb OTA	Current response at 5s (nA)	Mean (nA)	SD	CV (%)
1	0 (std)	5370	5718		
2	0 (std)	6066			
3	0.6	4629			
4	0.6	4183	4235	306.6	7.2
5	0.6	4244			
6	0.6	3883			
7	2.6	6786			
8	2.6	6808	6459	396.5	6.1
9	2.6	6201			
10	2.6	6039			
11	2.4 (std)	5736	5604		
12	2.4 (std)	5472			

The first observation is that the average current responses for the two standards (0 and 2.4 ppb) do show the correct ranking, ie. 2.4ppb gives a lower response. However, based on these figures, there is a very small working current range, and the value obtained for sensor number 1 seems anomalous. If the response for sensor number 2 was taken as the value for 0ppb, then this would give a more realistic working current range of up to 500 nA between 0 and 2.4 ppb. Really it is necessary to see an entire current range and to obtain several repeat readings.

On a positive note, the CV values for repeat sensors measuring the real wheat samples containing 0.6 and 2.6 ppb OTA showed sensible grouping, with values of 7.2 and 6.1%. However, the ranking order of these mean values was not correct for a competitive assay and did not fall within the current range seen for the two standards.

This result implies that there is a strong matrix effect which differs for different wheat samples. In this experiment, blank sensors were not included for each sample in order to correct for any matrix responses/shifts. Clearly, there is evidence here that blanks will be required if chronoamperometry is to be used as the measurement technique on different wheat samples.

Further experiments on real wheat samples were planned. Unfortunately, a technical fault developed in the auto-instrument, necessitating its return to Uniscan Instruments for repair. Hopefully it will be possible to complete these studies at a later date.

Due to a power cut and subsequent instrument breakdown not all the samples were analysed. Those that were suggested that there was a significant matrix effect on the results which remains to be resolved.

Reduction of the instrument run time (currently 77mins) is an area that the end users felt would be required for a successful commercial instrument.

Publications

Papers

Studies towards the development of a screen-printed carbon electrochemical immunosensor array for mycotoxins: a sensor for Aflatoxin B1. R.M.Pemberton, R.Pittson, N.Biddle, G.A.Drago & J.P.Hart. Analytical Letters (2006) 39: 1573-1586.

Progress towards a commercial test for mycotoxins in grain: an automated instrument for ochratoxin A based on a screen-printed carbon electrochemical immunosensor array. R.M.Pemberton, R.Pittson, N.Biddle, G.A.Drago, D.J.Lonsdale, M.Piano & J.P.Hart.(in preparation).

Posters

Electrochem 2005, September 2005, Newcastle, UK: A screen-printed carbon electrochemical immunosensor array for the determination of mycotoxins in grain extracts. R.M.Pemberton, R.Pittson & J.P.Hart.

2nd International Workshop on Biosensors for Food Safety and Environmental Monitoring, Agadir, Morocco, November 2005: A screen-printed carbon electrochemical immunosensor array for the determination of mycotoxins in grain extracts. R.M.Pemberton, R.Pittson, N.Biddle, G.A.Drago & J.P.Hart.

Biosensors 2006 in Toronto, Canada: A screen-printed carbon electrochemical immunosensor for the determination of mycotoxins in grain. R.M.Pemberton, R.Pittson, N.Biddle, G.A.Drago, D.J.Lonsdale & J.P.Hart.

The 57th Annual Meeting of the International Society for Electrochemistry, September 2006 at Heriot-Watt University, Edinburgh, UK: Towards a commercial instrument based on an immunosensor array for automated electrochemical detection of mycotoxins in grain. R.M.Pemberton, R.Pittson, N.Biddle, G.A.Drago, D.J.Lonsdale & J.P.Hart.

Non-refereed

A poster detailing the project was produced for Cereals 2006.
Partners had the opportunity to review all posters prior to printing.

References

Hart,J.P., Pemberton,R.M., Luxton,R. & Wedge,R. (1997). Studies towards a disposable screen-printed amperometric biosensor for progesterone. Biosensors Bioelectron., 12: 1113-1121.

Pemberton,R.M., Hart,J.P. & Foulkes,J.A. (1998). Development of a sensitive, selective electrochemical immunoassay for progesterone in cow's milk based on a disposable screen-printed amperometric biosensor. Electrochim.Acta., 42: 3567-3574.

Pemberton,R.M., Hart,J.P., Stoddard,P. & Foulkes,J.A. (1999). A comparison of 1-naphthyl phosphate and 4-aminophenyl phosphate as enzyme substrates for use with a screen-printed amperometric immunosensor for progesterone in cows' milk. Biosensors.Bioelectron., 14: 495-503.

Pemberton,R.M. & Hart, J.P. (2001). An electrochemical immunosensor for milk progesterone using a continuous flow system. Biosensors.Bioelectron., 16: 715-723.

Pemberton, R.M. & Hart, J.P. (2005). Development of a screen-printed carbon electrochemical immunosensor for picomolar concentrations of estradiol and in human serum extracts. J.Biochem.Biophys.Methods, 6: 201-212.

Hart, J.P., Crew, A., Crouch, E., Honeychurch, K.C. & Pemberton, R.M. (2004). Some recent designs and developments of carbon screen-printed electrochemical sensors for biomedical, environmental and industrial analyses. Anal.Lett., 37 (5) 789-830.

Micheli, L., Grecco, R., Badea, M., Moscone, D and Palleschi, G. 2005. An electrochemical immunosensor for aflatoxin M1 determination in milk using screen-printed electrodes. Biosens.Bioelectron., 12: 588-596.

Appendix 1

HPLC Conditions

A Perkin Elmer Quaternary pump with series 200 Autosampler were used for HPLC separation with the following conditions.

Column: Waters Spherisorb 5m C18

Mobile phase:

A: 95% Water/5% Methanol + 10mM ammonium acetate
B: 95% Methanol/5% Water + 10mM ammonium acetate

Gradient over 15 minutes at a flow rate of 1500 ml/min

Mass Spectrometry Conditions - Tricothecenes

Mass Spectrometer: Applied Biosystems/MDS Sciex API 4000™LC/MS/MS System

Ionisation	Heated nebuliser (APCI)
CUR	25
GS1	40
CAD	10

Temperature: 500 °C

Nebuliser current: -4 (neg) +4 (pos)

Negative Ion Tricothecenes

Parameter	MRM	DP	CE
NIV	371>59	-30	-22
	371>280	-30	-22
DON	355>59	-40	-40
	355>295	-40	-16
FUS	413>59	-35	-40
	413>187	-35	-38
ADON	317>59	-60	-50
	317>337	-60	-12

Positive Ion Tricothecenes

Parameter	MRM	DP	CE
NEO	484>305	56	19
	484>185	56	29
DAS	400>185	46	31
	400>215	46	23
HT-2	442>263	41	19
	442>215	41	17
T-2	384>307	51	19
	384>247	51	13

Mass Spectrometry Conditions – Aflatoxins/Tricothecenes

Mass Spectrometer Applied Biosystems/MDS Sciex API 4000™LC/MS/MS System

Ionisation :	TurboIonSpray™
CUR	25
GS1	40
CAD	10

Temperature: 500 °C
Ionspray voltage: -4500(neg)/+5500(pos)

Positive Ion Aflatoxins

Parameter	MRM	DP	CE
B1	313>285	100	31
	313>241	100	49
B2	315>287	106	37
	315>259	106	43
G1	329>243	96	37
	329>200	96	55
G2	331>245	101	43
	331>257	101	43

Negative Ion Tricothecenes (Electrospray)

Parameter	MRM	DP	CE
ZAN	371>59	-30	-22
	371>280	-30	-20

Appendix 2

Operating Procedure for Uniscan computer-controlled 12-channel electrochemical immunoassay instrument.

1) Prepare 96-well plate as follows (example given is OTA assay):
Lay plate out so that well H12 is at top left.
So Row H is Row 1, Row G is Row 2, Row F is Row 3, Row E is Row 4 and Row D is Row 5.
Add reagents to Row 1 as follows: 100 μl 1/5000 OTA-biotin/PBS; 100 μl wheat (or spiked wheat) in PBS/20% MeOH/0.1% Tween 80; 100 μl PBS/20% MeOH/0.1% Tween 80 alone or containing OTA standards. Mix thoroughly using Gilson.
Add 300 μl PBS to Row 2.
Add 300 μl 1/500 SA-ALP in PBS to Row 3.
Add 300 μl 0.1M Tris-HCl/10mM $MgCl_2$ to Row 4.
Add 300 μl 2mg/ml 1-naphthyl phosphate in 0.1M Tris-HCl/10 mM $MgCl_2$ to Row 5.

2) Place prepared 96-well plate on stage (well A1 is now at top left)
3) Place comb of biosensors into connector bank (unscrew wing-nuts, remove white plate, place comb onto pegs, replace plate and wing-nuts (finger-tight)).
4) Configure the instrument using the computer as follows:
In the UiEchem software, open a New file as follows:
Click on the "mycotoxin.cpp" icon (opens a new window)
Click "Yes" to continue
UiEchem - [macroexperiment] window appears
Now configure Rows 1-5:
Click on green configure icon
Parameter window appears
Click "Load"
Look in c:/UiEChem
Double-click "MK2OTArow1.cma"
Parameters for Row 1 will appear in window
Click "OK" to accept
Click "OK" to continue
"? initialise equipment"
Click "Cancel"
Return to green configuration icon and repeat for Rows 2-5 by selecting MK2OTArow2, row3, row4 or row5
When Row 5 is loaded and "OK"ed, click "OK" to initialise equipment
The stage position will now be initialised
Single click on green forward (start) arrow
Potatiostats will "Bleep"
"Prime pump?"
Click "OK"
Stop pump as soon as air bubbles are removed from supply tube
"Do you wish 5 min temperature soak?"
Click "No"

5) The instrument will now "seek Row 1" and begin/run the experiment.

6) At the end of the experiment, current values for Potentiostats 1-12 (corresponding to sensors 1-12 in plate wells D12-D1 respectively) will appear in the data window.
7) Export the data and save it, and save the File before proceeding.
8) To commence a further experiment, open a new File and repeat the above procedure, configuring each Row in turn as before.

Do not attempt a further experiment simply by pressing the start arrow, or by reconfiguring the row parameters within the same open window. This will result in a wrongly-sequenced experiment.
You must start a completely new file for every experiment.